2013

Learning, self-organisation and homeostasis in spiking neuron networks using spike-timing dependent plasticity

Humble, James

Learning, self-organisation and homeostasis in spiking neuron networks using spike-timing dependent plasticity.

James Humble

Plymouth University

A thesis submitted in partial fulfillment of the requirements for the degree of:

Ph.D

March 2013

Abstract

Learning, self-organisation and homeostasis in spiking neuron networks using spike-timing dependent plasticity.

James Humble.

Spike-timing dependent plasticity is a learning mechanism used extensively within neural modelling. The learning rule has been shown to allow a neuron to find the onset of a spatio-temporal pattern repeated among its afferents. In this thesis, the first question addressed is 'what does this neuron learn?' With a spiking neuron model and linear prediction, evidence is adduced that the neuron learns two components: (1) the level of average background activity and (2) specific spike times of a pattern.

Taking advantage of these findings, a network is developed that can train recognisers for longer spatio-temporal input signals using spike-timing dependent plasticity. Using a number of neurons that are mutually connected by plastic synapses and subject to a global winner-takes-all mechanism, chains of neurons can form where each neuron is selective to a different segment of a repeating input pattern, and the neurons are feedforwardly connected in such a way that both the correct stimulus and the firing of the previous neurons are required in order to activate the next neuron in the chain. This is akin to a simple class of finite state automata.

Following this, a novel resource-based STDP learning rule is introduced. The learning rule has several advantages over typical implementations of STDP and results in synaptic statistics which match favourably with those observed experimentally. For example, synaptic weight distributions and the presence of silent synapses match experimental data.

Contents

List of Figures

Acknowledgements

I would like to thank my friends, family and colleagues. There has been the occasional difficult period over the last few years and having someone to discuss and moan with has helped greatly. In both cases, moaning or discussing, you helped more than you know.

I also want to thank Thomas Wennekers and Sue Denham for their support and guidance. Their critical eyes were a major driving force that lead to the work presented here.

Finally, I am indebted to coffee, different teas, RedBull and crosswords.

Authors declaration

At no time during the registration for the degree of Doctor of Philosophy has the author been registered for any other University award.

Relevant scientific seminars and conferences were regularly attended at which work has been presented. Two papers have been accepted for publication.

Signed: _____

Date: _____

Publications :

Humble, J., Furber, S., Denham, S. and Wennekers, T. *STDP pattern onset learning depends on background activity* in Proceedings of BICS 2010 - Brain Inspired Cognitive Systems **2010**

Humble, J., Denham, S. and Wennekers, T. *Spatio-temporal pattern recognizers using spiking neurons and spike-timing-dependent plasticity* Frontiers in Computational Neuroscience **2012 , 6:October**

Humble, J., Denham , S. and Wennekers, T. *What can a neuron learn with STDP?* **in prearation**

Humble, J., Denham , S. and Wennekers, T. *Synaptic homeostasis arising from spike-timing-dependent plasticity with heterostasis.* **in prearation**

Word count for the main body of this thesis: 23588

Chapter 1

Introduction

1.1 Biological background

1.1.1 Neurons and synapses

A typical neuron is divided into three parts: the soma, the axon and dendrites. For simplicity, dendrites can be thought of as input, axon as output and the soma as the decision segment. Input typically gets integrated on dendrites and, when this activity (membrane potential) reaches the soma, if it is great enough, an action potential is propagated down the axon to other neurons. These action potentials form the communication substrate of the brain and nervous system.

Communication of these action potentials is facilitated between neurons by synapses, these are structures that permit activity to pass from one neuron to another. An action potential is transmitted through a synapse via neurotransmitters which are released presynaptically, and bind to receptors postsynaptically, this in turn allows ions to flow into the postsynaptic neuron and change the membrane potential. Many different neurotransmitters are present, and many different types of receptors mediate different ionic currents and ions pre- and postsynaptically. Essentially, specific neurotransmitters bind with specific receptors; this allows for individual postsynaptic currents to be controlled presynaptically.

Furthermore, many synapses are ‘plastic’; this means their efficacy is not fixed. A synapse can have a very weak effect on postsynaptic activity, a strong efficacy towards activity, or an efficacy somewhere in between. Moreover, this synaptic efficacy is controlled by many factors including those found presynaptically such as neurotransmitter release rate, postsynaptic factors such as receptor quantity and receptor type and mechanisms found both pre- and postsynaptically like synapse size. ‘Plasticity’ describes the process of changing synapses’ efficacies.

Different receptors are crucial to different forms of plasticity and changes in receptor presence or quantity, effect different plastic mechanisms, which subsequently alter synaptic efficacy. It has been observed that pre- and postsynaptic activity can affect a synapses efficacy: activity-dependent plasticity .

1.1.2 Long-term potentiation and depression

Two examples of plasticity are long-term potentiation (LTP) and long-term depression (LTD). These refer to two types of plasticity (Bliss and Gardner-Medwin 1973; Levy and Steward 1983; Siegelbaum and Kandel 1991; Bliss and Collingridge 1993; Linden and Connor 1995; Nicoll and Malenka 1995). Both forms are activity-dependent and can result in either a long-term increase (LTP) or decrease (LTD) in the efficacy of synapses.

Commonly studied receptors implicated in LTP and LTD are AMPA (2-amino-3-(3-hydroxy-5-methyl-isoaxazol-4-yl)propanoic acid) (Hayashi et al. 2000; Shi et al. 2001; Carroll et al. 1999; Shi et al. 2001; Takahashi et al. 2003; Bredt and Nicoll 2003; Oh et al. 2006; Park et al. 2006; Serulle et al. 2007; Yang et al. 2008) and NMDA (N-methyl-D-aspartic acid) receptors. AMPA receptors allow the passage of Na^+ and K^+ and NMDA receptors, Na^+.

An important mechanism of NMDA receptors for plasticity is their voltage-dependent activation: Mg^{2+} ions extracellularly block the channel until the membrane voltage reaches a certain amount. This is important as calcium ion flow through NMDA receptors is critical in synaptic plasticity.

1.1.3 Spike-timing-dependent plasticity

Another well established plasticity mechanism is spike-timing dependent plasticity (STDP). STDP permits spike time differences between pre- and postsynaptic activities to affect changes in synaptic efficacy (Bastrikova et al. 2008; Bell et al. 1997; Bi and Poo 1998, 1999; Markram et al. 1997; Pratt et al. 2008): if presynaptic activity precedes postsynaptic activity, the conjoining synapse is strengthened—usually according to some STDP function—and if the reverse is observed, the synapse is depressed. See figure 1.1 for STDP data and fitted exponential functions. This form of synaptic plasticity, which relies on temporal differences between pre- and postsynaptic activity, was found using electrophysiology; for example Bell et al. (1997) found that in cerebellum-like structures in fish, synaptic plasticity depended on the sequence of pre- and postsynaptic events and Markram et al. (1997) found a similar effect in pyramidal neurons.

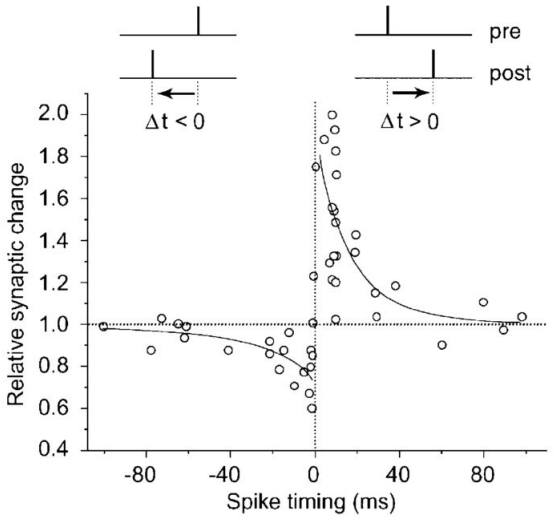

Figure 1.1: Spike-timing-dependent plasticity observed in hippocampal neurons. Relative changes of evoked postsynaptic currents are shown for repeated pre- and postsynaptic spike pairs with different temporal differences. Two exponential functions are fitted with time constants τ_p=19 and τ_d=34ms. (Image from Bi (2002).)

1.1.4 Further forms of plasticity

LTP, LTD and STDP are not alone–other mechanisms of plasticity have been discovered including heterosynaptic plasticity, homeostasis, synaptic scaling, and presynaptic plasticity. Heterosynaptic plasticity for example describes cases where LTP is induced at some afferents, and LTD is sometimes induced at other afferents (Dunwiddie and Lynch 1978; Tsumoto et al. 1978; Hirsch et al. 1992). There are also findings of the reverse: LTD inducing LTP (Royer and Paré 2003; Wöhrl et al. 2007). Synaptic scaling describes a homeostatic regulation of synapses across a neuron. For example, artificially blocking or increasing a neuron's activity can lead to an increase, or decrease, of AMPA receptors (O'Brien et al. 1998; Turrigiano et al. 1998; Watt et al. 2000).

1.2 Computational models

1.2.1 Neuron models

There are many different computational models with features of biological neurons: for example (in increasing complexity) integrate-and-fire model (Lapicque 1907), leaky integrate-and-fire

model (LIF) (Stein 1967) and Hodgkin-Huxley model (Hodgkin and Huxley 1952). Integrate-and-fire neurons integrate some input, I, with a membrane time constant, τ_m=10ms, until a threshold, θ, is reached and the membrane potential, V, is reset, Eq. 1.1. Leaky integrate-and-fire neurons compute the same, although they have a leak current which represents current loss due to a leak across a neuron's membrane potential, Eq. 1.2. A more complex model is the Hodgkin-Huxley neuron model, which models different channel types, and exhibits more realistic behaviour such as refractory periods. For many purposes, however, a leaky integrate-and-fire neuron is used as it is computationally cheaper, and captures the fundamental properties of the membrane potential.

$$\tau_m \frac{dV}{dt} = I \qquad \text{if } V \geq \theta \text{ then reset } V = 0 \tag{1.1}$$

$$\tau_m \frac{dV}{dt} = -V + I \qquad \text{if } V \geq \theta \text{ then reset } V = 0 \tag{1.2}$$

1.2.2 Long-term potentiation and depression

Computational rules of LTP and LTD are usually based on firing rates . For example, an increase in afferent firing rate leads to an increase in synaptic efficacy, and a decrease in firing rate a decreased in synaptic efficacy. LTP and LTD computational learning rules are not considered in this thesis as the emphasis is on spike-timing-dependent plasticity.

1.2.3 Spike-timing-dependent plasticity

The amount of change for different intervals between pre- and postsynaptic activity, τ, is dependent on an STDP function, $f(\tau)$. A commonly used function is an exponential decay with maximum synaptic change and minimal temporal difference between pre- and postsynaptic activity, Fig. 1.1 and Eq. 1.3 where A_p and A_d are learning rates and τ_p and τ_d are time constants for potentiation and depression respectively.

$$\begin{aligned} f(\tau) &= A_p \times \exp\left(\frac{-\tau}{\tau_p}\right) \qquad \text{if } \tau \geq 0 \\ f(\tau) &= A_d \times \exp\left(\frac{\tau}{\tau_d}\right) \qquad \text{if } \tau < 0 \end{aligned} \tag{1.3}$$

Spike-timing-dependent plasticity has been studied extensively, and is commonly used as a substrate of many forms of learning (Linsker 1988; MacKay and Miller 1990; Swindale 1982). Linsker (1988) demonstrated that through Hebb-type synaptic plasticity, structured receptive fields could be developed. Furthermore, since the discovery of temporal synaptic plasticity, many potential benefits have been proposed. For example, STDP can (1) increase the mutual information between inputs and outputs of simple networks (Masquelier et al. (2009) used information theory to quantify learning performance), (2) provide a function for Hebbian and development and (3) capture the causality of determining the direction of synaptic change that is implied by Hebb's original postulate. Plasticity rules based on such temporal differences have consequently been studied extensively, and have been applied successfully to both simple pattern learning and complicated competitive pattern learning (Guyonneau et al. 2005; Masquelier et al. 2008, 2009; Masquelier and Thorpe 2007; Song et al. 2000; Izhikevich and Desai 2003; Bush et al. 2010; Gerstner and Kistler 2002).

Masquelier and colleagues (2008) demonstrated that a leaky-integrate and fire neuron equipped with STDP can learn repeated spatio-temporal spike patterns, even when embedded in a statistically identical distractor signal—a somewhat non-trivial task. In their setup a singular neuron received Poisson input on 2000 afferents. Half of these afferents always presented this Poisson noise, however the other half alternated between Poisson noise and a repeated spatio-temporal stimulus with identical Poisson statistics. The neuron was able to distinguish the repeated pattern from a background signal even though the firing rates of both were equal. Furthermore, after the neuron had learnt a part of the pattern it reduced the response latency—relative to the beginning of the pattern—until it responded within a few milliseconds after the onset of the pattern. It is proposed that such learning may take advantage of the view that a pattern is a succession of spike coincidences (Masquelier et al. 2008).

Masquelier et al. (2009) later extended their network with multiple neurons. As in their previous

work each neuron was learning a repeated spatio-temporal spike pattern, however the neurons competed to learn a pattern through lateral winner-takes-all inhibition. Due to this inhibitory competition each neuron learnt a different segment of a pattern. Specifically, it was found that neurons learnt to respond near the onset, as in (Masquelier et al. 2008), however remaining neurons then 'stacked' on this neuron so their response latencies increased.

However, an important question is 'what is a neuron learning in this case?' After learning, is the neuron sensitive to spike-count, spike-timing, firing rates or some other property of the stimulus? Is the neuron only sensitive to one stimulus component, or are multiple features learnt? These questions are the first main topic of this thesis.

1.3 Biological and computational comparison

Synaptic statistics of computational studies rarely match those found biologically. For example, synaptic weight distributions resulting from computational learning are either bi-modal (Masquelier et al. 2008, 2009; Barbour et al. 2007), or uni-modal with a peak near the midpoint of the weight range (van Rossum et al. 2000; Burkitt et al. 2004). To the contrary, biological distributions are mostly unimodal with a peak near zero (Montgomery et al. 2001; Song et al. 2005; Frerking et al. 1995; Isope and Barbour 2002).

Two other biological factors often left out of computational studies are non-potentiable synapses and silent synapses. Non-potentiable or non-plastic synapses have been reported in area CA1 of hippocampal slices (Petersen et al. 1998), and silent synapses (synapses with a lack of AMPA receptors) are one of five discrete observed synaptic states (reviewed by Montgomery et al. (2004)).

The observation that computational results do not match those found experimentally questions whether typical computational STDP implementations are complete. For example, do common implementations of STDP require additional properties/mechanisms to better match the synaptic distributions found in biology? And does the lack of non-potentiable and silent synapses in typical computational STDP

have an effect on how significant the results are? These questions form the last main topic of this thesis.

1.4 Synfire chains and self-organising maps

In 1982, when trying to account for observed precise sequences of neural firing with long inter-spike delays, Abeles coined the term "synfire chain" (Abeles 1982, 1991). Some delays seen between spikes of simultaneously recorded neurons were extremely long, but repeated with a precision in the millisecond range. This was difficult to understand given that the firing patterns of single neurons look very noisy, and can often be well described as rate-modulated Poisson processes. A possible mechanism to produce these delays, was the postulated synfire chain consisting of feed-forwardly connected populations of cells. Each population would contain neurons with excitatory "diverging-converging" connections to neurons in the next population. The populations are defined by their connectivity, and therefore symbolise the order of activation; individual neurons may take part in more than one (and in fact many) populations. Experimental evidence supporting synfire chains is limited, however precisely repeating firing patterns have been observed (Prut et al. 1998; Nádasdy et al. 1999; Ikegaya et al. 2004).

There have been some attempts to learn synfire chains using computational models (Bienenstock 1991; Hertz and Prügel-Bennett 1996). There are, however, limitations to these studies. For example, closed loops form in which once activity enters, it never exits again.

Along side synfire chains, the formation of topographically ordered maps has been a focus of research within neuroscience. The research is driven by findings of topographically organised maps in nervous systems; for example, Fox et al. (2008) found somatosensory maps in barrel cortex, Wandell et al. (2011) demonstrate a retinotopic map, and Horton et al. (1996) and Casagrande et al. (1994) show ocular dominance maps. Whether these maps self-organise is a topic of ongoing debate, although some evidence suggests that maps may be half formed during neural development and fully organised by plasticity (Rosa 2002).

A seminal self-organising map algorithm is that of Kohonen (1995). Kohonen's SOM algorithm firstly compares input with synaptic weights. A "winning" neuron is selected: usually that

which has synaptic weights most accurately matching the input. This winner and neighbouring neurons (within a certain neighbourhood distance function), have their weights adjusted slightly to more accurately match the input. Finally, the neighbourhood distance decreases during a simulation. This leads to the formation of a feature map, where similar features are represented by neurons spatially close to each other and dissimilar features by those far apart.

Self-organising map algorithms, such as Kohonen's, commonly have limited biological evidence supporting their function, and any evidence is usually considered after algorithm design. On the other hand, very few computational studies look at self-organising maps arising from simple computational rules.

> The formation of topographically ordered maps, and the evidence adduced for synfire chains suggests that there is one or many computational rule(s) underlying the formation and organisation of ordered neural activity. There have been attempts to elucidate these rules. Studies looking at synfire chains have found computational limitations. Therefore a main topic of this thesis considers synfire chains and SOMs: 'how can a simple learning rule, such as STDP, produce synfire chain like structures?' If a neuron with STDP is able to learn synfire chains, it may be possible to use STDP as a substrate to learn the experimentally observed topographically ordered maps.

1.5 Thesis layout

Throughout the introduction above, several crucial questions have been presented, that will be the centre of this thesis:

- *What stimulus properties does a neuron with STDP learn?*
  - Does a neuron with STDP learn spike-count, spike-timing or firing rate? Does the spatial or temporal structure of a stimulus make a difference? Is only one property of a stimulus learnt, or are combinations learnt? - We shall adduce evidence that a neuron learns two components: (1) the level of average background activity and

(2) specific spike times of a pattern. Some of this work is presented in a conference contribution (Humble et al. 2010) and the rest will be included in a forthcoming paper (Humble, in preparation A).

- *How can a simple learning rule, such as STDP, produce synfire chain like structures or self-organised ordered maps?*
  - Assuming synfire chain like structures and self-organising maps are the product of simple learning rules which can be reproduced computationally and that these structures are mostly formed through plasticity, is STDP—or a modified form thereof—a substrate? - We take advantage of the answer from the previous main question and a network is developed that can train recognisers for spatio-temporal input signals using STDP. Furthermore, the setup is such that a recognising neuron only responds if the correct stimulus and the firing of all previous neurons is present. This is akin to a simple class of finite state automata. This work is all presented in a recent paper (Humble et al. 2012)
- *Do current computational rules fully represent the biology and if not, what is missing?*
  - Why do computational synaptic distributions not match those found experimentally? Are missing mechanisms/properties that are found experimentally, such as non-potentiable synapses, important, and how can these be reproduced with computational learning rules? - To answer these questions a novel resource-based STDP learning rule is introduced. The learning rule results in synaptic statistics which match those observed experimentally and also has several advantages over currently existing STDP learning rules. This work will be presented in an upcoming paper (Humble in preparation B).

This thesis has three main chapters addressing the questions above in three mostly separate studies. Methods common throughout the thesis are described next and methods distinct to a study are described in their own chapters. Unless otherwise stated methods in the main methods chapter (next) apply throughout the thesis. Similar to the methods, distinct background infor-

mation is described at the beginning of chapters in a distinct introduction and each chapter also includes its own discussion.

Firstly, results are presented in chapter 3 which address the first question: 'What can a neuron learn with STDP?' We use both a spiking neuron model and linear prediction to study in detail what stimulus properties are learnt through STDP, and find that more than one property is important. This question is addressed first, as answers have implications for the subsequent questions. For example, our finding that a neuron with STDP learns both firing rate and spike-timings, is important when approaching the learning of structures such as synfire chains.

Secondly, chapter 4 describes a successful attempt to learn synfire chains with a typical STDP implementation. Simple synfire chain structures are learnt with nearest-neighbour STDP, and more complex chains learnt with all-to-all STDP (see (Morrison et al. 2008)). Furthermore, learnt synfire chains behave as simple finite state automata: one or more accepting neurons are present which only respond when a stimulus is presented in full. Limitations found in this chapter, such as weight normalisation, motivate the next.

Finally, in chapter 5 we look at our last question and address missing properties of typical STDP implementations. A novel resource-based STDP learning rule is proposed, and supporting evidence discussed. Our proposed learning rule produces synaptic statistics comparatively more similar to biological findings than typical STDP. It also solves the weight normalisation limitation of our previous synfire chain learning study.

Chapter 2

Methods

Some methods are common across all chapters; these are presented here. Unless otherwise stated these methods and terms apply throughout the thesis. Any distinct methods specific for a certain chapter are presented at the beginning of the respective chapter. See table 2.1 for a table of parameters that are common across all chapters.

2.1 Network structure and stimulus

A spiking neuron model is used in all chapters. The basic network structure is similar to that of Masquelier et al. (2008): 2000, N_{input}, afferents converging on an excitatory neuron (see figure 2.1). These 2000 afferents carry Poisson spike trains which are produced 'on the fly', with 1000 of these afferents occasionally conveying a repeated spatio-temporal pattern of 50ms duration.

Input, I, consists of one half continuously transmitting independent Poisson spike trains, I^{noise}. The other half, I^{in}, alternate between independent Poisson spike trains and a fixed spatio-temporal pattern. The simulation is segmented into 50ms segments, and the spatio-temporal pattern is inserted into random segments with a probability of 0.25 per segment. These 50ms patterns are generated by Poisson processes as well, but the patterns are fixed for the duration of the simulations. The rate of the Poisson spike trains and the repeated spatio-temporal pattern were 54Hz. Additionally, 10Hz Poisson noise is added to all afferents including during the presentation of the frozen patterns. This provides a scenario where a pattern is embedded in a statistically identical carrier signal.

All simulations use forward Euler-integration with a time-step of dt=0.1ms.

2.2 Neuron model

All spiking neurons were leaky-integrate-and-fire cells, Eq. (2.1), with synaptic currents described by alpha functions, S_r and S_f, Eq. (2.2). The membrane potentials of all neurons followed a low-pass dynamics with time-constant τ_m=10ms and a reset when they reached firing threshold; a firing threshold θ=1 was used. τ_m=10ms is the membrane time constant, τ_r=1ms is the rise time constant of the alpha synapse and τ_f=5ms the decay constant.

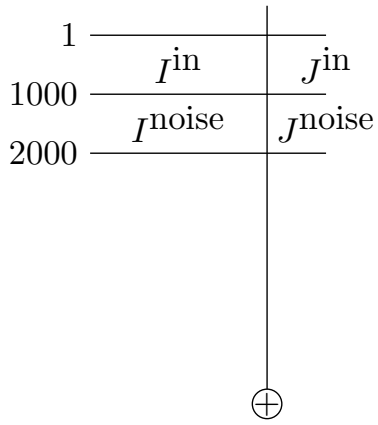

Figure 2.1: An excitatory neuron receives input consisting of a total of N_{input}=2000 afferents. Half of these, I^{in}, alternate between presenting a repeated spatio-temporal pattern (for 50ms) and Poisson input (for at least 50ms). The other half, I^{noise}, continuously present Poisson input. All input synapses, J^{in} and J^{noise}, are plastic.

$$\tau_m \frac{dV}{dt} = -V + S_f \qquad \text{if } V \geq \theta \text{ then reset } V = 0 \tag{2.1}$$

$$\begin{aligned} \tau_r \tfrac{dS_r}{dt} &= -S_r + I \\ \tau_f \tfrac{dS_f}{dt} &= -S_f + S_r \end{aligned} \tag{2.2}$$

2.3 Spike-timing-dependent plasticity

The spike-timing-dependent plasticity (STDP) rule used in chapters 3 and 4 is a typical additive exponential STDP update rule. Pre- and post-synaptic spike-pairs evoked synaptic changes given by a function f of their temporal distance τ, see Eq. (2.3). We used both, all-to-all and nearest-neighbour spike implementations (see (Morrison et al. 2008)), which differ only with respect to how many pre-synaptic spikes are considered: an all-to-all rule considers all pre-synaptic spikes whereas a nearest-neighbour implementation will only consider the pre-synaptic spike that is received closest to the time of post-synaptic activity. Equation (2.3) describes the STDP function used, where τ_p=τ_d=20ms. τ_p and τ_d were chosen similar to those

observed experimentally (Bi and Poo 1998; Levy and Steward 1983; Wittenberg and Wang 2006) where the strongest synaptic modifications occur within a window of $\pm$20ms. These constants vary from previous studies such as Masquelier et al. (2008; 2009) who used τ_+=16.8ms and τ_-=33.7ms. Learning rates A_p and A_d for potentiation and depression were assigned using (2.4) where λ=1.05. The assignment of these is in accordance with the finding by Song et al. (2000; 2003; 2010) that $\frac{A_d}{A_p}$ needs to be slightly larger than one to maintain reasonable postsynaptic activity.

$$\begin{aligned} f(\tau) &= A_p \times \exp\left(\frac{-\tau}{\tau_p}\right) \qquad \text{if } \tau \geq 0 \\ f(\tau) &= A_d \times \exp\left(\frac{\tau}{\tau_d}\right) \qquad \text{if } \tau < 0 \end{aligned} \tag{2.3}$$

$$\begin{aligned} A_p &= 0.002 \times W_{\max}^{\mathrm{P}} \\ A_d &= -A_p \times \left(\frac{\tau_p}{\tau_d}\right) \times \lambda \end{aligned} \tag{2.4}$$

2.4 Maximum synaptic weight

Many studies into STDP pattern learning use weight bounding to control synaptic change; such saturation limits unstable forms of STDP based learning changing synaptic efficacies *ad infinitum*. Furthermore, the maximum synaptic weight can have a great impact on the learning process: if too low, postsynaptic activity may not reach threshold, and if too high, postsynaptic activity may be erratic and uninformative.

The maximum synaptic weight $W_{\max}^{\mathrm{P}}$ for Poisson afferents was thus assigned such that the difference in membrane potential required to go from resting to threshold is divided by the total number of afferents. This value may further be adjusted to allow fluctuations in the membrane potential to reach the neuron's threshold because (1) all afferents in the pattern may not be learnt through STDP, (2) synapses are not guaranteed to converge fully to weight boundaries and (3) the afferents are not guaranteed to fire at the average firing rate or sufficiently within the membrane time constant. To this end, an appropriately selected value (considering the above points)

can allow STDP to be affected by positive fluctuations in input and membrane potential—found to be crucial by Song et al. (2000; 2003; 2010) and designed into a learning rule by Senn et al. (2005). It was found that STDP trained best with A=20.

This choice of $W_{\max}^{\mathrm{P}}$ allows for a reliable activation of neurons when the pattern is presented after training, but only few occasional output spikes due to random inputs. Furthermore, the cumulative change in weights from random activity approximates to < 0; see Eq. (2.5).

$$\int_{-\infty}^{\infty} f(\tau)dt < 0 \tag{2.5}$$

Crucially, this is a 'best guess' approach to assigning maximum synaptic weights because a 'best' value will depend on how many afferents are fully potentiated at the end of learning, and this changes between simulations depending on the stimulus, chance during learning and random initial synaptic weights. Specifically, the rheobase will stay the same across simulations but the number of synapses contributing and their individual contributions will change.

2.5 Initial synaptic weights

The initial strength of synaptic weights can be as important as their maximum efficacies. Several different approaches are used to set initial weights; the approach we adopted is to set weights, $\mathbf{w}$, with random values drawn from a uniform distribution between 0 and $W_{\max}^{\mathrm{P}}$ as in Eq. (2.6).

$$0 < \mathbf{w} \leq W_{\max}^{\mathrm{P}} \tag{2.6}$$

Initial weights should be set such that fluctuations from all afferents cause the output neuron to fire frequently. This is important because it allows all synapses contributing to postsynaptic activity to be affected by STDP (Song et al. 2000; Izhikevich and Desai 2003; Bush et al. 2010), and thus be potentiated or depressed.

Table 2.1: Table of parameters

Parameter	Description	Value
N_{input}	Number of input afferents.	2000
I	Input.	-
I^{in}	Input transmitting the repeated pattern.	-
I^{noise}	Input not transmitting the repeated pattern.	-
dt	Euler-integration time step.	0.1ms
τ_m	Membrane time constant.	10ms
θ	Firing threshold.	1
θ_r	Rise time constant for alpha function.	1ms
θ_f	Fall time constant for alpha function.	5ms
S_r	Rise synaptic current of alpha function.	-
S_f	Fall synaptic current of alpha function.	-
$f(\tau)$	STDP function.	-
τ	Temporal distance between pre- and postsynaptic activity.	-
τ_p	Potentiation time constant for STDP function.	20ms
τ_d	Depression time constant for STDP function.	20ms
A_p	Positive learning rate.	$0.002 \times W_{\text{max}}^{\text{P}}$
A_d	Negative learning rate.	$-A_p \times \left(\frac{\tau_p}{\tau_d}\right) \times \lambda$
λ	Parameter adjusting the proportionality of the learning rates.	1.05
$W_{\text{max}}^{\text{P}}$	Maximum synaptic weight for input afferents.	$1/N_{\text{input}}$

Chapter 3

What can a neuron learn with STDP?

3.1 Introduction

As described in the main introduction, Masquelier et al. (2008) found that a singular neuron with STDP is able to learn to respond to the start of a repeated spatio-temporal pattern. However, a question arises: what exactly do the STDP synapses 'learn'? Are they adjusted so a neuron is sensitive to spike-counts on a subset of its afferents or does the neuron become sensitive to some temporal properties, perhaps spike timing, and if so, at what resolution?

Some indication comes from recent studies. It has been found that when sustained neuronal noise is included in simulations and *in vitro* experiments, a neuron's input-output relationship is changed (Chance et al. 2002; Hô and Destexhe 2000; Stacey and Durand 2001; Shu et al. 2003; Wolfart et al. 2005; Fellous et al. 2003) (see (Silver 2010) for an excellent review). In fact, neurons are continually receiving spikes from thousands of neurons (White 1989; Abeles 1991), and the sheer number of these can have strong effects on the activity of a neuron (Hô and Destexhe 2000; Chance et al. 2002; Fellous et al. 2003). Shu et al. (2003) and Hô et al. (2000) found that background synaptic activity increased the probability of a neuron responding to small inputs. Shu and colleagues also found that it decreased the latency and jitter of spikes. Furthermore, Shu et al. and Stacey et al. (2001) found that an increase in background activity can increase the correlation between a neuron responding and a stimulus. Hô et al. (2000) have shown additionally that background activity can be split into a tonically active conductance and voltage fluctuations. Interestingly, these fluctuations were found to be crucial to Hebbian learning by Song et al. (2000). Song et al. found that with an STDP function with $\int_{-\infty}^{\infty} f(\tau)dt < 0$, presynaptic activity positively correlated with membrane potential fluctuations was crucial to STDP learning. Considering these, a hypothesis on learnt features might include a combination of background activity, small inputs and voltage fluctuations.

With these findings in mind, we address our proposed question. To do this we use a combination of a spiking neural model and linear prediction. Linear prediction is used instead of a spiking neural model due to the time requirement to run many spiking neural model simulations. More specifically, when studying whether timing is important when using STDP, we would have to run thousands of spiking neural model simulations to cover the several parameters; the linear

prediction model can be used to look at these parameters more timely. However, because the linear prediction misses some of the non-linearities of the spiking neural model we return to the spiking neuron after using the linear prediction model to pinpoint a much smaller parameter space to study.

We adduce that a neuron learns a pattern's spike times 'on top' of background activity and due to a change in this background activity level, the temporal accuracy—the latency relative to the onset of the pattern—of the learning can become unstable. Subsequently, insights into the neuron's encoding are possible, *viz.* that a neuron with STDP appears to learn both background activity and specific pattern spike times with millisecond precision.

3.2 Methods

In this chapter, two models are used: one spiking and the other based on linear prediction. See table 3.1 for a table of parameters for this chapter.

3.2.1 Spiking model

The spiking model is identical to that described in the methods section, confer chapter 2. Each full simulation ran for up to 3000s. During typical simulations it was found that any individual weight could converge (change from one weight limit to the other) in typically 200s, therefore weight values are recorded every 2s allowing sufficient resolution of weight trajectories and distributions.

3.2.2 Linear prediction

A linear predictor was used because each spiking simulation takes considerable time to simulate due to computational costs, and an investigation into specific features in such a large stimulus space could be infeasible because of the sheer number and type of features such as spike timing and spike count.

If one considers a neuron as a stimulus-response transducer that is driven by sensory stimulation (a pattern), one can use linear prediction described below to study how neurons integrate input from receptive fields in time and space.

Spatio-temporal receptive field

Firstly, one computes the spatio-temporal receptive field (STRF) of a neuron. This STRF is a matrix, **S**, see Eq. 3.1. It has dimensions $j = 1,\ldots,\frac{\tau_m}{\Delta}$ and $i = 1,\ldots,N_{\text{input}}$ where Δ is a binning factor (in our simulations we used $\Delta = dt$=0.1ms therefore our STRF matrix has dimensions 100x1000). **S** is produced by recording the previous τ_m=10ms of the input, $I^{\text{in}}(t)$ (which in our simulations is also 100x1000), whenever the output neuron discharges. These recordings continue for every output spike for 200s after the neuron has learnt the pattern (1000–1200s). The arithmetic mean (angular brackets) is taken across all these spikes/trials. The STRF is finally multiplied by learnt weights to take into account any learning.

$$\mathbf{S}_{j=0,\ldots,\frac{\tau_m}{\Delta},i=1,\ldots,N_{\text{input}}} = \left\langle I_i^{\text{in}}(t-j)\right\rangle w_i \tag{3.1}$$

Linear prediction

The linear predictor, $C(t)$, can then be taken between this STRF and different test inputs, $I^{\text{test}}(t)$, to predict the response from a learnt neuron: Eq. 3.2. This effectively convolves $C(t)$ and will be maximum when $I^{\text{test}}(t)$ equals the STRF, and will decrease as $I^{\text{test}}(t)$ becomes less similar to the STRF. Therefore, any change in $I^{\text{test}}(t)$ is matched with a change in $C(t)$.

$$C(t) = \sum_{i=1}^{N_{\text{input}}} \sum_{j=0}^{\frac{\tau_m}{\Delta}} \mathbf{S}_{i,j} I_i^{\text{test}}(t-j) \tag{3.2}$$

Spike train metric

During experiments we altered the pattern. We either temporally jittered spikes on individual afferents by varying amounts, temporally reversed the entire pattern or swapped pattern segments around, for example we swapped the beginning half and end half of a pattern while still maintaining the precise spike times and afferents within each half. To observe any effect this had on the neuron's response the linear prediction error, Φ, was calculated with Eq. 3.3 where arg max is the maximum linear predictor value for a test input and a modified van Rossum spike

train metric (van Rossum 2001) was used to record the alteration amount.

$$\Phi = \arg\max\left(C_{\text{before}(t)}\right) - \arg\max\left(C_{\text{after}(t)}\right) \tag{3.3}$$

Before we compute the spike train metric we cumulatively sum the spike trains over afferents as in 3.5, where $\mathbf{P_{orig}}$ is the original binary pattern matrix, $\mathbf{P_{perm}}$ is the altered binary pattern matrix and P_{orig} and P_{perm} are resulting vectors of the original and altered matrices.

$$P_{\text{orig}}(t) = \sum_{i=1}^{N_{\text{input}}} \mathbf{P_{orig}}_i(t) \tag{3.4}$$

$$P_{\text{perm}}(t) = \sum_{i=1}^{N_{\text{input}}} \mathbf{P_{perm}}_i(t) \tag{3.5}$$

The van Rossum spike train metric can be computed between P_{orig} and P_{perm} by firstly adding an exponential tail to the spikes—Eq. 3.6a where M is the number of spikes in the original pattern, M' the number in the altered pattern and τ_c is appropriately chosen to take into account coincidence detection and total spike count, cf. van Rossum (2001)—and secondly by calculating the Euclidean distance, Eq. 3.6b. (After pattern alteration, some spikes may no longer be in the pattern hence M and M'.)

$$\begin{aligned} h(t) &= \sum_{i}^{M} P_{\text{orig}}(t - t_i)\, e^{-(t-t_i)/\tau_c} \\ g(t) &= \sum_{i}^{M'} P_{\text{perm}}(t - t_i)\, e^{-(t-t_i)/\tau_c} \end{aligned} \tag{3.6a}$$

$$D^2(h,g)_{\tau_c} = \frac{1}{\tau_c} \int_{t=0}^{\infty} \left[h(t) - g(t)\right]^2 dt \tag{3.6b}$$

Table 3.1: Table of parameters

Parameter	Description	Value
N_{input}	Number of input afferents.	2000
I	Input.	-
I^{in}	Input transmitting the repeated pattern.	-
I^{noise}	Input not transmitting the repeated pattern.	-
dt	Euler-integration time step.	0.1ms
τ_m	Membrane time constant.	10ms
θ	Firing threshold.	1
θ_r	Rise time constant for alpha function.	1ms
θ_f	Fall time constant for alpha function.	5ms
S_r	Rise synaptic current of alpha function.	-
S_f	Fall synaptic current of alpha function.	-
$f(\tau)$	STDP function.	-
τ	Temporal distance between pre- and postsynaptic activity.	-
τ_p	Potentiation time constant for STDP function.	20ms
τ_d	Depression time constant for STDP function.	20ms
A_p	Positive learning rate.	$0.002 \times W_{\text{max}}^{\text{P}}$
A_d	Negative learning rate.	$-A_p \times \left(\frac{\tau_p}{\tau_d}\right) \times \lambda$
λ	Parameter adjusting the proportionality of the learning rates.	1.05
$W_{\text{max}}^{\text{P}}$	Maximum synaptic weight for input afferents.	$1/N_{\text{input}}$
$\mathbf{S}$	The spatio-temporal receptive field.	-
Δ	Binning factor in the implementation of $\mathbf{S}$.	0.1ms
w_i	Weight vector indexed by i.	-
$C(t)$	Linear predictor.	-
I^{test}	Test input spike train.	-
Φ	Linear prediction error.	-
P_{orig}	Original pattern matrix.	-
P_{perm}	Altered pattern matrix.	-
$\mathbf{P_{orig}}$	Original pattern vector.	-
$\mathbf{P_{orig}}$	Altered pattern vector.	-
M	Number of spikes in original pattern.	-
M'	Number of spikes in altered pattern.	-
$h(t)$	Function used in implementation of van Rossum spike train metric.	-
$g(t)$	Function used in implementation of van Rossum spike train metric.	-
D^2	van Rossum spike train metric.	-

3.3 Results

3.3.1 Background activity

During a typical simulation of the spiking neural network, a neuron's responses can be characterised by three temporal phases—first observed by Masquelier et al. (2008). In our simulations the first two phases are identical to (Masquelier et al. 2008) and the third differs; it is the last phase we investigate in more detail in this section. The results suggest that the level of background activity is one feature of stimulus space which a neuron with STDP learns. Moreover, the firing rate of the background activity—consisting of afferents not transmitting the pattern during a pattern presentation and all afferents when not—stays constant (64Hz), as described in the methods, but its effect on the neuron's membrane potential is modulated through the synapses and as these are plastic, the resulting effect can be non-trivial.

Typical background activity

A typical simulation of the spiking model for 1000s is depicted in Fig. 3.1. There are three clear phases within the simulation: (1) when the neuron fires tonically due to high initial synaptic weights; (2) when the neuron has recognised the repeating pattern and reduces its response onset latency to $\approx$10ms; and (3) when the neuron responds near the onset of the pattern but drifts a little increasing the latency.

These results reinforce those of Masquelier et al. *viz.* that a neuron equipped with STDP is able to effectively find and train to the onset of a repeated spatio-temporal pattern embedded within a statistically identical signal. This is not surprising as the mechanism presented by Masquelier et al. is very general. However, Masquelier et al. found that once a neuron had trained to a pattern it had "converged towards a fast and reliable pattern detector" and usually responded at the onset of a pattern. In our simulations we further found that a learnt neuron's response latency appeared to drift backwards through the pattern, as in phase 3 in Fig. 3.1.

To study this drift in more detail, longer simulations (3000s) were run to see how much drift would occur and whether the latency would stabilise—figure 3.2 shows the results of such a simulation. Figure 3.2A depicts a neuron's response onset-latency as a function of simulation

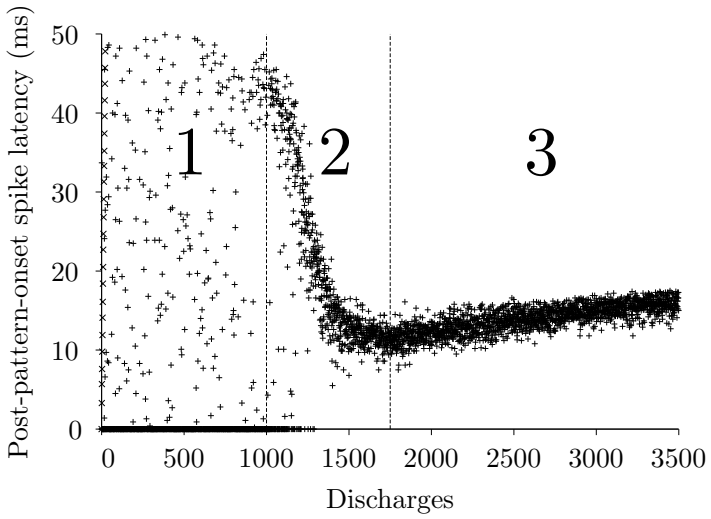

Figure 3.1: Post-pattern-onset latency—relative to the pattern start—as a function of discharges. When the neuron discharges outside of the pattern a latency of 0 is shown. The neuron clearly learns the pattern and has similar periods to those observed by Masquelier et al.: (1) the neuron is non-selective to the pattern and most weights are being depressed due to $\int_{-\infty}^{\infty} f(\tau) < 0$; (2) the neuron is training to the beginning of the pattern; and (3) the neuron consistently fires within the pattern.

time. The phases described earlier are still visible, (albeit compressed due to a change in the independent variable). Notably, the neuron responds as early as 13ms, but saturates at ≈18ms and this backward drift through the pattern has a longer time scale than the second phase.

To elucidate the mechanism behind this slower component, synaptic weight values were recorded every 2s (Figs. 3.2B–E). Weight distributions and trajectories are fairly stable after 1000–2000s and are bimodal (as expected; see Masquelier et al. (2008) and Rubin et al. (2001)). The first phase, when the neuron learns the pattern, can be seen in the weights' distributions and trajectories of afferents transmitting the pattern (Figs. 3.2B and 3.2D): the weights quickly converge to either weight bound. This convergence of weights to the pattern is mostly complete before 250s with very few weights still varying throughout the rest of the simulation. In contrast, synapses not transmitting the pattern take relatively much longer to stabilise— ≈1000–2000s—with some never stabilising (Figs. 3.2C and 3.2E). These non-pattern weights are depressed over this longer period (the desired effect of STDP as they are not transmitting the repeated pattern). The time scale is longer as the neuron is no longer firing tonically and only responds to the pat-

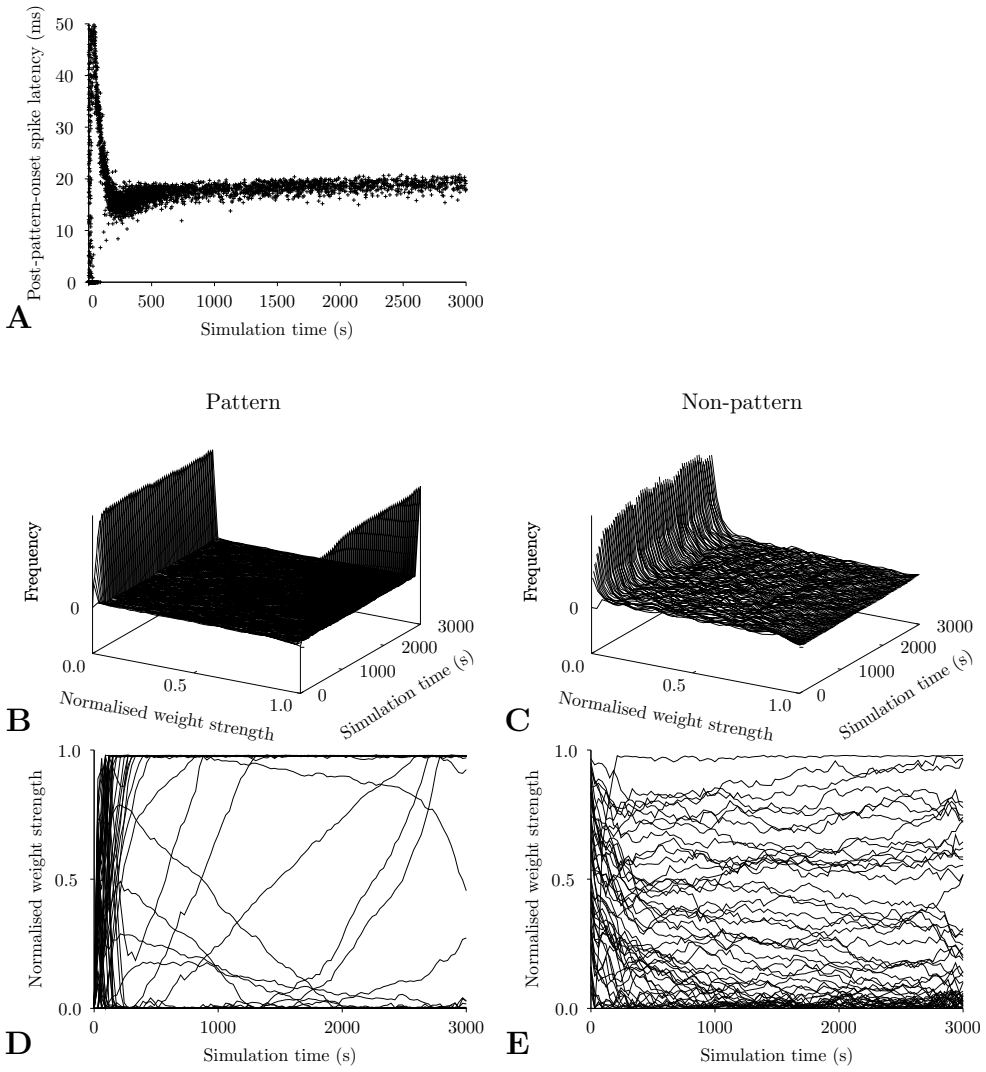

Figure 3.2: Results of a long simulation (3000s) including weight distributions and trajectories. (A) depicts post-pattern-onset discharge latency as a function of simulation time (cf. Fig. 3.1). (B) depicts the evolution of the weight distribution of afferents in the pattern and (C) of those not in the pattern. (D) shows the weight trajectories of 50 afferents in the pattern and (E) 50 of those not in the pattern.

tern and thus the learning is slowed. This longer time scale has a possible side-effect however: the latency drift described above.

Explicitly, during the first phase, the neuron does not fire specifically to the pattern, and thus STDP depresses most weights. This continues until stimulus-driven fluctuations in the neuron's membrane potential facilitate STDP learning (Song et al. 2000; Izhikevich and Desai 2003; Bush et al. 2010): phase two. These fluctuations are based on a background activity level consisting of the activity of the synaptic weights of *all* afferents at *that time* (≈200–250ms). We hypothesised that it was this level of background activity and the subsequent change in this level that causes the drift.

Artificial change in background activity *after* learning

To test this hypothesis, an additional constant electrical current was applied to the output neuron after it had learnt a pattern and remained present for the rest of the simulation. This additional constant is analogous to raising the level of background activity. (We chose to inject current into the neuron instead of raising the background activity level through the afferents as the first guarantees a set effective amount.)

If a trained neuron learns a short succession of coincidences, as has been postulated before (Masquelier et al. 2008), it may have little if any reliance on the background activity. Therefore, our constant current—if small relative to the membrane potential range—should not disturb the neuron's response latency; figure 3.3 shows the results of such an experiment.

When constant current is applied to the neuron at 2000s there is a significant change in weights (Fig. 3.3B–E). Moreover, Fig. 3.3A shows a significant change in the neuron's firing latency during this additional current: the latency is reduced. Interestingly the neuron's latency then drifts again. The synapses are plastic for the entirety of the simulation.

An analysis of the weight distributions and trajectories from 2000s onwards helps to postulate as to the cause of this second drift: some afferents which convey the pattern change their efficacy significantly—either going from 0 to $W_{\max}$ or vice-versa. Accompanying these changes is a reduction in weights for afferents not conveying the pattern—similar to the initial training

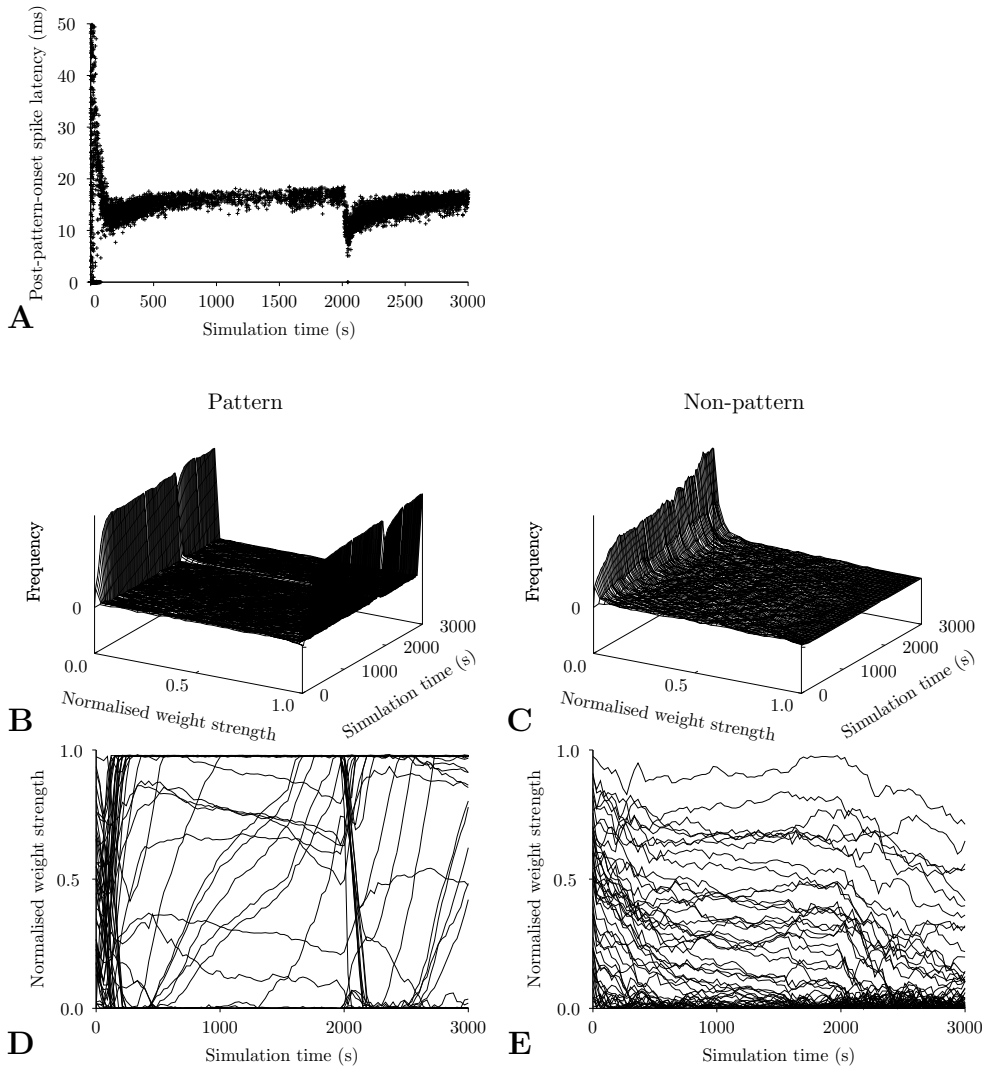

Figure 3.3: Results of a long simulation (3000s) with an additional injection of constant electrical current at 2000s. (A) clearly shows a decrease in latency at the current onset; the latency then increases and levels off. As with Fig. 3.2, weight distributions (B and C) and weight trajectories (D and E) were recorded every 2s.

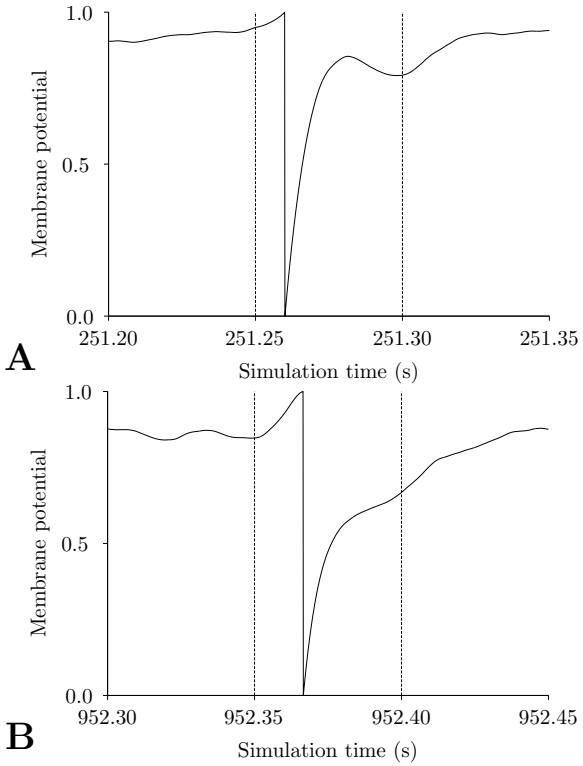

Figure 3.4: A neuron's membrane potential depicting a lower background activity and consequently a longer integration time. (A) reaches threshold with a latency of ≈10ms, whereas (B), with ≈15ms due to level of membrane potential being lower before pattern presentation (dotted lines). Patterns started at 251.25s and 952.35s.

phases. We suggest the neuron is adjusting to its new background activity.

To further clarify the reliance on background activity, Fig. 3.4 depicts a neuron's membrane potential during two different presentations of a pattern in a simulation. Figure 3.4A is just after the neuron has trained to the pattern, and Fig. 3.4B is later in the simulation. One would expect the background activity—and thus the membrane potential—to be higher just after learning than after some drift because the background activity is continuously decreasing due to non-pattern weights being depressed. We found that the level of membrane potential is higher before pattern presentation (dashed lines) just after learning, Fig. 3.4A, than after some drift has occurred, Fig. 3.4B.

To summarise, if during the second phase the neuron learns to respond at t, the neuron is sensitive to coincident spikes in a window ranging from about $t - \tau_m$ to t. Ideally the neuron should

respond at t because there is some background activity present before the window and the neuron's membrane potential is near threshold allowing the activity in the window to contribute to reaching threshold. However, if the initial activity before the window is reduced the neuron may not respond until $t + x$ where x is the extra time required to temporally sum the activity, as in Fig. 3.4. These results suggest that during the drift and after the latency has stabilised the neuron is still sensitive to the onset of the pattern, however, the background activity modulates the neuron's response latency.

Artificial change in background activity *during* learning

Next we questioned what happens when the level of background activity is modulated *during* learning. To this point, neurons trained to the beginning of the pattern, however if Gaussian white noise with positive mean is added directly to a neuron's membrane potential at every dt, this is no longer the case. Figure 3.5 depicts two typical results with noise (both with μ=0.05 and σ=0.013): in Fig. 3.5A the shortest latency is $\approx$20ms, and in Fig. 3.5B it is $\approx$38ms. It appears the noise interferes with the learning phase (Fig. 3.1). In fact, with noise we found that a neuron's learnt latency varied greatly, Fig. 3.6; increasing amounts of noise changed the distribution of learnt response latencies.

Depicted in figure 3.6A are learnt response latency distributions for simulations with different amounts of noise added to a neuron learning a 50ms long pattern. Initially, with no or little noise the neurons respond near the onset (Fig. 3.6A). However, as the noise amount increases the neurons stop responding near the onset and respond later and later in the pattern. To test whether this was an artefact of a pattern with length 50ms, we also tried adding varying amounts of noise to patterns of length 75 and 100ms (Fig. 3.6B): we found the noise's effect was independent of pattern length.

Further, we fitted right censored gamma distributions to the response latency distributions. The peaks of these distributions are shown in figure 3.7A and show a general result, *viz.* that an increase in noise disrupts the neuron's ability to train to the beginning of the pattern and the peak latency drifts backwards through the pattern. In addition, there is a negative side effect of this additional noise: a drop in learning performance. Figure 3.7B depicts a major drop in

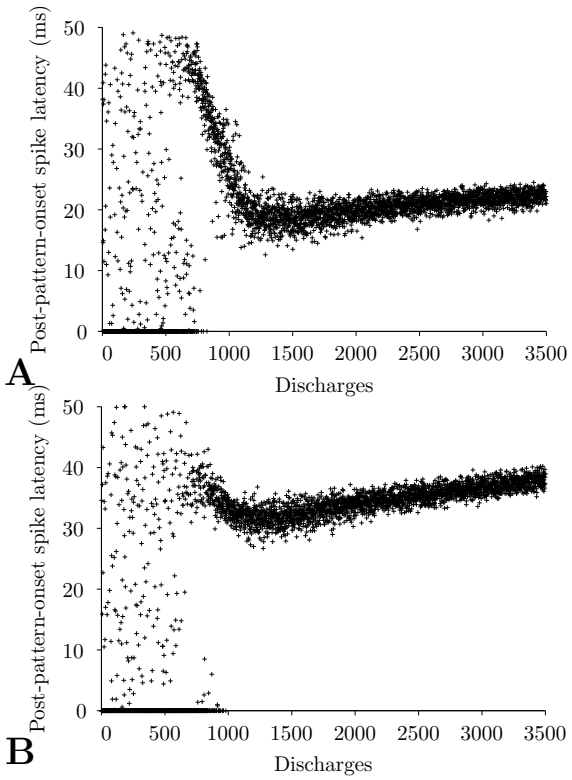

Figure 3.5: Raster plots of different trials when Gaussian noise (μ=0.05 and σ=0.013) is added directly to the membrane potential at every dt. In the two trials the neurons learn to different temporal positions within their patterns.

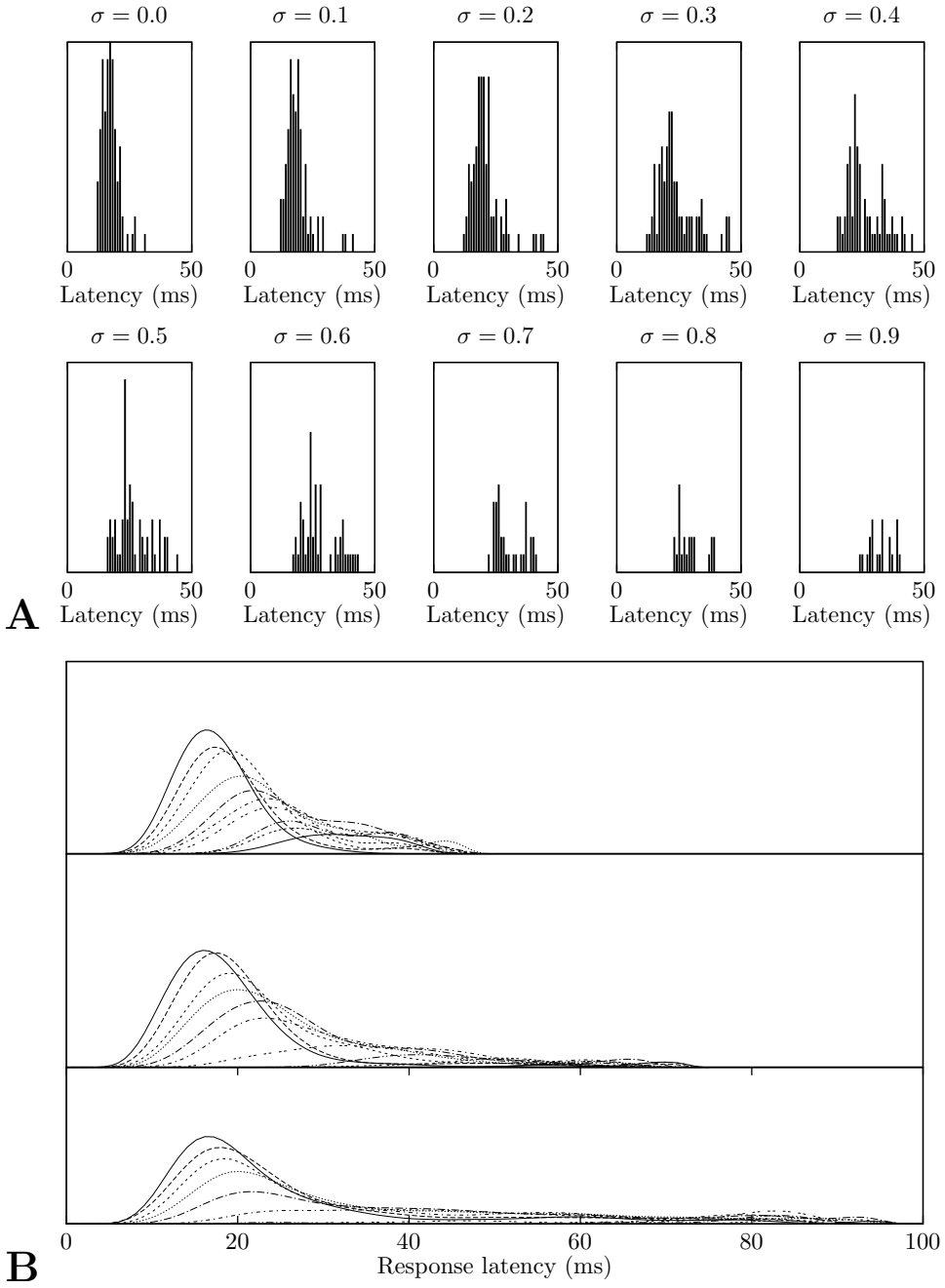

Figure 3.6: When additional noise is added, the response latency distributions are affected (N=100). (A) Response latency distributions for varying amounts of background noise (from σ=0.0 to σ=0.9; all with μ=0.05) for a pattern of length 50ms. (B) Fitted Bezier curves to response latency distributions for patterns of length 50, 75 and 100ms.

performance for larger values of σ. Specifically for σ=0.9, performance drops to just below 20% for 50ms patterns, $\approx$ 3% for 75ms and does not learn a 100ms pattern at all.

Masquelier et al. (2008) also noted that the final learnt latency may not be at the onset of the pattern and suggest this might be due to a zone of low spike density. We postulate that adding extra noise to a neuron increases the likeliness that the neuron stops during one of these low spike density zones, however also reduces its ability to learn the pattern at all with high amounts of noise.

3.3.2 Stimulus spike features

The level of background activity described hereto does not alone allow a neuron to learn to fire specifically at the onset of a pattern—it merely increases a neuron's sensitivity to smaller inputs via a raised membrane potential consequently adjusting a learnt neuron's response latency; therefore we subsequently investigated what additional features in input space are learnt: spike-counts, spike-order, spike-timing etc. Specifically, we found that spike-timings within the pattern are further learnt by neuron's with STDP and allow a neuron to become sensitive to a specific segment of the stimulus.

To facilitate our investigation into the input space we used linear prediction. Firstly, we tested the linear predictor's ability to predict the output neuron's activity with the original pattern used during the learning. If the linear predictor predicts a neuron's activity accurately there should be a peak in $C(t)$ at approximately the same time in the pattern as the neuron spikes. Results are shown in Fig. 3.8, where (A) is the original neuron's behaviour during the simulation, (B) is the prediction with the original pattern and (C) is the STRF: there is a peak in the value of the linear predictor at the learnt latency.

Spike-count, spike-order or spike-timing

As the linear predictor accurately mimics a neurons activity (membrane potential excluding action potentials) from our spiking model, it can be used to elucidate whether, and if so, what, spike features are crucial for a neuron to learn a segment of the repeated pattern. If we take a neuron that has learnt to fire at the onset of the pattern (13ms) and swap the first 25ms (half)

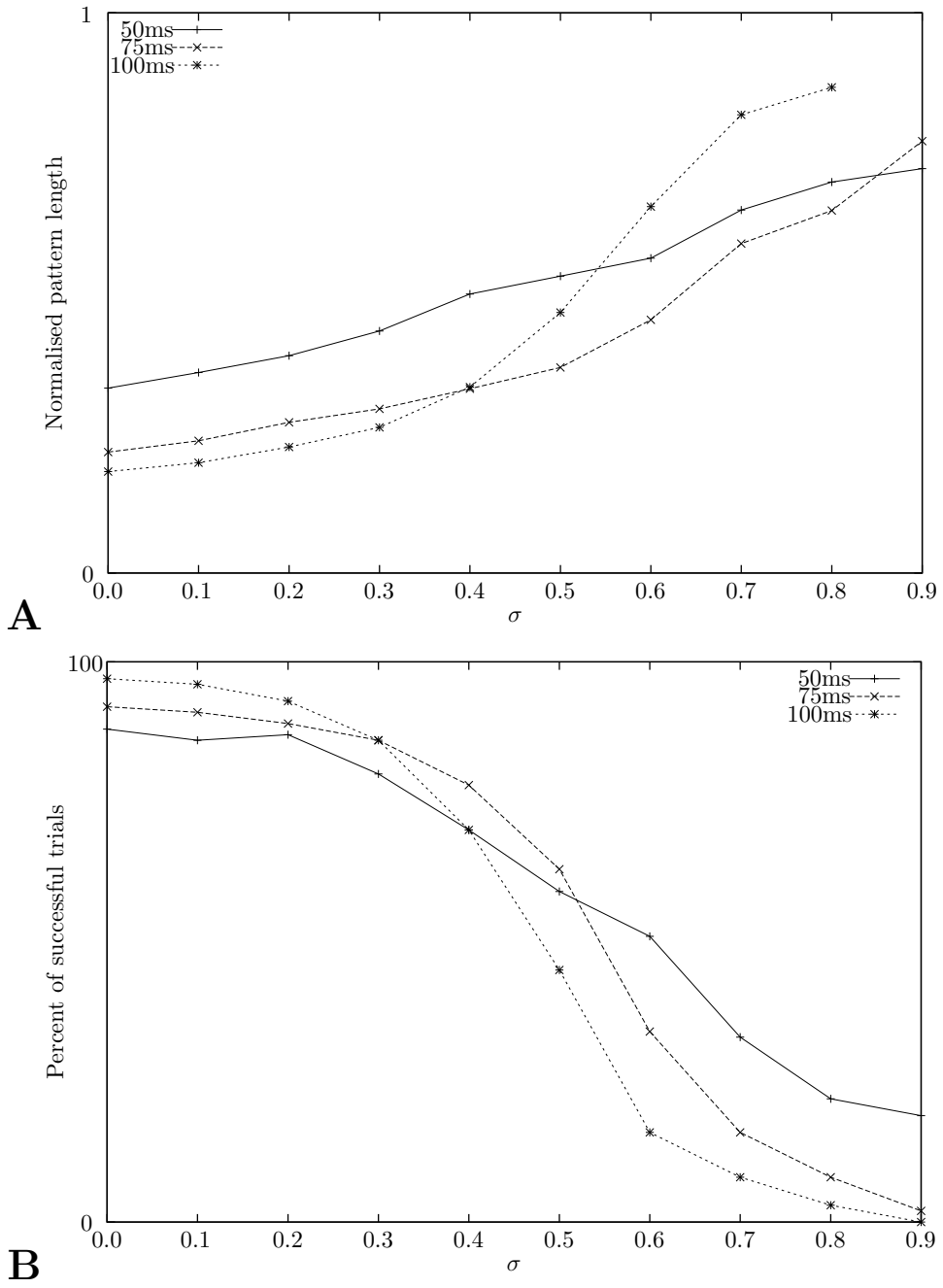

Figure 3.7: Adding increasing amounts of noise not only disrupts the response latency distribution but also produces a drop in performance. (A) The peak of fitted right censored gamma distributions and (B) the learning performance.

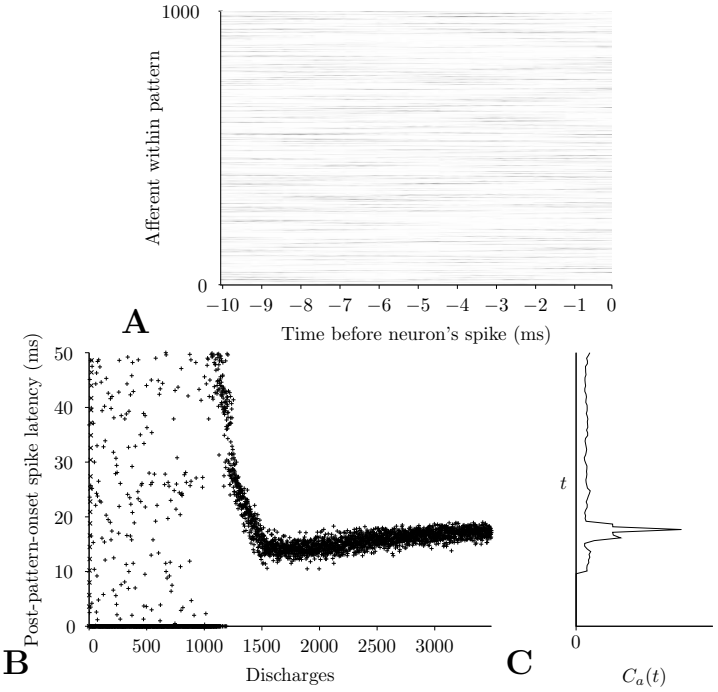

Figure 3.8: Typical results using linear prediction. The STRF (A) shows the average position of input spikes preceding a response. (B) depicts the progress of learning as previously described. The response latency after learning is approximately 18ms (B). When the linear predictor was tested with the original pattern used during training (C), $C(t)$ peaks at the same response latency as the spiking neural model confirming that the linear predictor is replicating the spiking model.

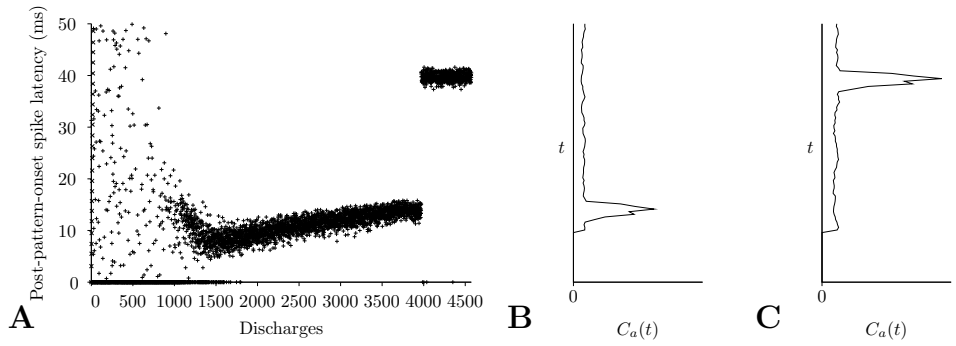

Figure 3.9: Typical results before and after swapping two halves of a pattern at 4000s. The neuron's activity (A) shows the point where the pattern was flipped. Specifically, before swapping the neuron responds with a latency of approximately 15ms, and after swapping the latency increases to 40ms. This change in latency is mirrored by the linear predictor (B and C) by peaks in $C(t)$.

with the second 25ms, and vice-versa, the order of the spikes and timings within the learnt segment (now 28ms–38ms) are identical, therefore the linear predictor should be identical for the old and new positions: see Fig. 3.9 for an example. Such an experiment was also carried out with the spiking model (flipped after ≈4000 discharges in Fig. 3.9A)—the neuron responds as expected. Note that a very small amount of extra current (injected into the neuron) was needed to evoke the spikes after the flipping; we postulate this is due to a change in background activity as described before.

If the pattern is mirrored however—that is, temporally mirroring the pattern—the neuron no longer responds in the mirrored pattern; see Fig. 3.10 for an example. This is also reflected in the reduced result from the linear predictor. Extra input was also injected as with flipping the pattern, however this did not help evoke spikes at the reversed position; instead, the neuron started to fire unmeaningfully again, hence the spikes registered at 0ms.

To understand these results one must consider the different features which are available to the neuron. In the mirrored pattern, the learnt segment is at the end of the pattern (in the case in Fig. 3.10, 35ms–45ms), and the spike count within these 10ms is identical to the original pattern. The lack of response from the neuron with the mirrored pattern suggests that the spike count is not the determining feature: perhaps spike-order or spike-timing is?

If spike-order is important for a neuron to learn a repeated pattern, it is possible that spike-order

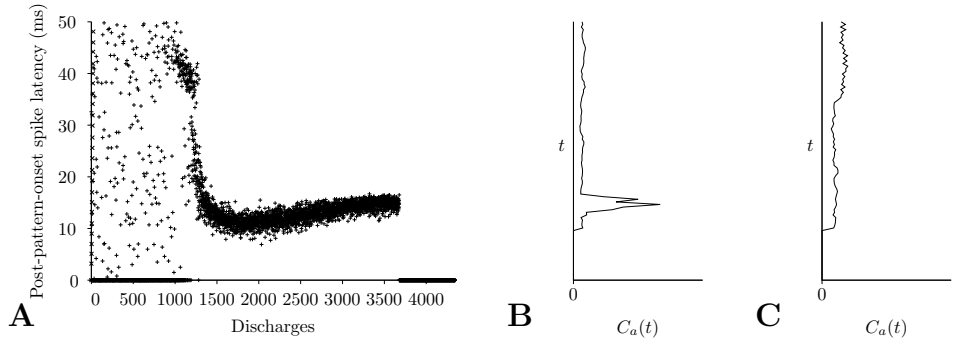

Figure 3.10: Typical results before and after mirroring a pattern at 4000s. The neuron's activity (A) shows the point where the pattern was mirrored and the neuron no longer responded. Specifically, before mirroring the neuron responded at approximately 13ms and after mirroring only responded outside the pattern. This is replicated in the linear predictor (B before and C after): before mirroring there is a peak in $C(t)$ however afterwards there is no peak and $C(t)$ stays low throughout.

will be correlated with synaptic weight. For example, if a neuron responds with a pattern onset latency of ≈15ms, spikes presented at 5ms could be strengthened more than those at 10ms, or vice-versa. Furthermore, if this were the case, the linear predictor we use would reflect this because spike-order is preserved in the STRF.

We tested this hypothesis and found that there was no correlation between spike-order and synaptic weight. In the example in figure 3.11, the neuron would respond with a pattern onset latency of ≈15ms. We therefore depict the time of pattern spikes which are presented between 0ms and 15ms, with their corresponding afferents' synaptic weights. There are two clusters of synaptic weights: one near zero, and the other near the upper maximum synaptic weight bound ($W^{\mathrm{P}}_{\mathrm{max}}$). This result is supported by the typical bimodal synaptic weight distribution for learning with additive STDP, such as that used in this chapter. The lack of correlation suggests that spike-order is not a feature a neuron with STDP uses when learning a repeated spatio-temporal pattern.

We therefore next studied spike-timing. We carried out an experiment where different window widths between 1 and 20ms were temporally moved through the pattern and only spikes within this window were jittered (±5ms). More specifically a window of 10ms would include spikes from 1ms to 10ms in the pattern initially. Only spikes within this window are jittered and the

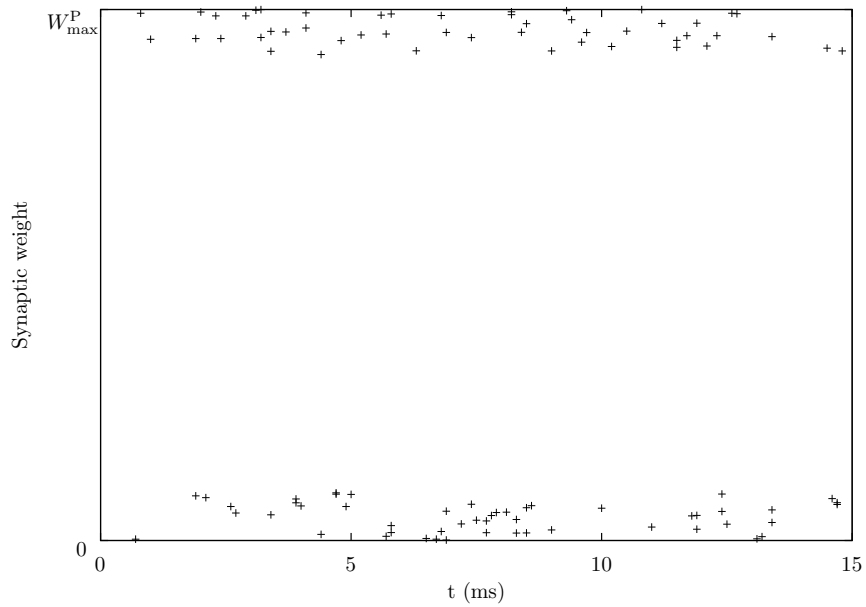

Figure 3.11: Spike-order and synaptic weight. In this example, the neuron will respond at ≈15ms. Therefore, we consider the order of spikes within the pattern from 0ms to 15ms (x-axis). The synaptic weight for each spike's corresponding afferent is also included (y-axis). There are two clusters, which correspond to the bimodal synaptic weight distribution: approximately half of the spikes' afferents have synaptic weights near zero, while the other half have synaptic weights near the upper maximum synaptic weight bound (W^{P}_{max}). There is no correlation between spike-order and synaptic weight.

Trial	Mean firing (ms)	Window of greatest error (ms)
1	13.7	5–15
2	17.0	8–18
3	20.1	11–21
4	16.7	7–17
5	17.2	8–18
6	14.4	5–15
7	15.9	7–17
8	14.8	6–16

Table 3.2: Results of jittering spikes ±5ms within a 10ms window where 'mean firing' is the recorded mean firing position of the neuron on a respective trial of the last 100 discharges, and 'window of greatest error' is the 10ms window that produced the biggest error

effect recorded. Next, this window is moved through the pattern in dt=0.1ms increments so the window will next include spikes from 1.1ms to 10.1ms and subsequently 1.2ms to 10.2ms. This was done with the various window widths noted above.

Logically one would expect that the linear predictor would be lowest when spikes before the temporal position of the learnt output neuron's response are changed, with less of an effect apparent for jitter elsewhere (especially after the discharge position as the spikes there should have no effect on when and/or if the neuron is to fire, unlike those immediately preceding the discharge). Results of this experiment are in table 3.2, where 'mean firing' is the recorded mean firing position of the neuron on a respective trial of the last 100 discharges, and 'window of greatest error' is the 10ms window that produced the biggest error (cf. section 3.2.2). Only the results from jittering spikes in a 10ms window is included herein as this had the greatest effect ($>$ 10 had an equal effect) and as τ_m=10ms. The results suggest that, as expected, the 10ms before the neuron's response latency are important, and crucially, jittering spike-times can be destructive.

Spike-timing tolerance

It appears that spike-timing is an important feature in stimulus space which allows for a neuron's sensitivity to a subset of a repeated pattern. To further understand what the STDP synapses are becoming sensitive to, spikes within the 10ms window before a neuron's response latency were jittered by varying amounts to find the spike-timing temporal tolerance of a neuron with its

respective pattern. Furthermore, a spike train metric was used to measure the amount of change in the stimulus and the linear prediction error (Φ) was used to gauge the erosive effect of the alterations.

Typical results of this experiment are shown in Fig. 3.12: (A) shows the mean linear prediction error (N=10) when spikes—on different numbers of afferents—are jittered by varying amounts and (C) the squared spike train distance between the original and altered patterns. The effect of jittering spikes is non-linear—error increases steeply with jitter amount and then plateaus; in contrast, error grows linearly with the number of afferents altered. Interestingly, we also found that some small jitters increased the linear prediction, suggesting that a neuron's learnt STRF is not always optimal.

Furthermore, returning to our spiking model and by just adjusting the jitter amount and keeping the number of afferents altered constant, we found a critical jitter amount which resulted in the neuron no longer firing. This was because the spike jitter prevented the neuron from reaching threshold. It was possible, however, to recover the neuron's correct response by adding an additional constant current. This increased the neuron's membrane potential to threshold. Another boundary was also found where a neuron stopped responding only within a pattern even if additional constant current was added to help the neuron reach threshold. In this case, when additional current was added, the neuron responded not only within the pattern but also outside the pattern at random times due to fluctuations in the membrane potential not stimulated by the pattern. These error boundaries form three parameter regions: Φ_α, Φ_β and Φ_γ. These are included in Fig. 3.12(A). In Fig. 3.12(B); cartoon membrane potentials are also included for each region.

We then tested the proposed segmentation of the parameter space with three experiments using the spiking model with adjustments to both jitter amount and number of afferents altered. When spikes on 300 afferents were jittered by 5ms the neuron still responded; when spikes on 500 afferents were jittered by 10ms the neuron no longer responded on its own but responded with additional input; and when spikes on 800 afferents were jittered by 20ms the neuron no longer responded informatively even with additional input.

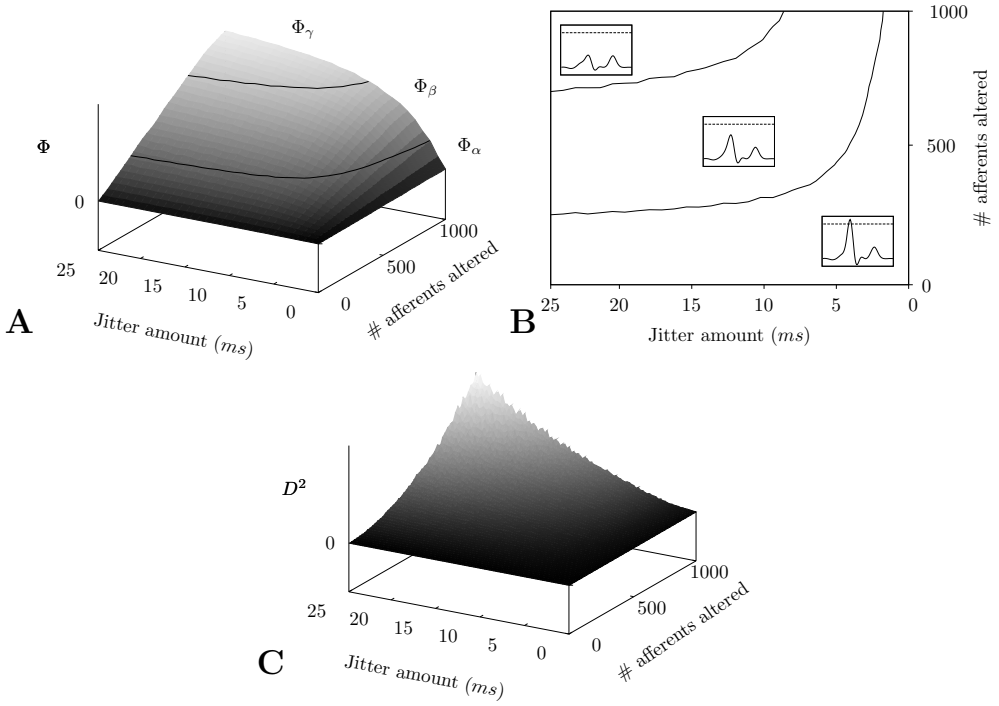

Figure 3.12: Results of jittering spikes on a varying number of afferents by varying jitter amounts. (A) shows the linear prediction error (Φ) as a function of jitter amount and number of afferents altered. When Φ increases it signifies a decrease in $C(t)$ and therefore implies a lower chance that a neuron will not respond to input correctly (either with an increased stimulus onset latency or not at all). As we increased the amount of temporal jitter the effect on Φ was non-linear; specifically, small amounts of jitter greatly increased Φ however once the jitter amounts were greater than 10ms, Φ increased more slowly. When we adjusted the number of afferents that were altered by this jittering the effect on Φ was linear.
We tested various sets of parameters from (A) with the spiking model and were able to further split the space in to three sub-spaces: Φ_α, Φ_β and Φ_γ. While in Φ_α, the spiking neuron responded correctly. But when the spiking neuron was tested with parameters from Φ_β additional current was required to permit the neuron to reach threshold. Further, this additional current no longer successfully worked with the jitter amounts and number of afferents altered in Φ_γ and the neuron was no longer able to respond correctly.
(B) is a contour plot of (A). (C) is the squared spike train distance between the original and altered patterns. Furthermore, (B) includes cartoons of membrane potentials.

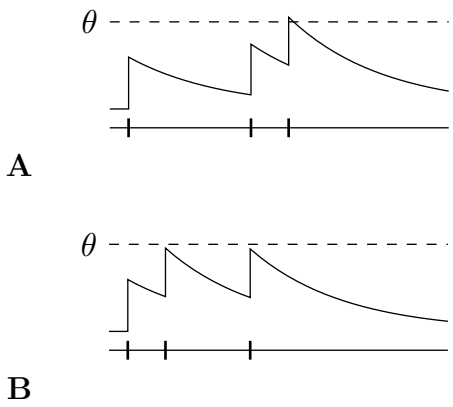

Figure 3.13: The leak current's effect on input integration. Two results of a singular neuron, with one afferent, integrating three input spikes. In (A) the three spikes are sufficient to integrate to threshold, however when they are jittered, as in (B), they are no longer sufficient even though the spikes occur over a shorter time span.

Finally, figure 3.13 depicts two results of a singular neuron's membrane potential, with only one afferent, integrating three spikes. In (A), the three spikes are sufficient to integrate to threshold, however in (B), these spikes are jittered and the input is no longer sufficient to reach threshold. This is the case even though the spikes in (B) occur over a shorter time span. This proof of principle demonstrates that the leak current present during inter-spike intervals can affect how latter input spikes are integrated and consequently affect a neuron's ability to produce an action potential.

Furthermore, the distribution of, below threshold (θ=1), membrane potential peaks is approximated by the left hand side of a Gaussian distribution: see figure 3.14. To produce this distribution, we recorded the peak value of a neuron's membrane potential during a pattern presentation if it did not respond. The distribution of peak membrane potentials spans from neuronal firing threshold to 0.85. The lower values, near 0.85, correspond to the background activity level (see Fig. 3.4).

Further work is needed to elucidate fully the mechanism behind how spike-timing is learnt by a neuron, however it appears that a neuron's leak current could be partly responsible. Essentially, a reduction of a neuron's membrane potential either due to a reduced background activity

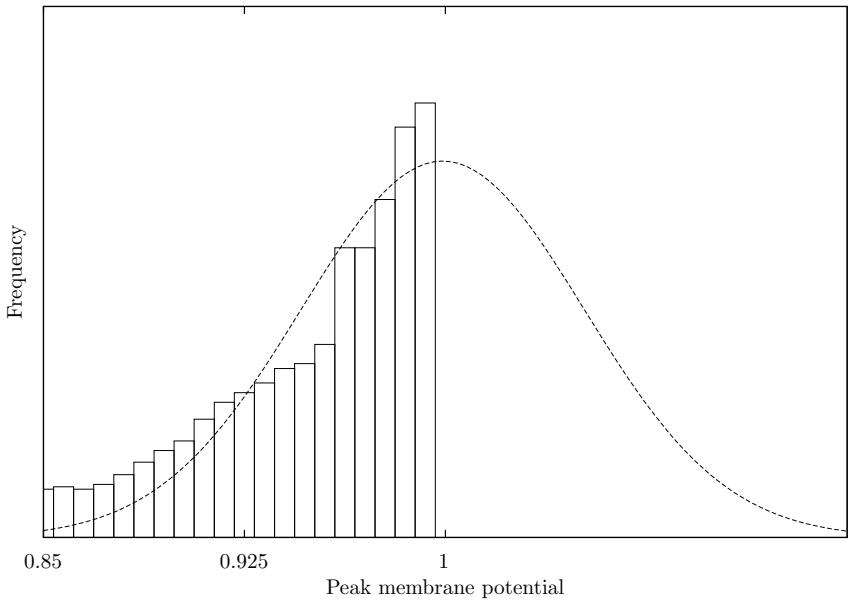

Figure 3.14: Below threshold peak membrane potential distribution. Peak values of a neuron's membrane potential was recorded for cases where the neuron did not respond to a pattern presentation (where the membrane potential was less than threshold, θ=1). The distribution is approximated by a the left hand side of a Gaussian distribution with, μ=0.99 and σ=0.35.

(Fig. 3.4) or a change in spike-timing (possible due to leak currents Fig. 3.13) can affect whether, and with what latency, a neuron responds.

3.4 Discussion

Firstly, we presented results that reconfirm the findings by Masquelier et al. (2008); even though we used a different STDP window and different learning rates, a neuron with STDP was able to distinguish a repeated pattern from random background activity, learn it and fire consistently within it. The main topic for this chapter however was our proposed question, what does this neuron learn? Using a combination of a spiking neuron model and linear prediction we found that a neuron learns both the level of background activity and spike timing of a pattern.

Using the spiking model, we found that with long simulations the latency of a learnt neuron's response increased with respect to the beginning of the pattern and saturated at a later time. (It is not clear if Masquelier et al. (2008) ran their simulations for longer than 450s or whether

they found this drift.) We demonstrated that the drift is due to two components: fast learning of the pattern and relatively slower unlearning of background activity. Specifically, STDP initially modifies afferents' weights which are transmitting the stimulus, promptly (within 250s) stabilising appropriate weights at either bound. Then remaining weights are depressed on a longer time scale (within 1000–2000s). This second longer time scale adjusts the level of background activity, and we hypothesised that this caused our observed drift. We verified this hypothesis and found that an artificial change in the level of background activity can change the response latency. Moreover, we found that the tuning of the pattern detector towards the pattern onset is unstable against noise: with increasing levels of background noise, the learnt latency increased.

We inferred from these results that the level of background activity is a feature that a neuron with STDP uses to learn a repeated pattern: it raises the membrane potential to near threshold so a presentation of the repeated pattern can evoke a response. Therefore, a change in the learnt level affects a neuron's responses. However, this did not fully answer our question. To expose any spike-count or spike-timing reliance we used linear prediction.

Using linear prediction we altered the spikes of the stimulus and observed the result: we found that neither spike-count nor spike-order are important features, however spike-timing is. Jitter of just $\pm$2ms significantly impacted the postsynaptic neuron's response. Masquelier (2008) also previously found that a small amount of jitter (3ms) degraded the ability of a neuron to learn a pattern. We extended these results and found that the effect on the linear predictor is non-linear with spike-timing jitter, and linear with an increase in the number of afferents affected. Our results suggest that spike timing is another feature that a neuron with STDP uses to learn a repeated pattern. Further, we found that a neuron's leak current is crucial to spike-timing, however, further work is needed to fully elucidate the mechanism behind the learning of spike-timing.

It must be noted that the results presented in this chapter and their conclusions only apply to leaky-integrate-and-fire neurons under the protocol of an input consisting of a constant firing rate. It is plausible that other neuron models, conductance based for example, may react differently to the stimulus, and therefore may result in a neuron with STDP learning different

features of stimuli. Furthermore, the results we present are applicable to unsupervised learning only; possible limits of supervised learning with STDP have been previously studied by Legenstein et al. (2005). It is also possible that a pattern embedded in a modulating firing rate stimulus may be learnt differently.

3.4.1 Functional consequences

We have adduced that different stimulus features are learnt by a neuron, so it is pertinent to consider their functional consequences. For example, it would be advantageous for resources if synapses which are depressed—and determined not to carry information—were eliminated. However if this was to occur, our results predict that a neuron may either not fire at all or fire with a much greater latency due to the reduction in background activity. Furthermore, even *after* learning a stationary patten, a neuron's ability to respond to the pattern may drop sharply with spike timing permutations of ≈2–3ms, even if only a relatively few number of spikes are changed. However, researchers have commented that the vast amount of input typically found on neurons may take part in many beneficial mechanisms (Shu et al. 2003; Bernander et al. 1991; Hirsch et al. 1998). Bernander et al. (1991) for example, found that as background firing rate increases, a neuron's ability to act as a coincidence detector also increases. Furthermore, Hô et al. (2000) postulated that background activity keeps a neuron in a highly responsive state, which our results support: the background activity allows the detection of normally sub-threshold activity, *viz.* the relatively smaller subset of learnt synapses presenting a pattern. Wolfart et al. (2005) further postulated that their results support an idea that the control of information transfer could be through a change in background activity intensity. It seems that these two mechanisms are crucial for pattern learning with STDP within the protocol used in this study.

Chapter 4

Sequence learning

4.1 Introduction

Synfire chains are a possible mechanism proposed to reproduce observed delays *in vivo*. They consist of feed-forwardly connected populations of cells. Activity propagates from population to population in a synchronous manner which can be shown to be a stable and precise process when the compound post-synaptic potential caused by neurons in one population converging in the next population is significantly larger than the noise level (Abeles 1991; Wennekers 2000; Wennekers and Palm 1996). As activity can travel through a synfire chain in the same manner many times, the delay between two neurons along the chain is fixed, as observed originally in the experimental recordings. Abeles' synfire chain model has homogeneous axonal delays between populations, an assumption that can be relaxed to include an axonal delay distribution. Connections may then straddle intermediate populations. Such a set-up was called a "synfire braid" by Bienenstock (1995). Izhikevich (2006) has shown that similar connectivity and activation patterns (called "polychronous waves") can be generated in networks of spiking neurons as a result of random excitation and a learning rule that depends on pre- and post-synaptic spike-times (STDP, "spike-timing-dependent plasticity", cf., (Bi and Poo 1998; Morrison et al. 2008)).

Experimental support for synfire chains is difficult to obtain as one needs to simultaneously record from many neurons at once in order to find correlated pairs. Current techniques are limited to record from up to a few 100 sparsely located neurons and are at best able to record a few neurons from a chain. Nevertheless, precisely repeating firing patterns have been observed (Prut et al. 1998; Nádasdy et al. 1999; Ikegaya et al. 2004). For example, Ikegaya et al. (2004) describe precise repetitions of spontaneous patterns in neocortical neurons *in vivo* and *in vitro* and Nádasdy et al. (1999) found repeating spike sequences in awake and asleep rat hippocampus. It has further been shown that sequences can be related to a monkey's behaviour (Prut et al. 1998; Shmiel and Drori 2006). Prut et al. (1998) observed both (1) precise firing sequences in cortical activity which spanned hundreds of milliseconds and (2) their correlation with animal behaviour in one study. Hahnloser et al. (2002) also reported repeating spike-patterns in the song-system of birds that are clearly related to syllable generation. More recently, Ayzenshtat

et al. (2010) described spatio-temporal patterns within and across early visual areas that contained enough information to reliably discriminate between stimulus categories. Some of these findings, however, have been challenged. For example Mokeichev et al. (2007) re-examined the observation of repeating spontaneous patterns and suggest that they may not be significant but appear by chance. Furthermore, even though the precisely repeating firing patterns could be the result of synfire chains, these patterns do not ultimately prove the existence of synfire chains.

A question following these ideas is "how can synfire chains form?". Early attempts to derive them in neural networks subject to some kind of self-organisation have been moderately successful. Bienenstock and Doursat (1991), for example, reported that exciting neurons synchronously in a random network could lead to the formation of synfire chains. Another study by Hertz and Prugel-Bennett (1996) also attempted to learn synfire chains in random networks but found that closed loops formed. These loops are a problem as once activity enters a loop it never exits again; consequently, activity may never propagate fully through a synfire chain. In these studies, the total synaptic strength for a neuron's efferent synapses was limited; if this was not the case, connections would strengthen uncontrollably. A more recent study by Izhikevich (2006) used STDP in spiking neuron networks subject to unspecific random excitation. In these very large scale simulations complex recurrently connected web-like structures of specific synaptic pathways formed that carried repeating "polychronous waves" with many properties of synfire chains, but a broad distribution of possible delays between neurons. In the more abstract set-up of Markov chains, Wennekers and Ay (2003) also demonstrated the formation of web-like nested transition structures in the joint state space of N units using timing-dependent plasticity. These transition structures could be linked to finite state automata (Wennekers and Ay 2005) which suggests that they could be employed for neural state-based computations. An alternative hypothesis for computing with polychronous waves has been suggested by Izhikevich (2009).

In this chapter we took a different approach to learn synfire chains assuming that they may not form autonomously in a network, but rather by spatio-temporal driving activity which may come from other areas or the sensory surfaces. Repeated inputs could cause their target neurons to

learn a specific firing pattern. Essentially, we attempted to recognise a repeated spatio-temporal pattern with a sequence of neurons. When successful, several neurons respond one after the other, each recognising a segment of the input pattern. The learning of short repeated spatio-temporal patterns has been studied and analysed previously (Masquelier et al. 2008, 2009; Humble et al. 2010) in chapter 3. It has been shown that a neuron with STDP is able to learn and respond to the beginning of a repeated spatio-temporal pattern even when it is embedded in a statistically identical carrier signal. Furthermore, Masquelier et al. (2009) reported that if, instead of one neuron, several neurons are competing for the ability to respond and learn the pattern, they each learn a segment of the pattern. When inspecting the whole learnt pattern, however, a limitation becomes apparent: each neuron is responding to a unique learnt segment of the input regardless of when it appears. Therefore one could take an input pattern, switch the segments around, and the same neurons in the trained network would fire, albeit in a different order. We therefore were interested in whether it was possible to learn the order of the responses. If so, the network would learn to recognise a spatio-temporal input pattern in such a way that a chain of activity in the trained network would only propagate if a specific spatio-temporal input pattern supported it from the beginning to its end.

To learn temporal order, it seems natural to introduce plastic lateral connections which reinforce and prime a subsequent neuron's firing. A neuron will then not only rely on the input pattern but also on previously responding neurons. We found that by including lateral connections with STDP the model could learn the order of neural firing activity and it was possible to have an 'accepting neuron' that only responded if a learnt pattern was presented fully, thereby signalling when the whole pattern was contained in the input stream.

Such a set-up is analogous to finite state automata where an accepting state is reached only if previous states are transitioned correctly. The currently firing neurons represent "the state" of a recogniser for the input pattern and the momentary inputs act as "symbols" that drive the recogniser through its states. If at the end of the input the final neurons of the synfire chain fire, this signifies that the sequence of input symbols has been recognised correctly. This is functionally a simple finite state automaton with no loops in the transition graph. In Wennekers

and Palm (2007) and Wennekers (2006) the authors argued how more complex neural systems of this sort can be systematically constructed.

In the present work we take a step towards algorithms that can learn spiking neuron automata with accepting states/neurons. We present a learning scenario whereby a biologically based learning rule learns temporal sequences comprised of several neurons firing one after another. Furthermore, we find that by using plastic lateral connections our network's neurons can learn to respond only when temporally appropriate. This differs from previous work such as that of Masquelier et al. (2009; 2010) and the previous chapter because we include plastic lateral connections.

The chapter is organised as follows. The next section introduces distinct methods from those described earlier. Section 4.3 presents the main results split into several subsections. At first, proof-of-concept simulations for sequence learning and recognition are given followed by some analyses of parameter dependences. It is then shown that previously learnt chains can be sequenced into longer chains. It is argued that learnt chains contain a high amount of information and a certain robustness against variations in the speed of stimuli. Factors that limit robustness and memory capacities are discussed. The discussion section finally puts the results into a wider context and outlines their relevance for state-based neural computing architectures.

4.2 Methods

4.2.1 Network structure and setup

The research presented in this chapter uses an extension of that presented in common methods. See table 4.1 for a table of parameters for this chapter.

The network comprised N=20 excitatory neurons with one inhibitory neuron providing winner-takes-all competition: see Fig. 4.1. The size of N can be small, if only short sequences are to be learned. The excitatory neurons were laterally connected to all other excitatory neurons with synapses that were plastic throughout a simulation. The input synapses, J^{in} and J^{noise}, and lateral synapses, J^{lat}, are plastic for the duration of the simulation.

The inhibitory neuron was an integrate and fire neuron with the same parameters as the exci-

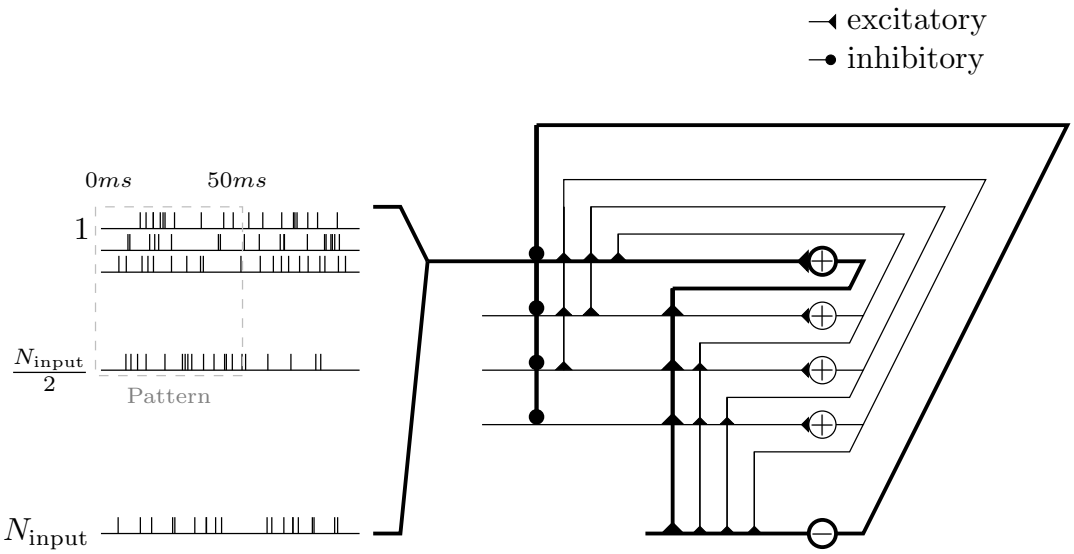

Figure 4.1: Network structure with several excitatory neurons (+) and one inhibitory neuron (−) with corresponding excitatory (triangle) and inhibitory (circle) synapses. Excitatory neurons are connected to one another with plastic mutual connections. They are in competition with each other via the one inhibitory neuron. Each excitatory neuron receives input consisting of a total of N_{input}=2000 afferents. Half of these alternate between presenting a repeated spatio-temporal pattern (for 50ms) and Poisson input (for at least 50ms). The other half continuously present Poisson trains. This input is presented to each of the excitatory neurons, however, across the excitatory neurons the input has only the repeated spatio-temporal pattern in common as the alternating and continuous Poisson trains are different. Furthermore, the repeated spatio-temporal pattern is presented to each neuron at the same time. All input synapses and lateral synapses are plastic. One pathway including input, excitatory lateral and inhibitory competition is emboldened for clarity.

tatory neurons. For convenience, inhibitory synapses had the same dynamics than excitatory ones, but were non-plastic. Likewise, excitatory synapses on the inhibitory cell did not learn. (Plastic synapses on the inhibitory neuron could be included although because the effect of these synapses changing could interfere with the competition–a potentially useful phenomena– this was left for future research.) Their values were all identical and set such that a spike in the excitatory network reliably triggered activity in the inhibitory neuron as well. Inhibitory synapses also had identical weights and were set such that a spike of the inhibitory neuron reliably suppressed firing in the excitatory sub-network for typically a few milliseconds after the firing of an excitatory neuron ("winner-takes-all" mechanism).

4.2.2 Weight normalisation

Similar to previous synfire chain learning studies, we included weight normalisation, Eq. (4.1), so that the total excitatory lateral input to a neuron was no greater than $W^{\mathrm{L}}_{\max}$=50. The value for $W^{\mathrm{L}}_{\max}$ was found experimentally, c.f., Fig. 4.5.

$$w_i = \begin{cases} \frac{w_i}{\sum w_i} W^{\mathrm{L}}_{\max} & \text{if} \quad \sum_{i=1}^{n} w_i > W^{\mathrm{L}}_{\max} \\ \\ w_i & \text{if} \quad \sum_{i=1}^{n} w_i \leq W^{\mathrm{L}}_{\max} \end{cases} \tag{4.1}$$

4.2.3 Simulations

Unless otherwise stated, training is run for a fixed duration of 200s, at which time weights have practically converged (Fig. 4.5). After training, the network performance is tested. We distinguish between 'learning of a pattern' and 'learning of a sequence'. This corresponds roughly to training of the feedforward and the recurrent synapses, respectively:

A spatio-temporal pattern counts as learnt if a fixed set of neurons responds reliably to segments of it. Neurons are considered part of a trained chain only if they fire with a probability of at least 50% during repeated presentations of the input pattern in the test phase. The majority of neurons are much more reliable than 50% after training.

A sequence counts as learnt if the pattern is learnt (as described above), none but the first

Table 4.1: Table of parameters

Parameter	Description	Value
N_{input}	Number of input afferents.	2000
I	Input.	-
I^{in}	Input transmitting the repeated pattern.	-
I^{noise}	Input not transmitting the repeated pattern.	-
dt	Euler-integration time step.	0.1ms
τ_m	Membrane time constant.	10ms
θ	Firing threshold.	1
θ_r	Rise time constant for alpha function.	1ms
θ_f	Fall time constant for alpha function.	5ms
S_r	Rise synaptic current of alpha function.	-
S_f	Fall synaptic current of alpha function.	-
$f(\tau)$	STDP function.	-
τ	Temporal distance between pre- and postsynaptic activity.	-
τ_p	Potentiation time constant for STDP function.	20ms
τ_d	Depression time constant for STDP function.	20ms
A_p	Positive learning rate.	$0.002 \times W_{\text{max}}^{\text{P}}$
A_d	Negative learning rate.	$-A_p \times \left(\frac{\tau_p}{\tau_d}\right) \times \lambda$
λ	Parameter adjusting the proportionality of the learning rates.	1.05
$W_{\text{max}}^{\text{P}}$	Maximum synaptic weight for input afferents.	$1/N_{\text{input}}$
N	Number of excitatory neurons.	20
J^{in}	Input synapses for I^{in}.	-
J^{noise}	Input synapses for I^{noise}.	-
J^{lateral}	Lateral synapses.	-
$W_{\text{max}}^{\text{L}}$	Maximum synaptic weight for lateral afferents.	50

neuron fires with recurrent input switched off in response to the learned pattern, but they do fire in fixed order with recurrent synapses present. This implies that both the feedforward and the recurrent input into a neuron are needed to make it fire. A sequence counts as recognised during a presentation if all neurons of a learnt chain fire; this signals that a complete pattern has been seen by the network.

Due to the Poisson spikes on 1000 input lines and additional 10Hz background spikes on all synapses, learning and retrieval are stochastic processes. Therefore, after training, neurons do not respond 100% reliable to the input pattern, but missing and spurious firings may occur caused by the random background input. This causes sequence recognition to fail and becomes more severe for longer sequences.

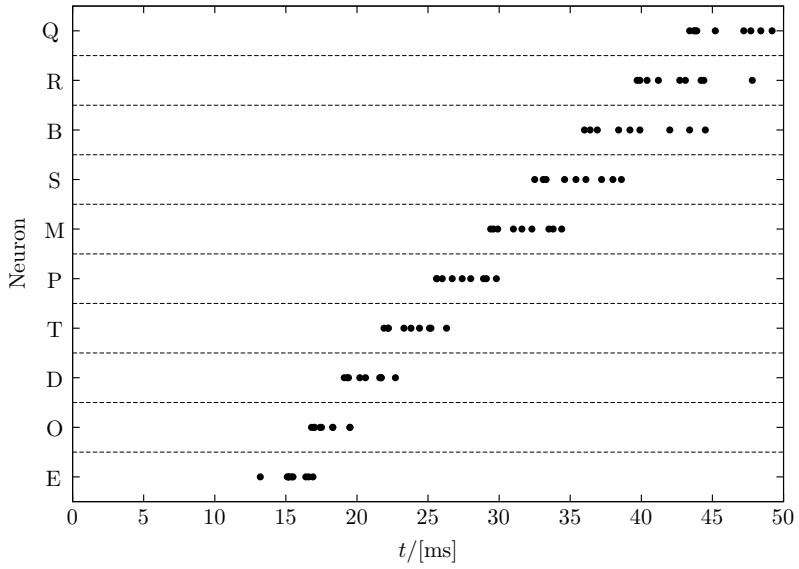

Figure 4.2: Typical raster plot of output spikes in response to 10 presentations of a trained sequence. After learning a repeated pattern of 50ms duration, neurons in the network responded to unique segments of the pattern. The cumulative responses of ten pattern presentations are shown, with jitter in the response times visible. The jitter in response latencies increases through the pattern as the variance is cumulative. Here, the order of firing is E→O→D→T→P→M→S→B→R→Q and each neuron responds in each trial but some spikes are printed on top of each other.

4.3 Results

4.3.1 Pattern learning for nearest-neighbour STDP

After learning a pattern with nearest-neighbour STDP, a set of neurons typically respond at different times during a pattern enforced by the winner-takes-all mechanism, see Fig. 4.2 for an example. The figure shows the cumulative spikes of ten neurons (Q to E) over time for ten presentations of the trained pattern starting at time zero. Each line contains ten accumulated firings (black dots; some printed on top of each other) reflecting proper sequence recognition for each individual pattern presentation.

Note that noise in the model is high – more than 75% of all spikes are noise spikes, because half of the input lines carry pure Poisson spike trains, the actual 50ms training patterns are shorter than the periods of intermittent noise between their presentations, and there is an additional

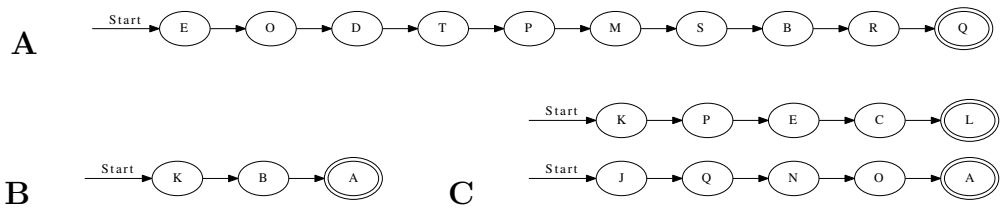

Figure 4.3: Three chains learnt with nearest-neighbour STDP. A is a relatively long sequence consisting of 10 neurons whereas B and C are shorter. In C, two chains were learnt; when the pattern was presented, two sets of neurons responded in sequence. Double-line neurons are accepting neurons. Only synapses that are greater than 5% of $W^{\mathrm{L}}_{\mathrm{max}}$ are displayed as these were deemed the most important.

10Hz Poisson noise on each synapse. Therefore, even after training finished, the membrane potential fluctuations (not shown) are large such that the spike times in Fig. 4.2 display a considerable jitter. The distribution of response times becomes greater later in the pattern. The first neuron responds after about 15ms reflecting the combined membrane and synaptic time-constants. These spikes are driven by the forward inputs only and quite reliable. Subsequent neurons fire in quicker succession driven by feedforward and recurrent input. Later spikes reveal a larger jitter because they rely on the feedforward input noise and the already jittered recurrent spike times. The large noise limits the recognition rates that can be reached (see section 4.3.4).

We found that with nearest-neighbour learning recurrent synapses between successive neurons were strengthened, leading to chains where each neuron in a sequence primed the next (Fig. 4.3). Sometimes multiple chains would be learnt (Fig. 4.3C), each responding to the same pattern. In such a case, all chains respond simultaneously to a pattern. This situation becomes more prominent when the number of neurons is increased. A 50ms pattern requires only a relatively small number of neurons to be represented (on average five). A significantly larger number of neurons then allows for multiple representations.

4.3.2 Convergence of Learning

Input to the model is stochastic. Even after long simulation times synaptic facilitation and depression events can happen by chance at individual synapses. Therefore, strictly speaking, weights never converge to deterministic limits but remain fluctuating even though with potentially small standard deviation. Whether, well-defined asymptotic weight distributions exist is

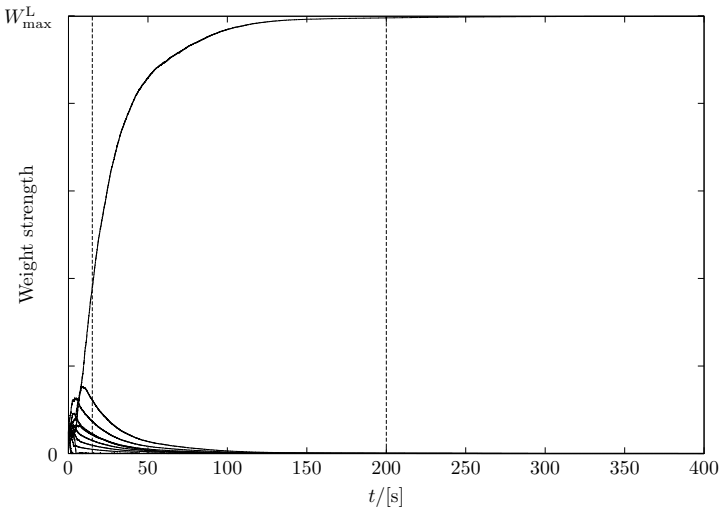

Figure 4.4: Weight changes over time for lateral excitatory synapses during learning. Only 10 synapses are depicted for simplicity. After 15s the pattern is already learnt, although the weights do not fully stabilise until about 200s.

likely, but given that winner-takes-all dynamics are difficult to understand those are difficult to predict. Beyond this general remark, Fig. 4.4 provides some insight into the learning dynamics of the recurrent connections (aspects of training the feedforward synapses are studied in (Masquelier et al. 2008; Humble et al. 2010) and the previous chapter).

Synapses start randomly initialised in a range $[0, W^L_{\mathrm{max}}/N]$ with N=20. Because total depression exceeds total excitation in the STDP learning curve, pure random spike trains depress synapses when output neurons fire noise-driven. This happens during the first few seconds of the simulation (cf. (Masquelier et al. 2008; Humble et al. 2010)). The repeating pattern counteracts this weakening, leading to the development of specific feedforward synapses for segments of the input in some output neurons. Subsequently recurrent synapses develop that chain output neurons together according to the temporal structure in the input.

The amount of time required for a network to learn a pattern according to our 50% criterion is a few seconds (simulated time) given the parameters in section 2. Sequences were learnt in between 10 and 20s, or at most 100 stimulus presentations. The mean length of learnt sequences was 5 neurons. The learning of weights continues after the sequence is learnt (15s in Fig. 4.4); weights stabilise much later (200s in Fig. 4.4). After learning, lateral weights had values close

to zero or the maximally possible value.

4.3.3 Effect of lateral weight bounds

To analyse the effect of $W^{\mathrm{L}}_{\mathrm{max}}$ on learning we varied the parameter and measured the percentage of neurons, which had learnt a pattern that responded with severed lateral connections (Fig. 4.5). When $W^{\mathrm{L}}_{\mathrm{max}}$ was increased the percentage of neurons that responded within the pattern *without* lateral connections decreased. In other words, as $W^{\mathrm{L}}_{\mathrm{max}}$ increased a neuron depended more on precedent neurons. Specifically, when $W^{\mathrm{L}}_{\mathrm{max}}$ was low ($W^{\mathrm{L}}_{\mathrm{max}}$=5), 80% of neurons responded without lateral synapses, however this decreased to ≈25% with stronger lateral synapses ($W^{\mathrm{L}}_{\mathrm{max}}$=55). Furthermore, very strong lateral synapses ($W^{\mathrm{L}}_{\mathrm{max}} \geq$60) interfered with the common Poisson input as they had a relatively strong efficacy towards a neuron's firing and therefore impeded with the learning.

When $W^{\mathrm{L}}_{\mathrm{max}}$=50, the start neuron was routinely the only neuron which responded without lateral connections. Furthermore, we found that an accepting neuron only responded when a pattern was presented in full. For example, if a pattern was reversed a chain's last neuron (and usually many more) would not respond. This effect was independent of the number of neurons and only depended on the absolute value of $W^{\mathrm{L}}_{\mathrm{max}}$.

4.3.4 Impact of other model parameters on learning and retrieval

Over 30 trials the success rate for learning patterns was 100% meaning that a reliable set of neurons practically always developed that reflects segments of the input patterns. These segments can then be chained in to a sequence to represent the entire pattern. However, this does not imply that individual neurons respond 100% reliably to their respective input segments. Given the large noise in the system, even after long learning periods a residual probability for missing or spurious firings remains. For sequence retrieval the probability of errors accumulates, which leads to a success rate for learning sequences of 62% given the parameters used.

The noise level can be adapted by changing the background firing rate or the number of background inputs. This, however, is possible only in limits due to the special nature of the model: the input noise is integrated over time by the membranes where it forms temporally correlated

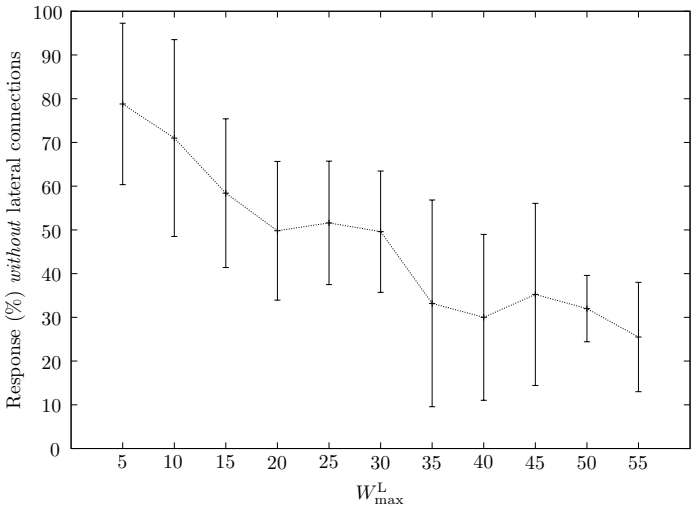

Figure 4.5: Effect of $W^{\mathrm{L}}_{\mathrm{max}}$ on a neuron's dependence on previous neurons. As the maximum strength of lateral connections, $W^{\mathrm{L}}_{\mathrm{max}}$, was increased, neurons became more dependent on the input from antecedent neurons. Due to STDP in the lateral connections the number of neurons responding without strengthened lateral connections decreased accordingly.

Gaussian noise (asymptotically for many inputs). Because all neurons receive precisely the same learning pattern reducing the standard deviation of the noise would make the membrane potentials of all neurons more and more similar. Noise is needed to break this symmetry and assign different neurons to different segments of the input pattern (with the additional help of the winner-takes-all mechanism). On the other hand, increasing the standard deviation of the noise also increases the error probabilities for spurious and missing spikes during retrieval. This can in turn lower recognition rates. Therefore, small changes in the background firing rate are theoretically tolerable however in practice even small changes, $\pm$5Hz, can negatively affect the learning of patterns/sequences.

Changing the pattern duration has previously been studied by Masquelier et al. (2008). Masquelier and colleagues found that as pattern duration increased the performance of pattern learning dropped to 59% with 100ms and further to 46% with 150ms; this effect would impede the learning of chains in this study and we therefore kept pattern duration at 50ms. The decrease is due to the STDP rule which depresses synapses if they see Poissonian input and output spikes, because overall LTD dominates LTP in the learning rule. A pattern embedded in noise must

therefore appear sufficiently frequently in order to facilitate synapses. As patterns get longer their presentation frequency decreases, which impairs learning.

The number of competing neurons (N) could be changed, but increasing the number too much interferes with learning for similar reasons as longer patterns: During the initial learning phase more neurons compete for a segment to learn, such that they respond less often because competitors do. Thereby the chance for facilitation becomes reduced and depression dominates.

Overall the parameter dependences discussed in this section suggest that the original model from (Masquelier et al. 2008, 2009) can be improved for optimal sequence learning. We come back to this point in the discussion.

4.3.5 Results for all-to-all STDP

When all-to-all STDP is used instead of nearest-neighbour STDP, more than one outbound/inbound connection per neuron was strengthened (Fig. 4.6). For example, if A→B→C→D was learnt with nearest-neighbour spike STDP, all-to-all STDP would add A→C and B→D, and possibly A→D, if the temporal window of the learning rule and the spike-times allowed for this. As with the last chain in Fig. 4.3, the connections do not always form in one single ordered sequence, but more complex situations are possible. For example, three accepting neurons are present Fig. 4.6A: neuron O will respond if the entire pattern is presented and neurons D and H will respond when the majority of the pattern is presented. However, these cases were rare and the majority of chains had one accepting neuron as in Fig. 4.6B. The presence of more than one accepting state was due to some neurons responding only just above 50% accuracy. In Fig. 4.6A for example, neurons D and O would not respond 100% of the time and in the cases where they did not respond neuron H was the final neuron.

4.3.6 Training more than one pattern at a time

Next we looked at presenting two patterns to see if more elaborate chains could form. The patterns were randomly presented but always non-overlapping. We usually found that both patterns were learnt (Fig. 4.7), although sometimes only one of the patterns was learnt. In addition to a neuron learning one pattern, some neurons learnt both patterns and took part in

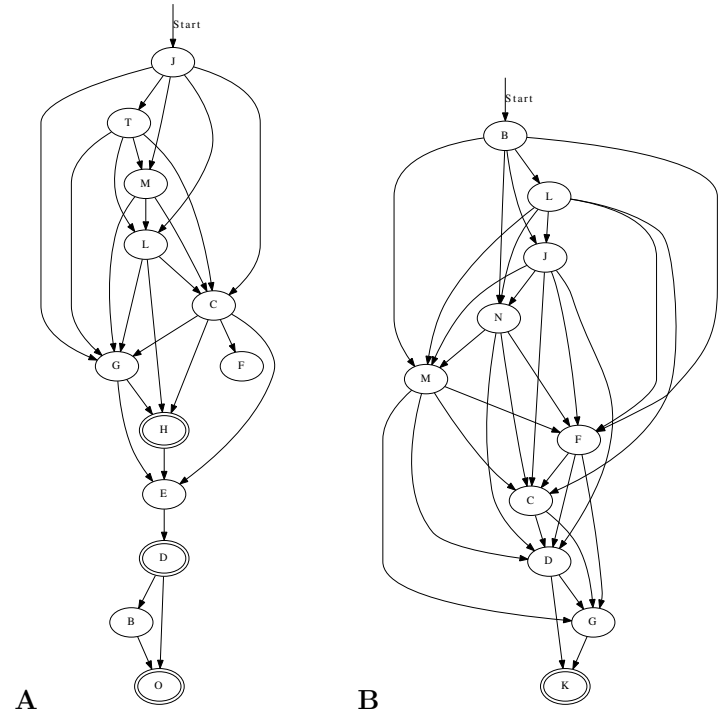

Figure 4.6: Two synfire chains learnt with all-to-all STDP. With all-to-all STDP, more synapses were strengthened resulting in some connections straddling subsequent neurons. For example, in (A) neuron C not only receives input from the previous neuron, L, but also J, M and T. The same is found in (B) where N not only receives input from the previous neuron, J, but also from B and L. Furthermore, it is possible to have more than one accepting neuron as in (A) where all D, H and O are accepting neurons. This is not always the cause though: in (B) only K is an accepting neuron. Double-line neurons are accepting neurons. Only synapses that are greater than 5% of $W_{\max}^{\mathrm{L}}$ are displayed as these were deemed the most important.

both chains. Networks therefore were often complicated with multiple pathways.

As several lateral connections now drove each neuron we analysed the strength of these synapses: generally the more direct the connection the stronger the synapse. In a chain A→B→C for example, the synapse between A and B would usually be stronger than that between A and C. Synaptic strengths are indicated in figures 4.7 and 4.8 to illustrate the fact.

4.3.7 Concatenating chains by training

In the previous sections we learnt only short patterns. The length of patterns can in principle be increased, but we tested an alternative option: the chaining of already learnt segments. For this purpose two patterns were stored as before, but in a second phase the two patterns were repeatedly presented consecutively. This allowed two chains to connect, see Fig. 4.8 for an example. If before learning two patterns were recognised by two unique chains, then the end of one would be linked to the beginning of the other. Still, recognition of the individual sub-chains remained possible using appropriate entry and exit nodes along the combined chain.

This mechanism in principle allows to train sequences hierarchically and potentially also to form more complex graph-like structures from simpler elements.

4.3.8 Notes on Memory Capacities

It may seem that using 20 neurons to store two patterns makes inefficient use of resources. This, however, deserves further consideration. Observe that two types of connections in the model store information, the feedforward synapses and the recurrent connections in the output layer.

Each trained neuron in the output layer responds specifically to a short segment in the input of length roughly similar to the duration of post-synaptic potentials; this is the time over which synaptic integration efficiently takes place in the feedforward synapses, and it is of the order of 10ms. Segments coded by subsequent output neurons overlap to some degree (see Fig. 4.2 where distinct output neurons fire about every 5ms).

The output network therefore basically uses a one-out-of-N code to represent short segments of the full spatio-temporal input pattern. If two spatio-temporal patterns each of 50ms duration are stored in 20 neurons this gets quite close to the maximally possible number of segments. The

Figure 4.7: Synfire chains learnt for two patterns, orange and yellow, presented separately to the same network. In A, each pattern is recognised by a different set of neurons. In contrast, the patterns in B are both recognised with two overlapping pools of neurons. The strength of synapses is represented by edge colour and thickness; for example, a thick black edge represents a strong synapse. If many synapses are strengthened they will all be relatively weaker than if only one was strengthened (due to weight normalization). For example, in (A) F only has one afferent and is relatively stronger than the three afferents to A. Double-line neurons are accepting neurons. Only synapses that are greater than 5% of $W_{\max}^{\mathrm{L}}$ are displayed as these were deemed the most important.

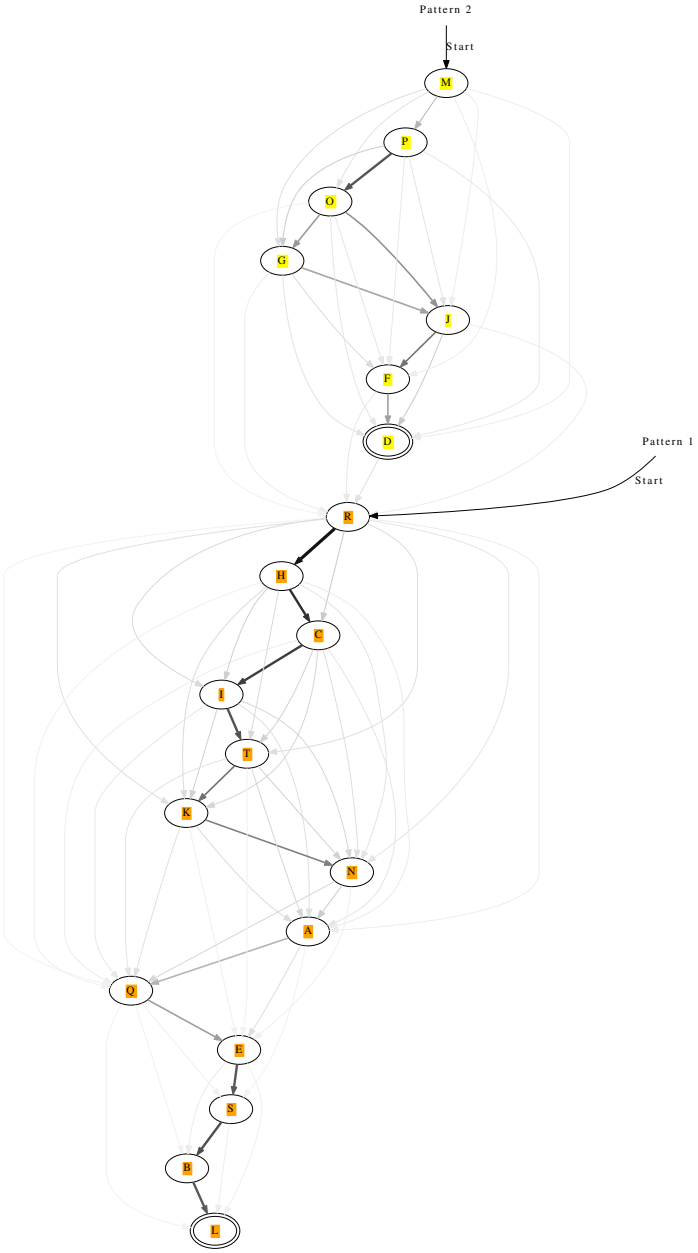

Figure 4.8: A long chain formed from two shorter ones each recognising a different pattern. After learning the two patterns separately, they were presented in succession: pattern two $\rightarrow$ pattern one. The end of pattern two connected to the beginning of pattern one. The strength of synapses is represented by edge colour and thickness; for example, a thick black edge represents a strong synapse. Double-line neurons are accepting neurons. Only synapses that are greater than 5% of $W_{\max}^{\mathrm{L}}$ are displayed as these were deemed the most important.

pattern capacity of a one-out-of-N code is $\alpha := P/N = 1$ or, informally, as many segments P can be represented as there are neurons, N. The recurrent connections chain these segments in the order of their occurrence.

It is known from theories of associative memories that sparse codes can have a much higher pattern capacity than dense codes and one-out-of-N codes. For example, the memory capacity of the Hopfield network with dense memory patterns (that is, a probability of $p = 1/2$ ones and minus ones each) is $\alpha = P/N \approx 0.14$, whereas for sparse codes with p percent ones (and zeros else) the capacity is of the order of $\alpha \sim -1/(p \log p)$. As p becomes small this number can become much bigger than 1 (as compared to a constant of 0.14 in the Hopfield net). Both results hold asymptotically in very large networks, but approximately also in smaller networks (Palm 1991).

This suggests that a k-winner-takes-all mechanism which selects k output neurons sparsely instead of only one, could be much more efficient regarding pattern storage capacities in the recurrent connections of the output layer. Unfortunately, it is not obvious how to design a neurally plausible mechanism that selects k neurons reliably and randomly during learning. Bienenstock noticed that the number of sets of k out of N neurons grows quickly in the sparse region, which makes a threshold mechanism to reach a controlled level of activity k and selects the same k neurons under the same input conditions unreliable (Bienenstock 1995). Also, in a case where learning is ongoing, some neurons will have already strengthened synapses relative to others which biases them towards higher firing probabilities and therefore a higher rate to be selected again. This is not only unwanted because it reduces memory capacities (high capacities assume independent neurons in patterns) but also in practice often leads to a core of neurons developing many mutual synapses, whereas other neurons never learn. The problem of designing a reliable k-winner-takes-all mechanism that avoids these problems has to be left to future work.

The amount of information contained in the forward synapses of the network is also quite close to a theoretical limit given a one-out-of-N code in the output layer. Note that given firing rates of roughly 50Hz (or 1 spike per 20ms) in the spatio-temporal patterns to learn, a neuron fires with probability 1/2 in a segment of about 10ms duration. Because binary patterns with independent

0/1-entries and p=1/2 contain maximally possible information, the learnt segments per output neuron in our model have a high information content close to maximum. This, of course is only an estimate; a more elaborate theory would have to take threshold and noise levels into account as well as jitter in spike times. Note also that again, sparse patterns in the input and output layers may potentially increase the pattern capacity or total information stored in the forward synapses.

4.3.9 Invariance against Stimulus Speed

Earlier work implies that it is possible to reach a certain amount of invariance in pattern recognition if the speed of the input pattern is changed. This may require an adjustment of the firing thresholds (Wennekers and Palm 1996; Wennekers 2000).

Figure 4.9 demonstrates the main mechanisms. Sub-plot A shows spike times of three consecutive neurons in the output layer, which for simplicity are assumed to fire at regular intervals. Each firing requires feedforward input from the spatio-temporal driving pattern. This is indicated in sub-plot B where the solid line applies to spike $i+1$ and the dashed line to spike i. These post-synaptic potentials are caused by brief segments before the spike that utilise trained pattern-specific synapses. After a spike in neuron i, the inhibitory loop is triggered as well as an excitatory post-synaptic potential is elicited on neuron $i+1$. The superposition of both is exhibited in sub-plot C. Sub-plot D shows the sums of the feedback inhibition and feedforward (ff) and feedback (fb) excitation for neurons i (dashed) and $i+1$ (solid). The neurons fire where the sum reaches the firing threshold (solid circles). The spikes times in A and the threshold crossing in D coincide for reasons of self-consistence.

Now assume that the input is slightly slower (or faster). In that case the curves in B will be slightly stretched and lower (or compressed and higher), whereas those in C stay the same. This will furthermore lead to slight changes in the summed curves in D, however, as long as the changes are small, the curves and changes are continuous. Therefore, the threshold can be slightly adapted to have neuron $i+1$ fire at a slower (or higher) speed as required by the input. Simulations actually show that the system tolerates a certain amount of noise in the input, which implies that the system is stable; for small enough speed changes a threshold adaptation is not

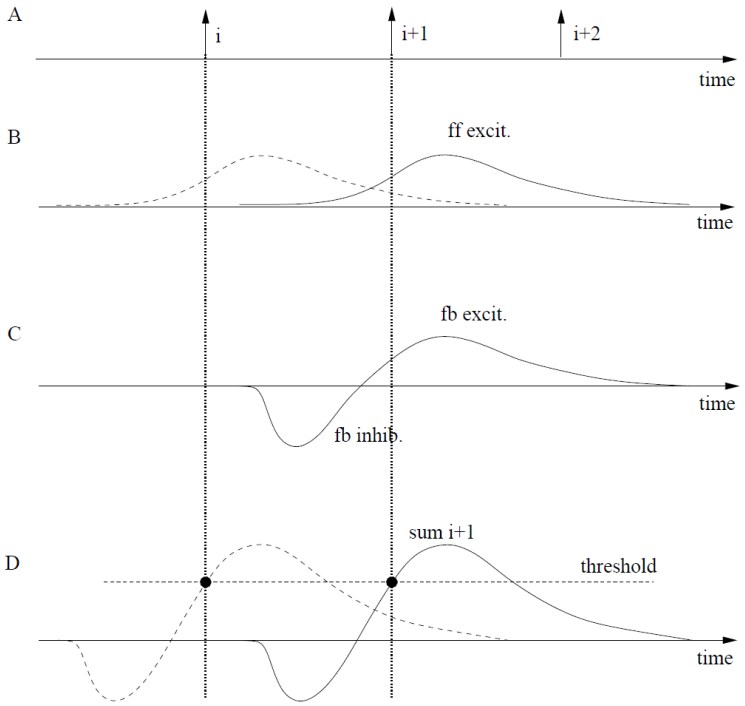

Figure 4.9: Robustness against input speed variations. A) shows spikes in three consecutively firing output neurons. These spikes are partly caused by specific feedforward input (B) and the recurrent feedback connections (C). The dashed post-synaptic potential in (B) contributes to the firing of neuron i, the solid line to $i+1$. C) shows excitatory-inhibitory post synaptic signals on neuron $i+1$ due to specific excitatory feedback (fb) from neuron i and the global inhibition also triggered by the firing of neuron i. (D) The feedforward and feedback signals superimpose on the output neurons and cause spikes where firing thresholds are crossed. These times must be the same as in (A) for consistency. If an input gets (slightly) faster than during training signals in B get compressed in time but larger in amplitude, which (slightly) moves the threshold crossing. By continuity, threshold variations can be used to speed up (or slow down) the recognition speed in the output network.

required. Changes of $< \pm 5$Hz are tolerable however greater variations impact pattern/sequence learning.

Even though the above analysis applies to the model in this chapter, the speed changes that can actually be tolerated are quite small for two reasons. At first, the rise times of the post-synaptic membrane potentials are small only (a few milliseconds). Because the threshold crossing causing the firing of neurons must fall on the rising edge, the maximum amount of speed tolerance is thereby limited. A second limiting factor is the large input noise for the parameters used in accordance with previous works. The input noise causes large membrane fluctuations which have an impact on the stability of wave propagation. On one hand, in order to allow any reliable retrieval, the threshold should be more than one standard deviation of the noise below the maximum in the summed potentials in Fig. 4.9; otherwise a neuron in the chain may miss firing by a significant probability which would terminate the chain. On the other end, the threshold must also be sufficiently bigger than the sum of both the feedforward and feedback excitation, again, by more than a standard deviation of the noise. Otherwise neurons may easily get excited randomly. It turns out that given the parameters used in the simulations the noise is so large that this leaves only a relatively small region for proper threshold settings. This is, for example, also indicated by Fig. 4.2 where even with a properly set threshold, spike jitter of output neurons in repeated simulations are around a few milliseconds, much comparable with the rise-times of the post-synaptic potentials.

Finally let us briefly mention that the above picture is not entirely complete. It leaves out a (constant) potential offset due to the Poisson inputs, membrane potential resets of the leaky-integrate-and-fire neurons after firing, and the fact that the recurrent inhibition acts globally. These effects have an impact on the precise shape of the membrane potential and firing times but do not change the main arguments qualitatively.

4.4 Discussion

It has previously been found that several neurons can learn to recognise different sections of a repeated spatio-temporal pattern (Masquelier et al. 2009). We studied whether it was possible to join these consecutively firing neurons into an ordered chain that recognises a spatio-temporal

input pattern. Using both nearest-neighbour and all-to-all STDP it was possible to form chains using a simple network of excitatory neurons laterally connected and one inhibitory neuron providing winner-takes-all competition.

Previous attempts to learn synfire chains (Bienenstock 1991; Hertz and Prügel-Bennett 1996; Hosaka et al. 2008) have set up random networks and some have excited neurons synchronously to strengthen connections. Our approach was different: we had a simple network that was driven mainly by a repeated spatio-temporal pattern where all excitatory connections were plastic for the duration of a simulation. Furthermore, a major limitation of some previous studies was that cyclical chains could form. When present, these closed loops interfered with the learning of long chains as once activity enters a loop it does not exit. None of our chains had cycles because the network was driven by a specific stimulus instead of random activity as with previous studies. This stimulus driven set-up deterred the formation of loops because the repeated patterns were separated by random activity that was not learnt.

An important result of having the lateral connections plastic throughout the learning process was that subsequent neurons in a chain not only recognised when a pattern segment was presented, but crucially only did so if the previous neuron had fired as well. The chains are therefore effectively simple finite automata that recognise linear sequences. However, the lateral connections only had this effect if they were allowed to strengthen enough (Fig. 4.5). When a neuron receives input through a lateral connection from a precedent neuron, this increases the membrane potential and primes the neuron to fire on appropriate input from the Poisson inputs.

We tested the possibility to learn longer sequences hierarchically from shorter segments representing two subsequent patterns. The longer chains that formed, included at least one accepting neuron that only responded if a learnt pattern was presented in full correctly. For example, if the pattern was reversed or split in half the accepting neuron would not respond. This multiple order dependence on previous neurons allowed for multiple paths through a network to be learnt.

Given that due to the random inputs firing was to some degree stochastic, the structures learned using nearest-neighbour learning may be considered to be similar to first-order Markov chains.

To extend this interpretation of learnt sequences as Markov chains, we found it was possible to learn higher order chains with all-to-all STDP. These produced neurons which not only relied on a previous neuron's response and the appropriate pattern input, but to a certain extent on the temporal pattern of activity across several neurons and time-steps. This dependence on previous neurons reinforced the concept of an accepting neuron only responding if a pattern had been presented in full.

These results take advantage of the finding in the previous chapter that a neuron with STDP learns both background activity and stimulus properties. In this case the lateral connections are modifying the background activity. For example, the background activity is increased slightly by lateral connections and when these are not present the combination of background activity and stimulus is not enough to reach threshold. Therefore a neuron is dependent on precedent neurons. However, it should also be noted, that the level of background activity allows the control of the speed of activation patterns in synfire chains (Wennekers 2000; Wennekers and Ay 2006). Such a mechanism can be used to gain a certain invariance against the replay speed of learned patterns. However, given the high noise level used in the present work (for better comparison with previous models of Masquelier et al., (2008) the controllable range is only small.

The high noise level also implies relatively low sequence recognition rates. The noise level, cannot be simply reduced because as discussed in section 4.3.4 at low noise levels membrane potentials become more and more similar because all neurons receive the same input. In this case the winner-takes-all mechanism has difficulties to reliably select only one neuron. Noise is needed to spread the membrane potential distribution and randomly select output neurons during learning. If neurons would not all see the same input, the noise level could likely be lowered and the recognition rates increased. This may improve the performance of the model.

Another drawback of the model is the relatively simple standard STDP learning rule. As mentioned in section 4.3.4 and already observed by Masquelier et al. (2008) the rule limits the maximum length of trainable patterns. In response to Poisson spikes synapses depress such that a certain minimum frequency for training patterns to repeat is required to facilitate synapses.

The inverse of this frequency limits the maximum duration of trainable patters.

The weight normalisation used in our study may be seen as a limitation. However, previous studies have used similar forms of weight normalisation; it seems to be crucial for the formation of synfire chains (Bienenstock 1991; Hertz and Prügel-Bennett 1996). Our implementation of weight normalisation is not local and would therefore require some signalling in biological neurons. Whether such signalling or weight normalisation is present within neurons is not known. Furthermore, the calculations for the maximal afferent weight for both input and lateral synapses ($W^P_{\max}$ and $W^L_{\max}$) would also require some, as yet, unknown signalling. However this would ideally be an "inbuilt" property of neurons. The resource-based STDP rule introduced in the next chapter addresses this problem.

Another limitation of our network is its small pattern capacity. Neurons can typically not be trained to participate in more than two patterns. This limitation is mainly due to the non-sparse input with 1000 inputs representing the signal and another 1000 carrying Poisson noise. The study of sparse input and output patterns suggested in section 4.3.8 remains an interesting but open problem. Sparse codes are known to drastically increase pattern capacities in associative memories (Palm 1991). In the present context they may similarly help with 1) overcoming the need to have about 20 neurons to recognise "only" 100ms of input and 2) increasing the number of different patterns stored within a network.

Experimental evidence is accumulating that cortical activity is often sparse and precisely timed in response to repeating stimuli. Wolfe et al. (2010) review evidence from a variety of species and cortical areas showing that neurons can respond highly selectively in response to brief periods of repeating inputs. The selectivity and sparseness is controlled by inhibitory networks of neurons which also chop the excitatory responses into bursts in the beta frequency range. Our model acts in a similar way causing sequences of neurons to fire in response to specific segments in the inputs. The firing activity in the model is rhythmic due to the winner-takes-all inhibition, ie., the firing of only a single neuron per recognised segment. A k-winner-takes-all mechanism may reflect the biological situation even closer. Our model, however, has the additional feature that on top of neurons that recognise single short segments of the input, we

also utilise lateral excitatory connections to encode longer patterns. It may be worthwhile to explore this possibility in experiments by stimuli that either support the propagation of activity (the original pattern) or not (the reverse pattern or scrambled segments). The possibility to stitch patterns together can also be tested experimentally. In the present work we have only shown this for two patterns (due to limitations of the learning rule) but in principle chains could be combined into more complex patterns that may underlie cortical computations.

Chapter 5

Resource-based STDP

5.1 Introduction

In this chapter we introduce a novel STDP learning rule. The learning rule addresses many issues that are common with typical STDP learning rules (such as that used in previous chapters). For example, computational and biological synaptic distributions do not match, the lack of non-potentiable and silent synapses, and computational problems with synaptic competition and bounds. Before background information is introduced on these limitations some additional forms of plasticity, that were only briefly mentioned in the main introduction, shall be discussed in more detail, *viz.* heterosynaptic plasticity and synaptic scaling.

In addition to typical experiments studying long-term potentiation (LTP), long-term depression (LTD) (Bliss and Gardner-Medwin 1973; Levy and Steward 1983; Siegelbaum and Kandel 1991; Bliss and Collingridge 1993; Linden and Connor 1995; Nicoll and Malenka 1995) and spike-timing dependent plasticity (STDP) (Bi and Poo 1998; Wang et al. 2005), several studies have found so called heterosynaptic plasticity. Heterosynaptic plasticity describes cases where the induction of one type of plasticity causes the expression of another type. For example, previous studies have found that LTP (Bradler and Barrionuevo 1989; Misgeld et al. 1979) or LTD (Muller et al. 1995; Staubli and Ji 1996; Cowan 1998) can spread postsynaptically to nearby synapses.

Furthermore, when LTP is induced at afferents, LTD is sometimes induced at other afferents in Schaffer collaterals (Dunwiddie and Lynch 1978), cortex (Tsumoto et al. 1978; Hirsch et al. 1992), dentate gyrus (Levy and Steward 1979; Abraham and Goddard 1983) and CA3 of hippocampus. The corollary are findings of LTD being induced by LTP in amygdala (Royer and Paré 2003) and the hippocampus (Wöhrl et al. 2007). In addition, Staubli and colleagues found that previous potentiation of a synapse would reduce the threshold for induction of LTD (Staubli and Lynch 1990), however Harvey et al. (2007) found that the induction of LTP at a synapse reduced the LTP threshold at neighbours ($\approx 10\mu$m) for approximately 10 minutes. The direction and magnitude of plasticity can also depend on the predisposition of a synapse to undergo plasticity (Chistiakova and Volgushev 2009) and heterosynaptic plasticity has also been found presynaptically (Kossel et al. 1990; Schuman and Madison 1994). These studies complicate the

picture of LTP and LTD being correlated with activity. The findings suggest that the induction of LTP or LTD is dependent on many complex and interlaced mechanisms and signals.

Synaptic scaling is another phenomenon recently discovered, and is a form of homeostatic plasticity. Synaptic scaling describes the homeostatic regulation of synapses across a neuron. Blocking a neuron's activity, or artificially inducing hyperactivity, leads to an increase, or decrease, of AMPA receptors (O'Brien et al. 1998; Turrigiano et al. 1998; Watt et al. 2000; Thiagarajan et al. 2005; Shepherd et al. 2006; Lissin et al. 1998; Wierenga et al. 2005; Stellwagen and Malenka 2006; Grunwald et al. 2004; Ju et al. 2004) and NMDA receptors (Watt et al. 2000; Rao and Ballard 1997; Mu et al. 2003) with a compensatory increase in current for both AMPA and NMDA receptors (Watt et al. 2000) and increase in insertion of AMPA receptors (Ju et al. 2004; Sutton et al. 2006). These effects last for hours to days (Turrigiano et al. 1998), can be seen from as early as 4 hours after intervention (Ibata et al. 2008) and have been found to occur across all synapses (Turrigiano et al. 1998; Thiagarajan et al. 2005; Ibata et al. 2008) and restricted subsets of synapses on a dendritic branch (Branco et al. 2008; Ju et al. 2004; Hou et al. 2008; Sutton et al. 2006; Ibata et al. 2008; Thiagarajan et al. 2005). The majority of studies are *in vitro*, however synaptic scaling has also been observed *in vivo* (Maffei et al. 2004; Desai et al. 2002; Goel et al. 2002).

Synaptic scaling is not confined postsynaptically and can be found presynaptically. For example, a blocking of activity leads to an increase in vesicle recycling (Moulder et al. 2006; Bacci et al. 2001; Burrone et al. 2002), an increase in the probability of vesicle release (Branco et al. 2008; Petersen et al. 1997) and an enlargement of the active zone and an increase in the number of vesicles (Moulder et al. 2006) with hyperactivity resulting in a reduction in the release probability (Branco et al. 2008; Petersen et al. 1997; Moulder et al. 2004).

5.1.1 Issues with typical STDP

Despite these biological findings of complicated interlaced forms of plasticity, common implementations of STDP do not include most of these phenomena; furthermore, STDP-based learning rules share several computational results which do not agree with those found experimentally. These include a non-biologically matching weight distribution, the lack of non-

potentiable synapses and silent synapses, synaptic stability and competition, and the implementation of synaptic bounds. Each shall now be described with reference to resource-based STDP results.

Synaptic distribution (Fig. 5.8). Recorded distributions of synaptic strengths are mostly exponential with a peak near zero; they have long tails with few relatively strong connections but many weak connections. Such distributions are found for excitatory synapses (Montgomery et al. 2001; Song et al. 2005; Frerking et al. 1995; Isope and Barbour 2002; Markram et al. 1997; Mason et al. 1991; Sayer et al. 1990; Feldmeyer et al. 2006; O'Brien et al. 1998; Holmgren et al. 2003; Thiagarajan et al. 2007) (AMPA and NMDA (Montgomery et al. 2001)), inhibitory synapses (Miles 1990; Holmgren et al. 2003) and for quantal distributions (Edwards et al. 1990), but see Feldmeyer et al. (1999). Furthermore, Sjostrom et al. found that 95% of synaptic connections were less than a threshold required for LTP (Sjöström et al. 2001) and Brunel et al. (2004) found—through a computational study—that the distribution of synaptic weights for optimal information storage was similar to those empirically recorded.

In contrast to biological distributions, computational studies have found synaptic distributions varying depending on STDP rule use. Specifically, multiplicative-STDP (weight-dependent) in general produces unimodal distributions with a peak between zero and the middle of the possible synaptic range (van Rossum et al. 2000; Burkitt et al. 2004; Barbour et al. 2007; Billings and Rossum 2009; Rubin et al. 2001) whereas additive-STDP (non-weight-dependent) produces bimodal distributions with a peak near zero and another near the upper bound (van Rossum et al. 2000; Barbour et al. 2007; Masquelier et al. 2008, 2009; Song et al. 2000; Izhikevich and Desai 2003; Bush et al. 2010; Billings and Rossum 2009; Câteau and Fukai 2003; Rubin et al. 2001; Song and Abbott 2001). Furthermore, Gutig et al. (2003) used a learning rule that allowed them to adjust the amount of weight dependence continuously and showed that the final distributions are not segregated into either uni- or bimodal, but can be interpolated in between these two extremes.

Nevertheless, no computational studies using a spiking learning rule have yet produced a synaptic distribution that qualitatively matches those found empirically. It has however been postu-

lated that perhaps both unimodal and bimodal distributions are stable. The unimodal distribution could represent unlearnt weights, and a bimodal distribution learnt synapses (Toyoizumi et al. 2007). This is still an open topic as one does not know when recording from synapses whether they are 'learnt' or not.

Non-potentiable synapses (Fig. 5.10). In addition to the distributions described above, studies have found that some synapses appear to be non-potentiable or non-plastic. For example, Debanne et al. (1999) found that 24% of EPSPs they studied did not show potentiation, and an identical proportion of non-potentiable synapses have been reported in area CA1 of hippocampal slices (Petersen et al. 1998). Moreover, Debanne et al. concluded that their non-potentiable connections had been previously potentiated to a saturating level (Debanne et al. 1999).

Silent synapses (Fig. 5.8). When synapses *are* plastic however, five discrete synaptic states have been defined (reviewed by Montgomery et al. (2004)): active, potentiated, depressed, silent and recently silent. Silent synapses are characterised by their lack of AMPA receptors (they still have NMDA receptors), and for this reason they could potentially be missed by studies recording synaptic distributions, such as those above, due to technical limitations. Some studies, however, have considered silent synapses and have estimated the number of undetected synapses. For example Brunel et al. (2004) included a Dirac delta of silent synapses into an empirically recorded distribution (Isope and Barbour 2002).

Synaptic stability (section 5.3.5). In addition to whether synapses are silent or not, many studies have found that after a tetanizing protocol, LTP decays back to a level similar to before tetanizing. Furthermore, three families of decay curves have been observed and defined as LTP1, LTP2 and LTP3 with time constants of 2.1 hour, 3.5 days and 20.3 days respectively. (Terming is from (Racine et al. 1983; Abraham et al. 1991) and decay time constants are from (Abraham et al. 1991, 1993).)

Contrary however, are other studies which find that LTP can be persistent for many months and even up to a year (Abraham et al. 2002). Moreover, other forms of LTP have been found intermediate to early and late phases including one protein synthesis independent (Winder et al. 1998) and another dependent on translation but not transcriptional processes (Raymond et al.

2000).

When taken together these studies suggest that LTP has a myriad of inducing and maintaining functions and mechanisms with greatly varying time constants, which are not often considered in computational studies of spiking learning rules. A few exceptions are a study by Billings et al. (2009) and those by Standage and Trappenberg (2007) and Standage et al. (2007). Billings and colleagues studied the weight persistence/stability for multiplicative (weight-dependent) and additive (non-weight-dependent) STDP. They found that additive STDP was fairly stable with weights decaying with a time constant of 18 hours, however multiplicative STDP was very unstable with weights decaying with a time constant of just 29 seconds. Furthermore, they found that even when the stability of receptive fields were studied the additive STDP rule was still more stable (93 hours) when compared to the multiplicative rule (1 hour); Standage et al. found similar results. In addition, when Standage and colleagues used a multiplicative STDP rule the learning was slow, and when the learning rate was increased, rapid forgetting was prominent due to noise.

There is however a fundamental difference between these computational studies and the empirical findings: the computational studies' time constants are for decaying exponentials fitted to autocorrelation functions whereas the empirical findings are decaying exponentials fitted to actual amplitude traces. Furthermore, whether the empirical studies were done *in vitro* or *in vivo* and the type of activity used computationally could greatly effect the results.

Synaptic competition and synaptic bounds (Figs. 5.8 and 5.10). Synaptic bounds can greatly affect the outcome of a STDP-based learning rule. For example, computational studies have found that additive STDP requires hard upper bounds or potentiating synapses will potentiate forever due to self reinforcement. Another method to control runaway synapses is with multiplicative (weight-dependent) STDP, which enforces a soft upper bound. Furthermore, multiplicative rules have very little synaptic competition (van Rossum et al. 2000) whereas additive rules have strong competition. Therefore, because learning must be both competitive and stable, when choosing between additive and multiplicative learning rules one has to consider competition, upper synaptic bound implementation and synaptic distribution realism (Brunel et al.

2004).

If global (hard or soft) upper bounds are used, this can constrict synaptic growth as synapses can only get so strong. Specifically, upper bounds have to be set prior to learning and can therefore limit learning if not chosen appropriately.

A possible solution is normalisation. Weight normalisation limits only the total amount of synaptic efficacy allowing for redistribution of synaptic efficacy and permits a setup with no global upper bounds. Normalisation introduces a simple form of competition that can be beneficial and is used for this reason in some computational studies. This does however lack supporting biological evidence as normalising computations often need to be neuron wide.

Another possible solution is to have local synaptic upper bounds instead of global bounds, however no computational studies have yet looked at intrinsic synaptic maxima (Standage and Trappenberg 2007; Standage et al. 2007). Local bounds may also be present in electrophysiological data. For example, it is possible that the synapses in Bi & Poo's data may not transition through the total range they recorded from and may saturate at their own maxima.

Weight dependence (section 5.3.6). In addition to a synapse depending on timing for potentiation polarity and amount of change, Bi & Poo (1998) also showed (independently of spike-timing) that the actual amount of change for depression was dependent on initial synaptic strength. This was later reconfirmed under more complicated protocols including triplet and quadruplet pairing relationships (Wang et al. 2005). Specifically, with spike-timing held constant, a strong synapse depresses (actual change of pA) more than a weak synapse; this dependence was not present (or not with such a strong dependence) for potentiation. This is not the full picture however as studies to the contrary find that LTP is dependent on potentiation too (Montgomery et al. 2001; Debanne et al. 1999); these studies however do not consider spike timing.

Several possible explanations have been proposed for these seemingly contradictory results:

- Firstly, the unsilencing of silent synapses and saturating of strong synapses is suggested to be responsible for the LTP weight dependence (Montgomery et al. 2001; Debanne et al.

1999), which differs from assumptions underlying Bi & Poo's data.

- Secondly, a standard computational interpretation of Bi & Poo's results on weight dependence includes an assumption that the data do not include saturated synapses (Standage et al. 2007) which could explain the lack of potentiation dependence. However, if the data reflect saturated synapses, synapses might need intrinsic synaptic maxima as the synapses may not transition through the total range Bi & Poo recorded from (Standage and Trappenberg 2007), leading to an extra complication for computational STDP implementations.

- Finally, it is possible that weight-dependency data reflect non-weight-dependency (Discussed by Debanne et al. (1999) and Standage et al. (2007)). The apparent weight-dependence could possibly be an artefact of limitations with the recording equipment and protocols (Standage and Trappenberg 2007). For example, extracellular stimulation is commonly used in STDP protocols, however may stimulate many synapses, and while intracellular stimulation eliminates this problem, neurons in culture may have multiple synapses between pre- and postsynaptic neurons (Koester and Johnston 2005; Markram et al. 1997; Silver et al. 2003).

Nevertheless, Bi & Poo's data suggest that computational STDP rules should include weight dependence for depression (and not for potentiation); many studies have done just this (Morrison et al. 2008; Standage and Trappenberg 2007; Standage et al. 2007; Kepecs et al. 2002; van Rossum et al. 2000), but highlight problems with weight-dependent STDP rules such as synaptic stability and synaptic competition—described above.

These limitations are rarely addressed in STDP learning rules and the phenomena mentioned above are not reproduced by current learning rules. Although our resource-based STDP learning rule was not specifically designed to, it addresses all of the above.

5.1.2 Resource-based STDP.

Even though synaptic scaling has been observed as multiplicative (Turrigiano et al. 1998; Goel and Lee 2007), and thus maintains the relative strengths of synapses stored through Hebbian-

like learning rules, studies finding homeostatic plasticity on a more local scale suggest that specific learnt synapses may be overwritten by synaptic scaling: an important computational problem which has previously been noted by Rabinowitch and Segev (2008). Rabinowitch and Segev proposed a solution to this with a local homeostatic plasticity mechanism, which has advantages over global homeostatic plasticity rules. Specifically, they suggest that if a synapse is potentiated, itself and its neighbours are depressed slightly to counter the increase in local mean activity. The reverse is also noted: to reflect a slight decrease in local mean activity when a synapse is depressed, itself and its neighbours are slightly potentiated.

This suggestion by Rabinowitch and Segev is the inspiration for the extension to STDP introduced in this chapter. Specifically, our learning rule includes the following: when a synapse is potentiated, its neighbours (not itself) are depressed by an amount depending on the neighbour's distance but totalling the same as the potentiating synapse. Moreover, when a synapse's neighbours have been fully depressed—and are therefore lacking in resources—a potentiating synapse can draw resources from a 'pool'. We do not include any compensatory change due to a synapse depressing–its resources are simply placed in the pool. Therefore, as one synapse potentiates, it becomes more specific and its neighbours, less specific. To complete this learning rule, the pool of resources decays over time (relatively much longer than all other time constants in the learning rule or neuron model). See figure 5.1 for a cartoon depicting the various scenarios in the learning rule. This resource-based STDP further addresses several phenomena, described above, that are often not considered in theoretical studies of typical STDP.

In the next section we firstly describe our resource-based STDP learning rule mathematically. Subsequently in the results section we first study how resource-based STDP compares with a typical STDP learning rule. Afterwards we show results that are qualitatively similar to those found experimentally. We specifically show synaptic weight distributions and results for synaptic stability, weight dependence and synaptic bounds. Finally we study a singular neuron's ability to learn two stimuli with both resource-based and typical STDP.

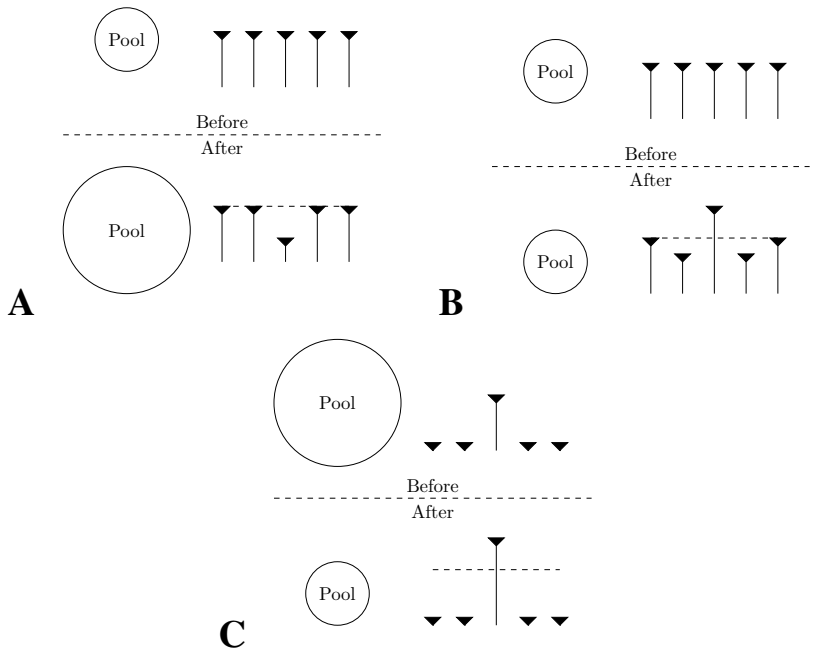

Figure 5.1: Resource based STDP has three scenarios: A) a synapse is depressed and its resources enter the pool; B) a synapse is potentiated and takes resources from neighbouring synapses with an exponential-distance dependent function and the pool remains unchanged; and C) a synapse is potentiated and takes resources from the pool as its neighbours are depleted. The height of the synapses signifies weight strength and there is no relation between the pool sizes of A, B and C.

5.2 Methods

In this chapter we introduce a new STDP learning rule: resource-based STDP. Therefore we refer to the form of STDP already introduced and used in the previous two chapters as 'typical' STDP. The following describes modifications made to typical STDP to formulate resource-based STDP. See table 5.1 for a table of parameters for this chapter.

5.2.1 Neuron model

In this chapter adaptation is introduced to the neuron model used in the last two chapters: Eq. 5.1 where τ_a=100ms and β=0.18. When a neuron reaches threshold and spikes, an amount of adaptation, a, increases slightly. The adaptation has a negative effect on a neuron's membrane potential. Therefore, after a neuron spikes it requires more input to reach threshold (the same threshold as introduced in the methods chapter) and spike again; consequently a third spike would require even more input. This type of adaptation is used to minimise the number of successive spikes a neuron can respond with.

$$\tau_m \frac{dV}{dt} = -V + S_f - a$$

$$\tau_a \frac{da}{dt} = -a \tag{5.1}$$

$$\text{if } V \geq \theta \text{ then increase adaptation } a \rightarrow a + \beta$$

5.2.2 Resource-based STDP

Heterosynaptic plasticity local to synapses (the sharing of 'resources') extends the typical additive weight update rule described in the methods chapter (and repeated here for convenience, Eq. 5.3). Furthermore, a pool of resources is included, P. Similar to many receptors and proteins which undergo degradation, the pool's resources decay with a time constant of τ_P=1000ms (Eq.5.2)

$$\tau_P \frac{dP}{dt} = -P \tag{5.2}$$

$$\begin{aligned} f(\tau) &= A_p \times \exp\left(\frac{-\tau}{\tau_p}\right) \qquad \text{if } \tau \geq 0 \\ f(\tau) &= A_d \times \exp\left(\frac{\tau}{\tau_d}\right) \qquad \text{if } \tau < 0 \end{aligned}$$

Depressing a synapse (A from Fig. 5.1) When depressing a synapse w_i by $f(\tau)$ if $\tau < 0$, its resources are relocated into the pool:

$$\begin{aligned} P &\rightarrow P + f(\tau) \\ w_i &\rightarrow w_i - f(\tau) \end{aligned} \tag{5.3}$$

Potentiating a synapse (B and C from Fig. 5.1) When potentiating a synapse w_i by $f(\tau)$ if $\tau > 0$, its neighbours are decreased by a function of their distance, x, and the potentiating amount, $f_{LH}[f(\tau), x]$, to a maximum distance, $x_{\max} \approx 10$ synapses, with resources drawn from the pool if necessary.

As neighbours may not have the required amount of resources a cumulative amount is used which includes only those resources that are available: Ω. When a neighbour has enough resources to donate, the full amount is added to Ω and subsequently to the potentiating synapse (lines 2 and 3 in pseudocode and 3a and 3b in equation 5.5). However, if a neighbour does not have enough resources, the amount they *do* have is added to Ω and the rest is taken from the pool (lines 5 to 7 in pseudocode and 5 and 6&7 in equation 5.5). And if the pool does not have enough the potentiating synapse does not get the full amount (lines 9 and 10 in pseudocode and 8 and 9&10 in equation 5.5).

```
1   FOR each neighbour
2       IF enough resources in neighbour
3           move resources directly from neighbour to potentiating synapse
4       IF NOT enough resources in neighbour
5           IF enough total resources in pool
6               move remaining resources from neighbour (depleting it)
                  to potentiating synapse
7               move resources from pool to potentiating synapse
8           IF NOT enough total resources in pool
9               move remaining resources from neighbour (depleting it)
                  to potentiating synapse
10              move remaining resources from pool (depleting it)
                  to potentiating synapse
```

$$w_i \rightarrow w_i + \Omega \tag{5.4}$$

$$
\begin{array}{rl}
1 & \text{for } x = 1 \text{ to } x_{\max}\text{:} \\
2 & \quad \text{if } w_{i\pm x} \geq f_{LH}\left[f(\tau), x\right] \\
3a & \quad\quad w_{i\pm x} \rightarrow w_{i\pm x} - f_{LH}\left[f(\tau), x\right] \\
3b & \quad\quad \Omega \rightarrow \Omega + f_{LH}\left[f(\tau), x\right] \\
4 & \quad \text{if } w_{i\pm x} < f_{LH}\left[f(\tau), x\right] \\
5 & \quad\quad \text{if } P \geq f_{LH}\left[f(\tau), x\right] - w_{i\pm x} \\
6\&7 & \quad\quad\quad \Omega \rightarrow \Omega + w_{i\pm x} \\
6\&7 & \quad\quad\quad \Omega \rightarrow \Omega + \left(f_{LH}\left[f(\tau), x\right] - w_{i\pm x}\right) \\
6\&7 & \quad\quad\quad P \rightarrow P - \left(f_{LH}\left[f(\tau), x\right] - w_{i\pm x}\right) \\
6\&7 & \quad\quad\quad w_{i\pm x} \rightarrow 0 \\
8 & \quad\quad \text{else} \\
9\&10 & \quad\quad\quad \Omega \rightarrow \Omega + w_{i\pm x} \\
9\&10 & \quad\quad\quad \Omega \rightarrow \Omega + P \\
9\&10 & \quad\quad\quad w_{i\pm x} \rightarrow 0 \\
9\&10 & \quad\quad\quad P \rightarrow 0
\end{array}
\tag{5.5}
$$

Specifically, the amount taken off synapse w_i's neighbours is a trapezoidal Riemann sum of a half-bounded interval $[x-1, x[$ for a specific synapse of a decaying exponential with a time constant $\tau_x \approx 3$ describing the maximum distance to retrieve resources from ($x_{\max} \approx 10$ synapses). This must be adjusted, ψ, because two sums total the amount required for potentiating (one in each direction away from the potentiating synapse) and is adjusted to match the potentiating amount, $f(\tau)$.

$$\psi = 0.5 \frac{1}{\int_{x=0}^{x_{\max}} e^{\left(\frac{-x}{\tau_x}\right)} dx} f(\tau)$$
$$f_{LH}[f(\tau), x] = \tfrac{1}{2}\left[e^{\left(\frac{-x-1}{\tau_x}\right)} + e^{\left(\frac{-x}{\tau_x}\right)}\right]\psi \tag{5.6}$$

Our typical STDP implementation uses learning rates assigned with λ=1.05 (cf. Eq. 2.4). This is suited because random activity results in the same number of spike pairings for both potentiation and depression, and thus overall depression slightly dominates (Song et al. 2000; Izhikevich and Desai 2003; Bush et al. 2010). However with local heterosynaptic plasticity, depression greatly dominates as every potentiation event is accompanied by an equal amount of depression (resources permitting); therefore λ has to be decreased. We adjusted λ and found that learning was best with $\lambda = 0.18$. If $\lambda > 0.18$, depression dominated too much and a pattern was not learnt, and if $\lambda < 0.18$, potentiation dominated. Essentially, we found the same balance between potentiation and depression where depression slightly dominates—as with λ=1.05—however adjusted for resource-based STDP. The resulting new STDP learning window is shown in figure 5.2.

5.3 Results

Our resource-based STDP (rbSTDP) includes extra computational aspects when compared to typical STDP (tSTDP); the first set of results will be comparing the two.

5.3.1 Learning rates, speed and accuracy

In order to compare the two learning rules, appropriate learning rates have to be chosen; as the learning rules have various time constants the learning rate can have a great impact on the learning. Therefore, we varied the learning rate while recording both the performance (the percentage of trials where a neuron learnt the stimulus) and the number of pattern presentations it took until the stimulus was learnt (its learning speed): see figure 5.3. When considering both the performance and the number of pattern presentations, resource-based STDP learns quicker for all learning rates and more accurately for most. We kept all other parameters in the learning rules constant and identical between the two learning rules.

Table 5.1: Table of parameters

Parameter	Description	Value
N_{input}	Number of input afferents.	2000
I	Input.	-
I^{in}	Input transmitting the repeated pattern.	-
I^{noise}	Input not transmitting the repeated pattern.	-
dt	Euler-integration time step.	0.1ms
τ_m	Membrane time constant.	10ms
θ	Firing threshold.	1
θ_r	Rise time constant for alpha function.	1ms
θ_f	Fall time constant for alpha function.	5ms
S_r	Rise synaptic current of alpha function.	-
S_f	Fall synaptic current of alpha function.	-
$f(\tau)$	STDP function.	-
τ	Temporal distance between pre- and postsynaptic activity.	-
τ_p	Potentiation time constant for STDP function.	20ms
τ_d	Depression time constant for STDP function.	20ms
A_p	Positive learning rate.	$0.002 \times W^{\text{P}}_{\text{max}}$
A_d	Negative learning rate.	$-A_p \times \left(\frac{\tau_p}{\tau_d}\right) \times \lambda$
λ	Parameter adjusting the proportionality of the learning rates.	0.18
$W^{\text{P}}_{\text{max}}$	Maximum synaptic weight for input afferents.	$1/N_{\text{input}}$
a	Adaptation amount.	-
τ_a	Time constant for adaptation.	100ms
β	Adaptation increment.	0.18
P	The pool of resources.	Initially 0.
τ_P	Time constant for decay of pool.	1000ms
$f_{LH}[f(\tau), x]$	Potentiating amount in resource-based STDP.	–
x_{max}	Maximum distance of neighbours.	10
Ω	Cumulative amount of resources.	Initially 0.
τ_x	Decay constant for neighbour distance.	≈ 3

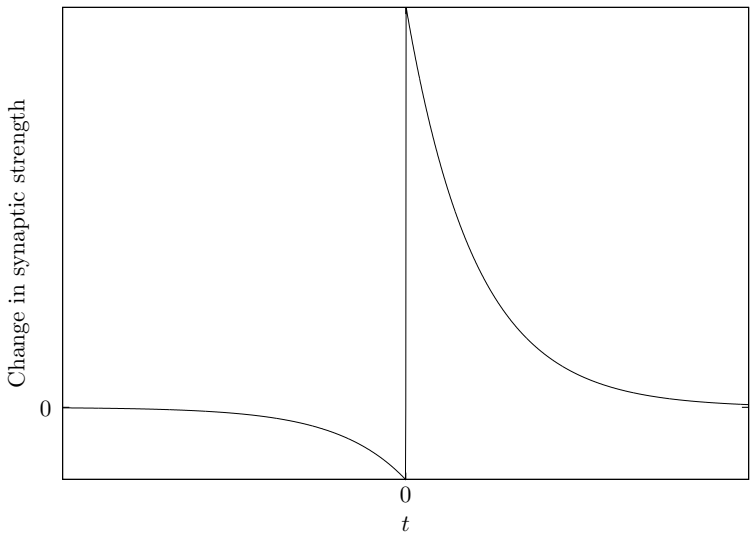

Figure 5.2: STDP curve for learning with resource-based STDP. The STDP curve for the learning rule being described herein is different from typical STDP functions. This is because depression dominates as every potentiation event is accompanied by an equal amount of depression. Therefore, the depression section of the function is reduced (by reducing λ) to negate this effect. λ=0.18 produces a STDP window with a greatly reduced depression half.

The learning accuracy of the rules further depends on whether adaptation is present or not: see figure 5.4. Resource-based STDP without adaptation performs the most accurately at 100% and with adaptation this performance only drops to 96%. Typical STDP, with and without adaptation, performs between 96% and 100%. Accuracy is the percentage of trials where the stimulus was learnt. For the rest of this chapter we used adaptation with both resource-based STDP and typical STDP to keep results comparable.

5.3.2 Number of responses to stimulus

We found that—similar to previous studies (Masquelier et al. 2008, 2009)—typical STDP allows a neuron to learn to respond with one action potential near the onset of the stimulus. Resource-based STDP on the other hand did not respond with only one action potential but with one or more and needed adaptation to bring the number of responses down to one: see figure 5.5.

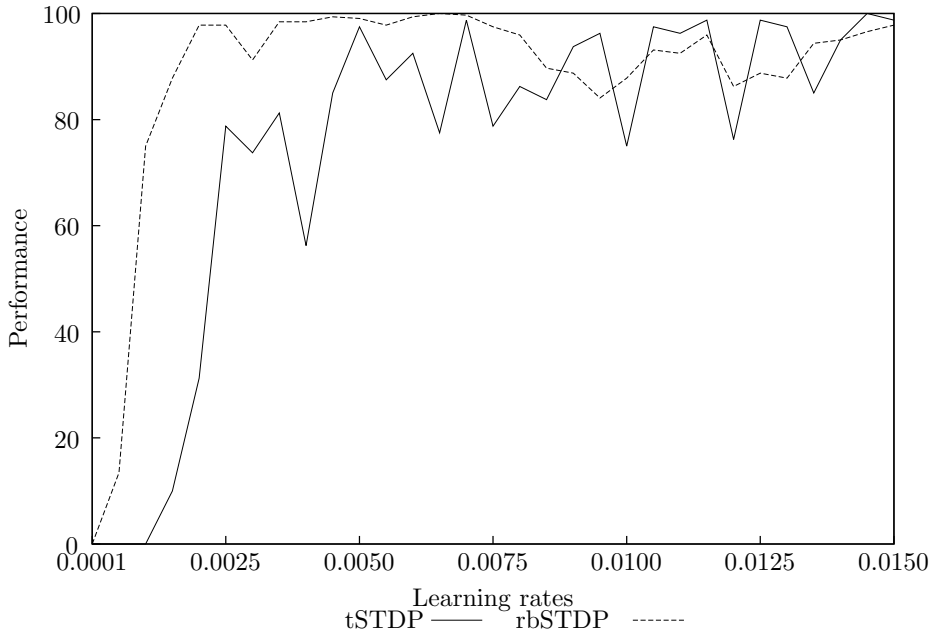

A

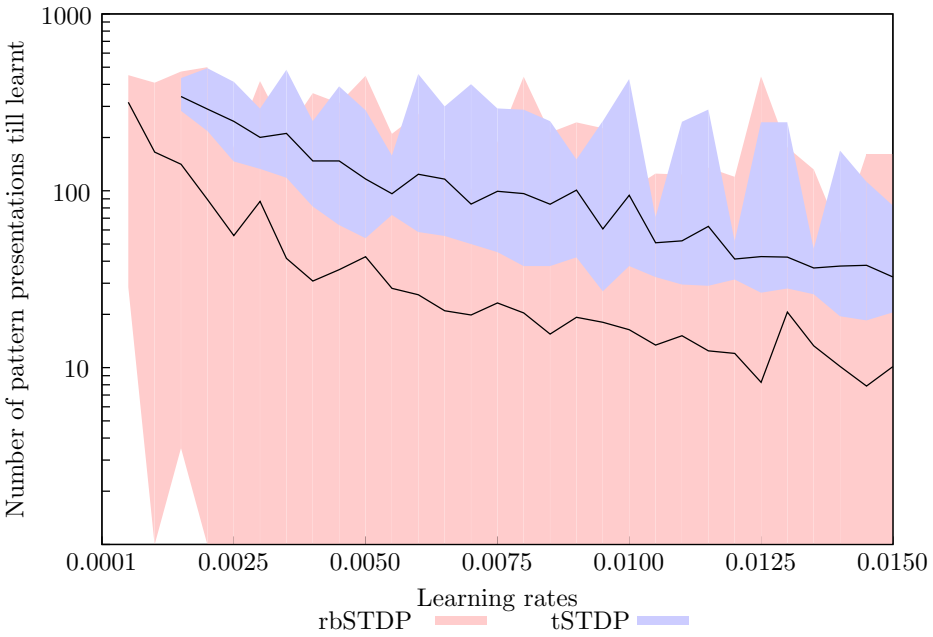

B

Figure 5.3: Effect of adjusting the learning rates. Adjusting the learning rates for both typical STDP rule (tSTDP) and resource-based STDP (rbSTDP) affects the speed and accuracy of learning. Firstly, it is clear that as the learning rate increases both the speed of learning (A) and the mean performance (B) increase. More specifically, the performance of resource-based STDP is greater or equal to that of typical STDP for most learning rates and learns much quicker (roughly a factor of 5 quicker) when considering both overall performance and number of pattern presentations required to learn.

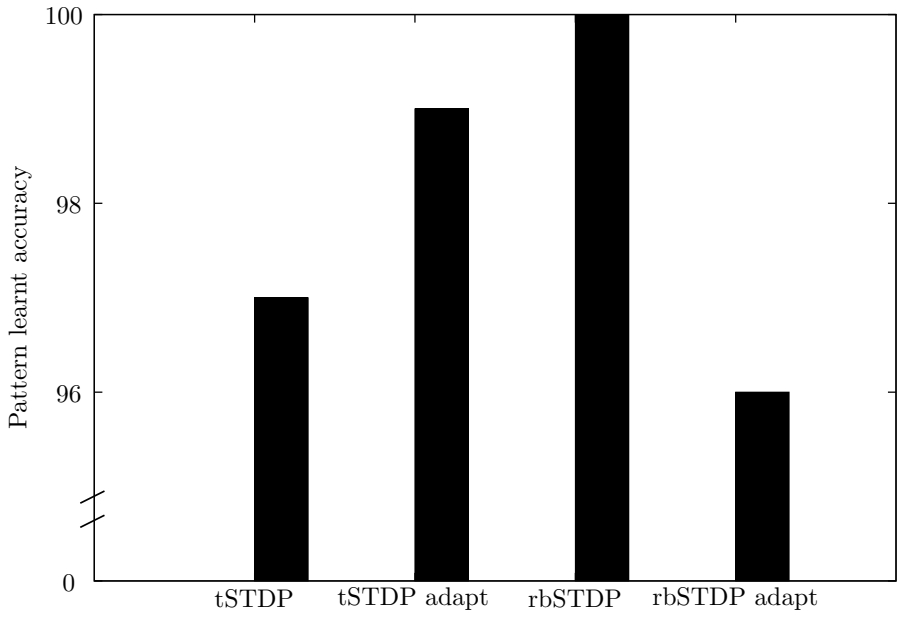

Figure 5.4: The learning accuracy is different for typical STDP and resource-based STDP. They further depend on adaptation. Specifically, resource-based STDP without adaptation has the best accuracy, 100%, and this coupled with adaptation only drops the performance to 96%. Typical STDP's performance with and without adaptation is in-between these two values.

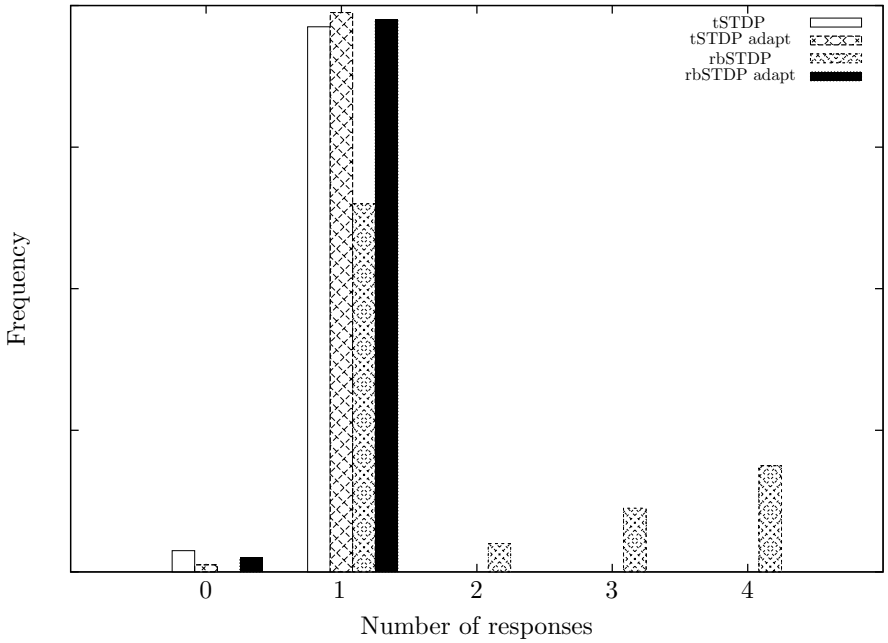

Figure 5.5: The number of response spikes within the stimulus. With and without adaptation typical STDP responds with one action potential the majority of the time, however resource-based STDP requires adaptation to respond with only one action potential, responding up to four times without adaptation.

5.3.3 Afferents' structure

Changing the structure of the afferents can have a negative effect on learning. For example, the structure can be changed such that there are 1600 afferents with 70% presenting the stimulus, or there can be 2400 afferents with only 30% presenting the stimulus. But, because STDP rules and networks have to commonly be set up to learn under strict parameters, such a change can result in a network no longer learning correctly. Figure 5.6 shows the results of such an experiment, where we modified the afferents' structure and recorded how well both typical STDP and resource-based STDP fair (both with and without adaptation).

As mentioned, implementations depend on set parameters for specific scenarios; in the typical STDP case, the maximum synaptic weight is set to facilitate learning on 2000 afferents with 50% presenting the stimulus; this could be changed to allow learning of different afferents' structures however as we are studying how well the learning rule can perform to an afferent structure that it is *not* specifically tuned to, we kept this constant. Resource-based STDP's parameters are set similarly to accommodate 2000 afferents with half presenting the stimulus.

The results in Fig. 5.6 show that typical STDP is only able to produce an ideal response for a small subset of afferents' structures with or without adaptation, whereas resource-based STDP with adaptation is able to respond ideally across a much greater range of afferents' structures. Specifically, a neuron with resource-based STDP is able to learn a pattern when presented on 240 afferents (600 total with 40% presenting the pattern), 2700 afferents (3000 total with 90% presenting the pattern) and all combination in-between. This is a multiple of more than 11 times the number of afferents presenting the pattern.

This is not the only advantage of resource-based STDP. It further only needs an approximate amount of resources set prior to be able to learn the stimulus when presented across a great range of afferents (320—2700): the initial total amount of resources can change by 15%.

5.3.4 Weight distribution

As described in the introduction empirical and computational synaptic weight distributions do not match; most biological distributions are unimodal with a peak near zero and have a distinc-

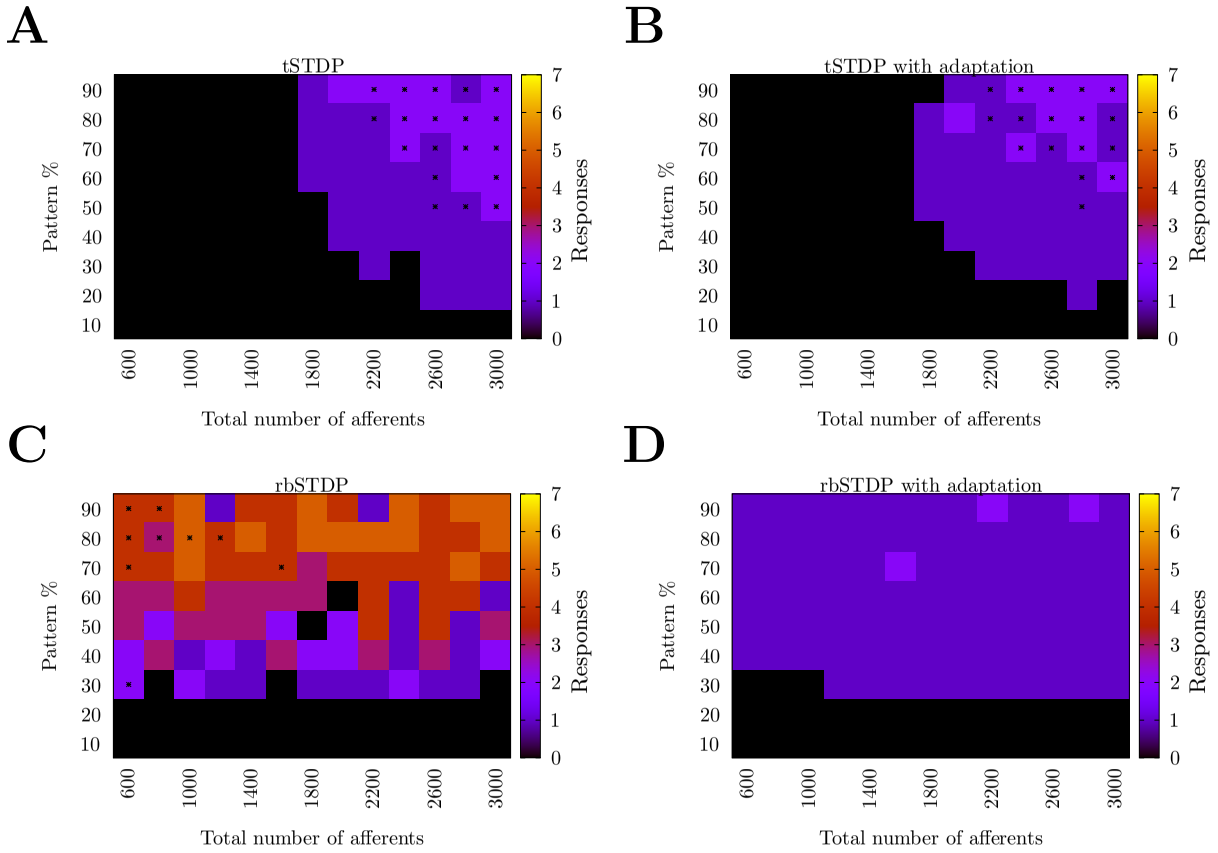

Figure 5.6: Response distributions for typical and resource-based STDP, both with and without adaptation. A) shows the number of responses to different structures for typical STDP; B), for typical STDP with adaptation; C), for resource-based STDP; and D), for resource-based STDP with adaptation. For all figures, the colour bar represents the number of responses within the stimulus (c.f. section 5.3.2) and the asterisk represents the presence of responses when a pattern is not presented. Therefore, the ideal response would be one action potential only when the stimulus is being presented—no asterisk. Such an ideal response is present for a much greater range of structures when using resource-based STDP with adaptation than typical STDP. Specifically, an ideal response can be elicited from 600 afferents with 40% presenting the pattern to 3000 afferents with 90% presenting the pattern.

tive long tail of strong connections with the majority of connections being weak, whereas additive STDP produces a bimodal distribution. Multiplicative STDP produces distributions which are unimodal, however their qualitative skew and peaks are dissimilar to empirical recordings. For example see figure 5.7 where biological and computational distributions are shown.

Figure 5.7A shows experimentally derived distributions which have peaks near zero and tails with fewer synapses of weaker efficacy even though the four distributions are from different sets of neurons/neural regions (Barbour et al. 2007). Furthermore, the distribution in figure 5.7B has the same distribution. This distribution also includes an extra peak at zero of undetected potentially 'silent' synapses. These were estimated from data (Brunel et al. 2004). On the other hand are the distributions resulting from computational studies. Figure 5.7C shows distributions of multiplicative and additive STDP and as described above they are unimodal or bimodal respectively. Gutig et al. (2003) further found that these distributions are not mutually exclusive and when they adjusted the extent to which STDP was multiplicative one can interpolate distributions between these two extremes.

Resource-based STDP, however, produces distributions which are very similar to those recorded: see figure 5.8. These results compare favourably to those in figure 5.7. Furthermore, without any mechanism to produce silent synapses they arise out of the resource sharing mechanisms: compare figure 5.7B with figure 5.8.

5.3.5 Weight stability

As described earlier previous studies have found that weights learnt with an additive STDP rule are much more stable than those learnt with a multiplicative STDP rule. To this end, we studied the weight stability of resource-based STDP and found that its stability is very similar to that of typical additive STDP.

Specifically, similar to (Billings and Rossum 2009), we calculated autocorrelations of individual weights and fitted decaying exponentials to these. The fitted time constants of these exponentials varied slightly depending on whether a weight was being potentiated or depressed. The distribution of time constants always had a high peak which we we took as the weight persistence time constant. We found that ordinary STDP decayed with a time constant of $\approx$85 minutes

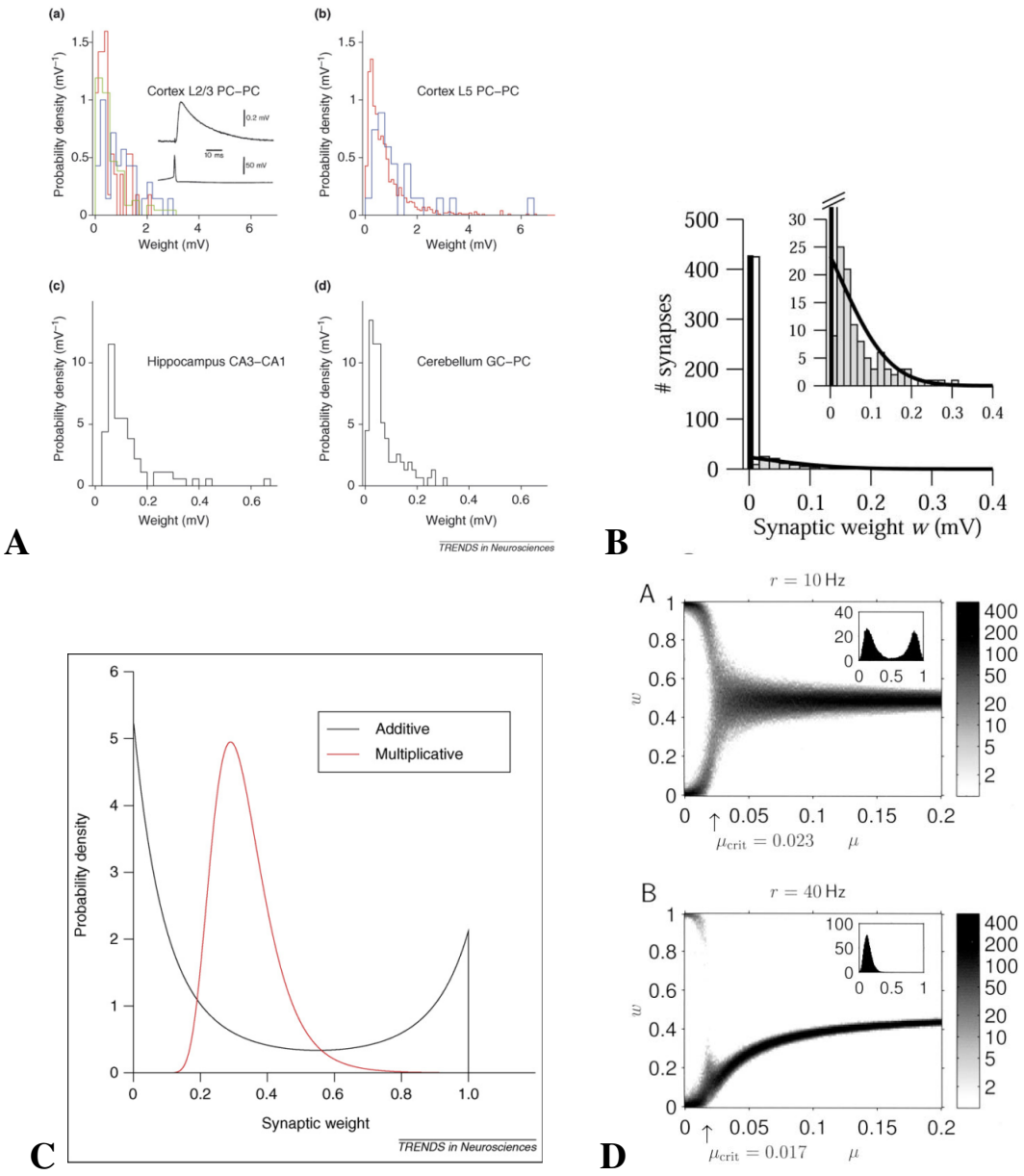

Figure 5.7: Biological and computational synaptic strength distributions. A are a collection of recorded distributions (image from (Barbour et al. 2007)); B is a study which included undetected, potentially 'silent' synapses—the peak at 0 (image from (Brunel et al. 2004)); C shows distributions for additive and multiplicative STDP (image from (Barbour et al. 2007)); and D shows distributions interpolating between additive and multiplicative STDP (image from (Gütig et al. 2003)).

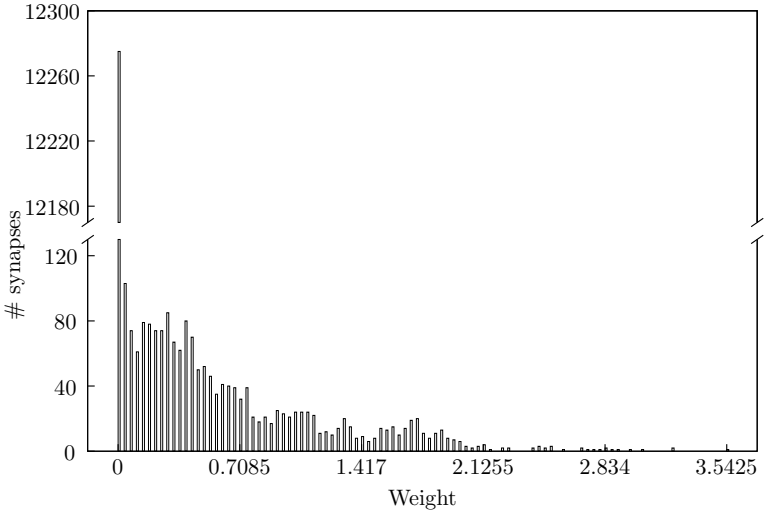

A

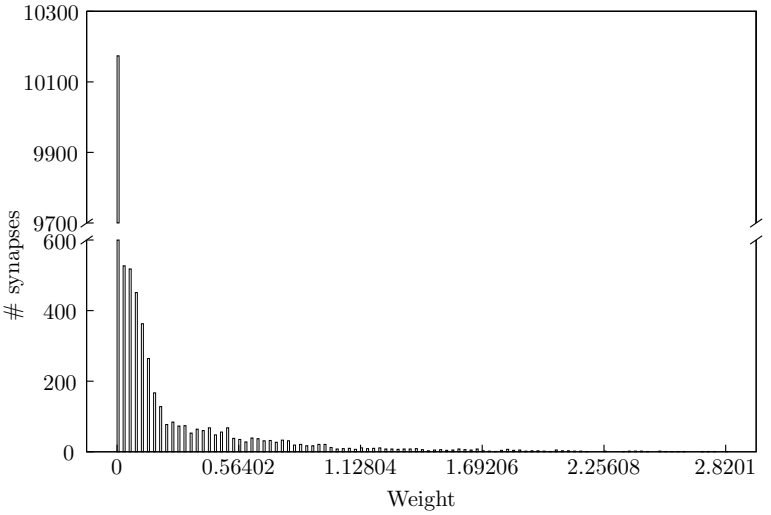

B

Figure 5.8: Two synaptic distributions from two trials of 10 neurons learning the same pattern with resource-based STDP. Both distributions are unimodel with a peak near zero; they have a large tail, and a very large peak of silent synapses. The difference between the two is due to differences in the number of learnt afferents in a pattern and random initial synaptic weights. For example, after learning a neuron may have potentiated 800 (out of the 1000 presenting the pattern) but it may have also potentiated just 200; this would affect the tail of the distribution. Each neuron has 2000 afferents so a total of 20000 data points are in each distribution.

and the proposed learning rule decayed with a time constant of ≈70 minutes.

As was discussed in (Billings and Rossum 2009) the learning rate will have a great effect on these results. We therefore ran our experiment with the optimal learning rates found in section 5.3.1. Therefore both typical and resource-based STDP were tested with their own individual optimal learning rates. If we proportionally adjust our time constants to match those of Billings et al. by matching our typical STDP without adaptation with theirs, resource-based STDP has a time constant of ≈14 hours compared with Billings finding of 18 hours for additive typical STDP and 29 seconds for multiplicative typical STDP.

5.3.6 Weight dependence

Even though the proposed learning rule does not include any weight dependence, we observed weight dependence for potentiation: see figure 5.9. During a simulation we recorded weights' strengths before and after an STDP learning event which would result in potentiation. Because the STDP curve determines the amount of synaptic change depending on the timing, we know the amount of 'required change' and can therefore calculate the percentage of this amount after the STDP event. This is the ordinate in figure 5.9 and is different from the ordinate in Bi and Poo's figure 5 (Bi and Poo 1998). The difference between ordinates is noted as several papers have found weight dependence experimentally but use different ordinates.

Figure 5.9 depicts two clusters of data: the cluster with an average lower synaptic weight are synapses that are not associated with the stimulus but are being potentiated by random (and subsequently depressed), and the cluster with a higher average weight are synapses associated with the stimulus. Our results suggest that resource-based STDP endows a weight dependence for potentiation. Moreover, the weight dependence is not always present as some times synapses will change by the full required amount, even if they are strong.

This weight dependence is due to a lack of resources; for example, if a synapse is attempting to potentiate, but the pool is nearly empty and its neighbours are completely depleted, then the synapse can only potentiate by an amount totalling the resources left in the pool.

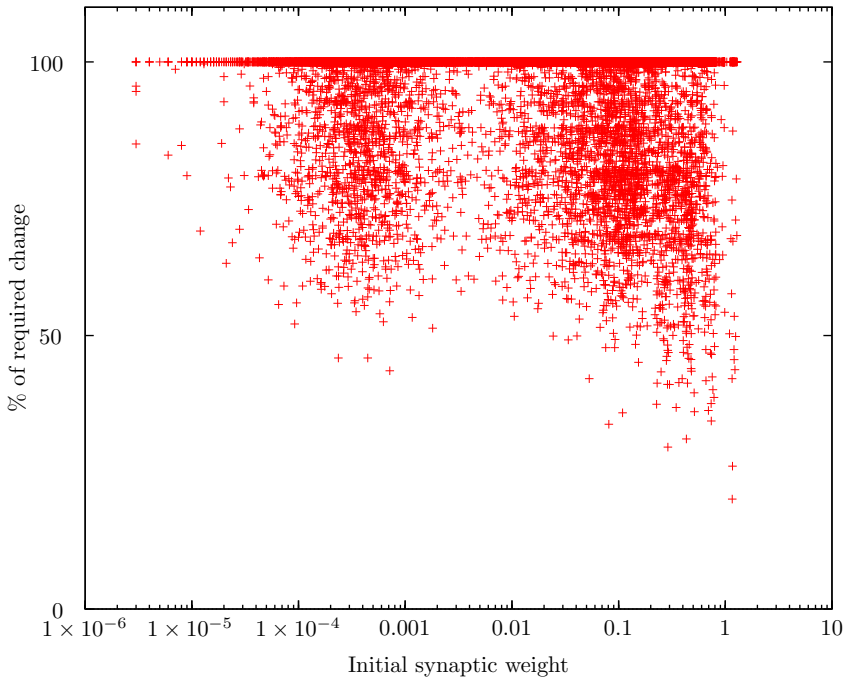

Figure 5.9: Weight dependency from resource-based STDP. A weight dependency was found for potentiation. The ordinate is percent change of the required amount after pairing (for details, see text).

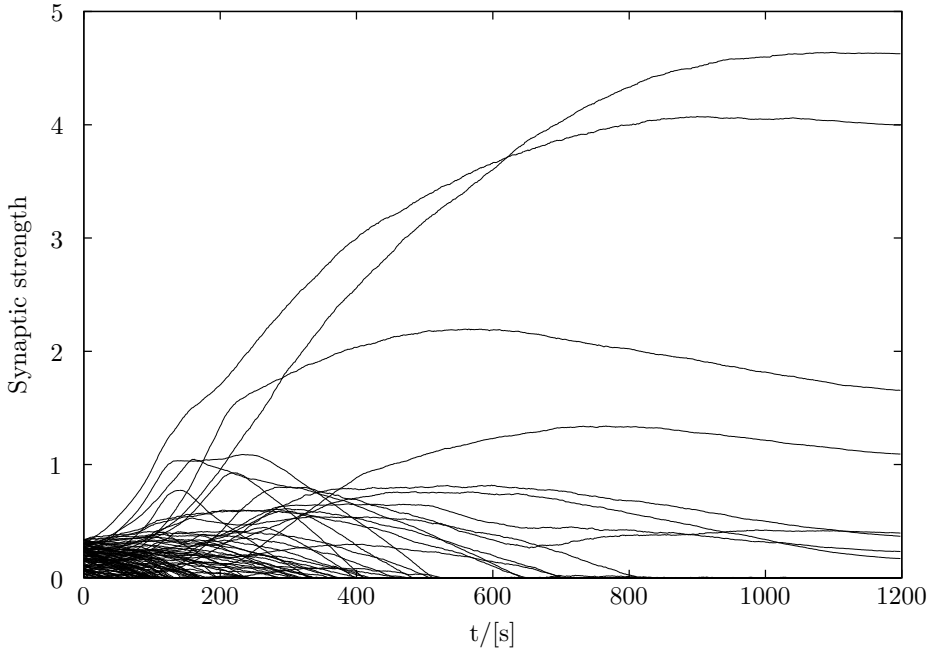

Figure 5.10: During a simulation synapses show plateaus at their own intrinsic upper bounds.

5.3.7 Synaptic bounds

As discussed earlier, many learning rules require global upper bounds (hard or soft) or explicit weight normalisation to control learning and stop runaway potentiating synapses. Resource-based STDP however has no set global upper bound and appears to implement a form of intrinsic synapse specific upper bound due to a limited amount of resources. Furthermore, due to the redistribution of resources, the learning rule implements weight normalisation indirectly. Figure 5.10 shows the learning of synapses during a simulation and depicts synapses saturating at different strengths.

5.3.8 Multiple patterns

In certain cases it is possible for a singular neuron to learn two patterns. With typical STDP these two patterns must be presented on relatively few afferents (600 or 800). Resource-based STDP on the other hand allows a single neuron to learn two patterns with a greater range of different afferent numbers. See figure 5.11 for results of typical STDP and resource-based STDP. Fig. 5.11A shows the percentage of trials when a neuron learnt two patterns when the

total number of afferents was adjusted and 5.11B when the percentage of afferents presenting the pattern was changed; resource-based STDP was able to learn two patterns across the full range of number of afferents and percentage of afferents while typical STDP, not.

5.4 Discussion

Due to limitations and missing phenomena when using typical additive exponential STDP learning rules, we developed a novel resource-based STDP learning rule. We found that resource-based STDP has many advantages over a typical STDP rule. We further found that it produces results which are comparable to biological results:

Learning accuracy and speed. Overall, a neuron with resource-based STDP learns as, or more, accurately than typical STDP. The learning speed is improved by approximately a factor of five.

Afferents' structure. Resource-based STDP displays a remarkable ability to allow a neuron to learn a stimulus presented across great numbers of different afferents (320—2700). More specifically, this is possible with only one set of parameters (which in themselves can change 15%). This is a major advantage over typical STDP whereby one must pick a set of parameter values prior to simulation depending on the number of afferents a stimulus is presented on and any prior change to these parameter values may lead to a total failure of learning.

Weight distributions and silent synapses. The weight distributions produced by resource-based STDP are a favourably better match to those recorded empirically than typical implementations of additive or multiplicative STDP. Specifically, a typical multiplicative STDP rule will produce a unimodal synaptic strength distribution with a peak near the mean of synaptic strengths and a typical additive STDP rule will produce a bimodal distributions with peaks at the upper and lower bounds. However, biological findings have found that synaptic efficacy distributions are unimodal with a peak near zero and a long tail of more potentiated synapses. Such a distribution is also produced by resource-based STDP.

Furthermore, estimates of silent synapses which may be missed by current recording

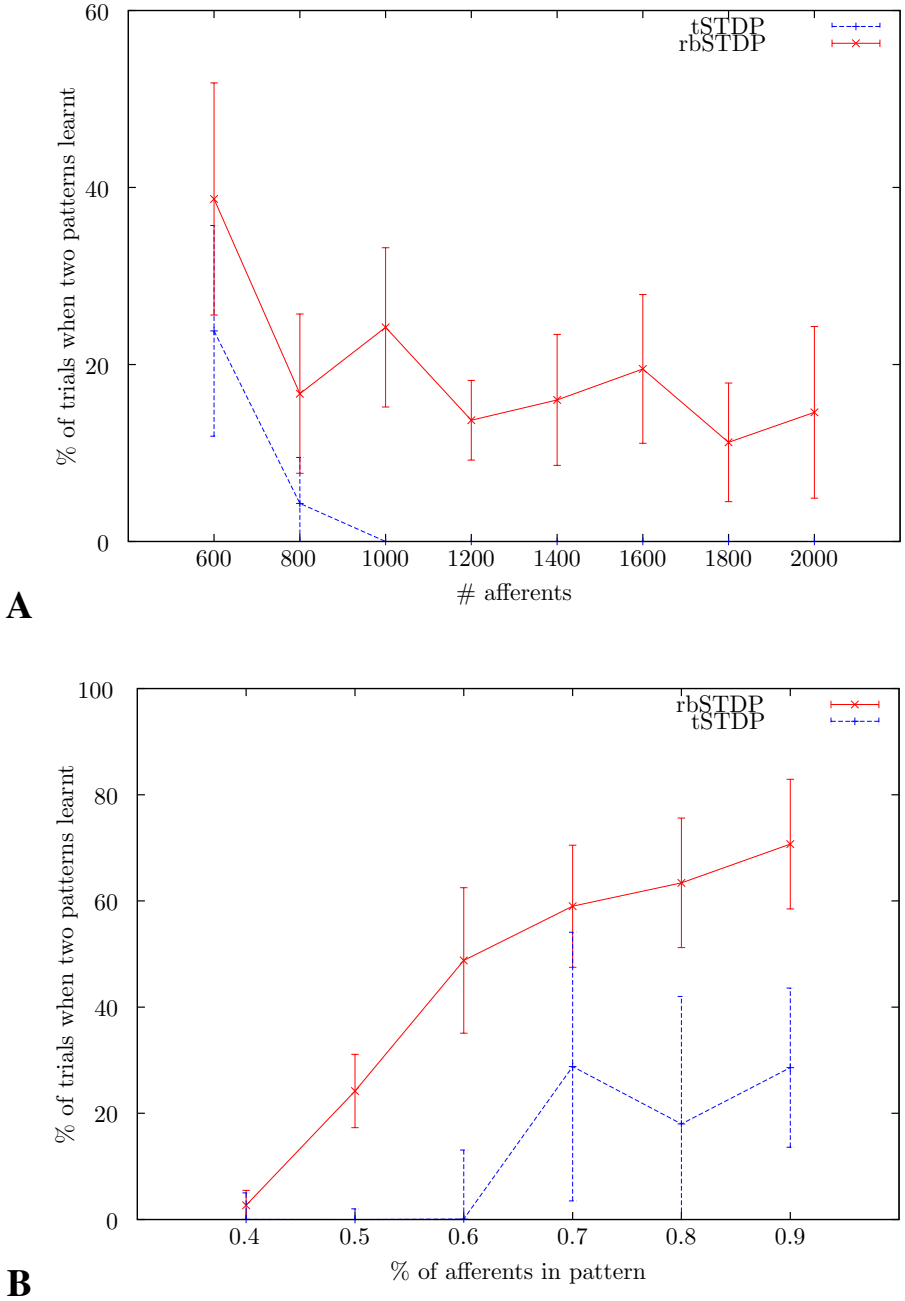

Figure 5.11: Comparing the ability of typical STDP with resource-based STDP to learn multiple patterns presented on the same afferents. A) depicts the ability of each learning rule to learn two patterns when the number of afferents is changed (while keeping the percentage of afferents constant at 50%) and B) shows the percentage of trials when the new learning rule learns two patterns when the percentage of afferents presenting the pattern is changed (while keeping the number of afferents constant at 1000).

technology and protocols show similar qualitative results to resource-based STDP. These silent synapses arise purely from the resource sharing mechanism as their is no explicit mechanism in the learning rule to produce them. Therefore this presents the hypothesis that perhaps 'silent' synapses found experimentally are the result of a synapse running out of 'resources'.

Weight stability and competition. A common problem with typical STDP is the trade off between weight stability (additive) and weight distribution (multiplicative). Resource-based STDP produces weight distributions more realistic than multiplicative typical STDP while still retaining the weight stability of additive typical STDP.

Another common distinction between multiplicative and additive STDP rules are their synaptic competition. Additive STDP produces strong competition whereas multiplicative rules have little to no competition between synapses. Resource-based STDP is still additive so retains its strong competition. In fact, the synaptic competition is stronger in the new learning rule as every potentiation can lead to a potentially unwanted depression in neighbours.

Weight dependence. As described in the introduction there are many studies finding weight dependence for depression when spike timing is considered and potentiation when spike timing is not considered; resource-based STDP has weight dependence for potentiation.

Our results are in accordance with the results of Bi & Poo (1998) because the rule is additive for both potentiation and depression; therefore, it is not expected that there would be a depressive dependence on initial weight strength. Furthermore the dependence for potentiation is an additional phenomenon predicted by resource based learning rule. This dependence on resources may be analogous to non-potentiable (run out of resources) and silent synapses (have had all resources depleted). As suggested previously, it is possible that weight dependence is not required directly, and perhaps the empirical results suggesting weight dependence are in fact indicative of an additive rule with some other mechanisms producing the results seen (suggested by Standage, et al (2007) and discussed by Debanne et al. (1999)).

Synaptic bounds and non-potentiable synapses. Typical STDP can either have global soft (multiplicative) or hard (additive) upper bounds with the choice greatly impacting the learning. Resource-based STDP has no such global upper synaptic constraint. Instead, a synapse can continue to potentiate until no more resources are available. Therefore, each synapse has its own intrinsic upper bound depending on its initial weight and the availability and competition of resources from its neighbours and the pool. Such intrinsic bounds have been considered before (Standage and Trappenberg 2007).

Having no upper bound is an advantage over typical STDP as the upper bound has to be set prior—with knowledge of the learning process and usually the stimulus—and if set incorrectly can lead to learning failure.

We also found that resource-based STDP allowed a single neuron to learn two patterns more consistently and across a greater range of afferents' structures than typical STDP. Having neurons that learn multiple patterns could be useful in a network; it is possible that a distributed and sparse code of patterns could be learnt with several neurons in a network representing more than one pattern.

5.4.1 Possible signalling mechanisms and resource molecules.

Even though our model is phenomenological it is interesting to consider what our resources could be and what mechanisms could fulfil the signalling requirements. Considering resources, a very attractive candidate is (among others) AMPA receptors:

AMPA receptors AMPA receptors are strongly implicated in LTP and LTD with a change in exocytosis (Hayashi et al. 2000; Shi et al. 2001; Carroll et al. 1999; Shi et al. 2001; Takahashi et al. 2003; Bredt and Nicoll 2003; Oh et al. 2006; Park et al. 2006; Serulle et al. 2007; Yang et al. 2008), endocytosis (Carroll et al. 1999; Seidenman et al. 2003; Beattie et al. 2000; Lissin et al. 1999; Carroll et al. 1999; Collingridge et al. 2004; Derkach et al. 2007; Bredt and Nicoll 2003; Luthi et al. 1999; Man et al. 2000), channel increase (Benke et al. 1998) and decrease, changes in recycling endosomes that process AMPA receptors (Oh et al. 2006; Park et al. 2004, 2006; Prekeris et al. 1998, 1999; Lee et al. 2001),

insertion (Sutton et al. 2006) and removal of endoplasmic reticulum and Golgi apparatus from spines which synthesize proteins for and related to AMPA receptors.

In addition to their critical role in LTP and LTD, AMPA receptors are present in several pools: (1) the recycling endosomes (Park et al. 2004, 2006) and early endosomes (Rácz et al. 2004) in/near spines which form part of their constitutive pathway of insertion and internalization; (2) endoplasmic reticulum and Golgi outposts which are present throughout dendrites (Horton and Ehlers 2004, 2003). Furthermore, Park et al. (2004) demonstrated that AMPA receptors move between plasma membrane and recycling compartments; this maintains AMPA receptors in a "dynamic pool" that is able to rapidly respond to any NMDA receptor activation.

In addition, AMPA receptors have been found to traffic long distances. For example, from the soma to dendrites on the neuron's membrane (Mammen et al. 1997), along dendritic membranes (Choquet and Triller 2003; Triller and Choquet 2005; Borgdorff and Choquet 2002; Passafaro et al. 2001; Shi et al. 1999), and along microtubules (Washbourne et al. 2002; Hirokawa and Takemura 2005; Lisé et al. 2006; Osterweil et al. 2005). More specifically, GluR1s can move rapidly (within 1 minute) through silenced synapses before remaining at a nearby active synapse (Ehlers et al. 2007) and evidence suggests that extrasynaptic receptors act as a reserve that can be mobilized on demand (Groc et al. 2004).

Several molecular mechanisms have been proposed for heterosynaptic plasticity including:

- Nitrogen oxide (NO) diffuses through cell membranes and mediates changes in the release probability of other synapses (Schuman and Madison 1994; Gally et al. 1990; Böhme et al. 1991; O'Dell et al. 1991)

- Calcium has been implicated in many signalling cascades so it is no surprise that it has also been theorised to contribute to heterosynaptic plasticity. For example, back propagating action potentials increase Ca^{2+} across broad areas of dendritic trees (Jaffe et al. 1992; Petrozzino and Connor 1994; Yuste et al. 1994; Schiller et al. 1995) and fast large

increases in intracellular Ca^{2+} lead to LTP (Yang et al. 1999) whereas brief small increases induces either LTP or LTD. Further, calcium diffusion is distance dependent and this has been hypothesised for heterosynptic plasticity which results in plasticity of opposite direction (Royer and Paré 2003; White et al. 1990; Coussens and Teyler 1996).

Furthermore, a myriad of possible mechanisms have been proposed for, or implicated in, synaptic scaling include intracellular calcium (Yu et al. 2009; Davis and Bezprozvanny 2001; Ibata et al. 2008; Thiagarajan et al. 2005; Abraham and Tate 1997), calcium buffers such as CaMKII (Turrigiano 1999) and CaMKIV (Ibata et al. 2008; Turrigiano 2008), a change in endocytic exit sites (Pérez-Otaño and Ehlers 2005), BDNF (Rutherford et al. 1998), ARC (Shepherd et al. 2006; Rial Verde et al. 2006; Tzingounis and Nicoll 2006), TNFα (Stellwagen and Malenka 2006; Popivanova et al. 2008) and Retanoic Acid (Aoto et al. 2008; Maghsoodi et al. 2008).

Below, are some of these and other candidates for signalling the local heterostatic modifications in our resource-based STDP.

PSD-95 PSD-95 binds to stargazin and other TARP family proteins and subsequently TARPs bind to all four subunits of AMPA receptors (Chen et al. 2000; Nicoll et al. 2006). This binding is crucial for AMPA receptor targeting to synapses (Chen et al. 2000; Tomita et al. 2005). PSD-95 also binds directly to NMDA receptors (Niethammer et al. 1996; O'Brien et al. 1998). It is the most abundant PSD component (Cheng et al. 2006; Niell et al. 2004; Sugiyama et al. 2005) so is potentially readily available for signalling. Furthermore, the stability of PSD-95 at synapses can be modulated by activity (Colledge et al. 2003; El-Husseini et al. 2002; Bingol and Schuman 2004; Okabe et al. 1999) and spines' volumes are proportional to postsynaptic domain (PSD) size (Harris and Stevens 1989) and synaptic strength (Nusser et al. 1998; Takumi et al. 1999). Taken together these results suggest that the prime mechanism for regulating synaptic strength is PSD-95 (Ehrlich et al. 2007).

PSD-95 is also very mobile, which is crucial for our signalling mechanism. Sharma et al. (2006) found that within 5 minutes $\approx$25% of spine PSD-95 had exchanged with pools of PSD-95 within the rest of the cell. Moreover, Sharma et al. found that PSD-95 exchanges with neighbouring spines by diffusion and spines therefore share a dynamic

pool of PSD-95. This spread of PSD-95 was bidirectional and after unbinding with a PSD the inter-synapse diffusion time was a remarkable ≈50ms (Sharma et al. 2006). Specifically Sharma et al. found that PSD-95 diffuses along the dendritic shaft until it is trapped by another active PSD, and the trapping properties of PSDs was proportional to their size and large spines held on to PSD-95 for longer.

CaMKII CaMKII is important for LTP because it is autophosphorylated by an increase in intracellular Ca^{2+} influx through NMDA receptors (Lisman 1994; Kennedy et al. 1990; Barria et al. 1997; Takahashi et al. 2003) and subsequently phosphorylates GluR1 (Roche et al. 1996) of AMPA receptors (Mammen et al. 1997; Barria et al. 1997; Hayashi et al. 2000; Shi et al. 2001) and increases their currents (Benke et al. 1998). Furthermore, CaMKII localises to postsynaptic densities (Hanson and Schulman 1992; Lisman et al. 2002; Leonard et al. 1999; Bayer et al. 2001; Ouyang et al. 1997) and causes insertion of AMPA receptors into excitatory synaptic sites (Barria et al. 1997; Lee et al. 2000; Hayashi et al. 2000; Poncer et al. 2002).

Pratt et al. (2003) extensively studied CaMKII and found several important phenomena: (1) correlated pre- and postsynaptic activity activates CaMKII; (2) CaMKII can selectively eliminate synaptic connections; and (3) conclude by commenting that their data "suggest that inputs that are effective at activating CaMKII, [...], will simultaneously enhance themselves and bias inactive synapses toward elimination." Moreover, "the ability of CaMKII to differentiate between active and inactive synapses may allow the activity-dependent activation of a single molecular signal to generate competitive structural rearrangements in synaptic connectivity." (Pratt et al. 2003).

Finally, there is a remarkable arrangement of CaMKII and PP1. These molecules have opposing effects on signalling synaptic efficacy and CaMKII is enhanced in activated PSDs whereas inactive synapses are abundant in PP1 (Ehlers 2003).

Ca^{2+} It is also possible that Ca^{2+} is potentially available as a signalling mechanism because it is critical for much of synaptic plasticity, as described above, however its diffusion can be severally limited by the spine neck.

Synapsis 1 and ProSAP2 Tsuriel et al. (2006) found that Synapsin molecules are continuously interchanging among presynaptic boutons on time-scales of tens of minutes. They further found that molecules of both Synapsin I and ProSAP2 can be reused and reassimilated into synaptic structures after leaving other synapses. This continues until the lifetime of a synaptic protein is reached and are thus replaced. These findings imply that dynamic pools may be shared by neighbouring synapses.

Finally, Royer et al. (2003) found that LTD was found at nearby synaptic sites when LTP was induced and the reverse, however Hou et al. (2008) found no change in GluR1 at neighbouring synapses due to LTP, leading to a contradiction in the current literature. Nevertheless, Miller et al. (1996) suggested that activity-dependent processes do not change a pool of synaptic resources, but merely allocated them.

The most attractive combination of resource molecule and signalling mechanism is AMPA receptors and PSD-95. PSD-95 could signal whether a synapse requires more resources or not and the number of AMPA receptors could be appropriately increased or decreased.

Chapter 6

Conclusions

6.1 What can a neuron learn with STDP?

In this thesis, we found that a neuron, equipped with STDP, learning a repeated spatio-temporal pattern under continuous constant stimulation learns two features of the stimulus to encode a pattern: the average background activity level and specific spikes times 'on top'. Furthermore, we found that modulations in either of these components can disrupt a neuron's ability to learn the onset of a pattern and can result in the neuron learning an arbitrary time in the pattern. For example, a typical unmodified setup will result in a neuron responding at the onset of the pattern however when one of these components are changed a neuron may respond in the middle or near the end of the pattern. Consequently, in a noisier framework—perhaps with greatly fluctuating non-pattern afferent activity as may be the case in biological situations—a neuron may no longer respond (or respond accurately) to its learnt pattern; however, fluctuating background activity, *viz.* oscillations have been used to facilitate learning (Masquelier et al. 2009).

This reliance on background activity has been noted before; for example, Silver (2010) commented that synaptic noise is a mechanism for neuronal arithmetic and Hô et al. (2000) and Shu et al. (2003) found that an increase in synaptic activity may increase the probability of a spike to small input, which is partially supported by our results. We have further adduced its importance during learning with STDP. These results suggest that background modulations on a slower temporal scale may underlie precise spike timing computations on a faster scale; such a segregation was shown by Hô et al. (2000) in reconstructed neocortical pyramidal neurons. Furthermore, our results suggest that when presenting a stimulus to a neuron, the neuron may not respond due to a lack of background activity and that a lack of a response may not necessarily mean a presented stimulus is not preferred by a neuron. Appropriately designed neurophysiological experiments might be able to (1) find such a phenomenon, which may have implications for finding preferred stimuli of neurons; (2) study the segregation of input; and (3) elucidate further its importance within STDP learning.

The emphasis has been pattern onset learning, however if the task was to simply fire within a learnt pattern the drift described herein does not present a problem. Furthermore, when additional noise was added—if relatively small ($\sigma < 0.4$)—it did not greatly impact on performance,

but did distort response latency distributions in favour for responding with an increased latency. A complete lack of background activity on the other hand may pose a significant complication, and indeed a great amount of additional noise severely impacted on learning performance.

The first half of this research has been presented as a conference contribution (Humble et al. 2010) and all of the work will be published in a forthcoming paper (Humble in preparation A).

6.2 Sequence learning

We extended the network in chapter 3 to include plastic excitatory lateral connections and an inhibitory neuron producing winner-takes-all competition. To summarise, we found that a simple network of laterally connected excitatory neurons can self-organise into spatio-temporal pattern recognisers. Simple Markov-like synfire chains were learnt with nearest-neighbour STDP and more complicated multiple order chains with all-to-all STDP. Furthermore chains recognising different patterns could be joined to represent longer, potentially nested patterns. Even though some limitations must be overcome, the latter offers the possibility to learn graph-like transition patterns with stronger computational capabilities than linear sequences, for example as suggested by Wennekers (2006) or Izhikevich (2009).

Previous attempts to learn synfire chains (Bienenstock 1991; Hertz and Prügel-Bennett 1996) have been somewhat successful. Cyclical chains formed in most previous studies and once activity enters these it never exits. This limitation was not present in our synfire chains and we posit that this is because our setup was stimulus driven–previous studies used random activity.

Our synfire chains took advantage of findings in the first chapter: specifically, lateral connections increase the background activity. When a neuron fires, its lateral connections increase the background activity of those it is connected to. This effectively primes these neurons to respond. This priming becomes crucial to a neuron firing. Therefore, our model has the advantage that if this priming does not take place, a neuron will not respond: the dependence of neurons in a chain on their preceding neurons' activity. This research presented in chapter 4 was published in a recent paper (Humble et al. 2012).

6.3 Resource-based STDP

Limitations of typical STDP implementations and the disparity between experimentally observed phenomena and computational results inspired our development of a novel resource-based STDP learning rule. Specifically, we included local heterosynaptic sharing of 'resources'. When a synapse is potentiated, its neighbours are depressed by an amount dependent on their distance from the potentiating synapse but totalling the same amount. Furthermore, when a synapse is depressed its resources are moved to a communal pool which decays with a time constant of 1000ms (significantly longer than all other time components in the model). This pool provides extra resources for potentiating synapses if their neighbours are depleted.

We found that resource-based STDP has advantages over typical STDP such as faster and more accurate learning. It also reproduces phenomena to this point missing from existing STDP learning rules: synaptic weight distributions, silent synapses, stable weights with competition and non-potentiable synapses. Resource-based STDP also exhibits weight dependence for potentiation and no upper global synaptic bound; instead individual intrinsic upper bounds are present for synapses.

Several candidate molecules were proposed to be 'resources' in our model: AMPA receptors, nitric oxide and calcium. Possible signalling mechanisms include PSD-95, CaMKII, calcium, synapsis 1 and ProSAP2. We propose that AMPA receptors and PSD-95 is a favourable combination for our model. This research with resource-based STDP presented in chapter 5 will be published in an upcoming paper (Humble in preparation B).

6.4 Future

Several further studies could be done to extend the work in this thesis. Firstly, the finding that a neuron with STDP learns two components—the average background activity level and stimulus' spike-timings—is only applicable to the setup used herein. This means that a model without constant input activity—perhaps with only periodic stimulus input, may learn different components of the stimulus. Therefore, different network and input setups should also be used to fully understand what a neuron with STDP learns in different scenarios. It is possible that our

findings may apply to other setups, but it is equally possible that computational STDP utilises different stimulus features depending on setup.

That any potentials studies may find different learnt components has implications for learning synfire chains. We took advantage of STDP learning the level of background activity to prime subsequent neurons in a synfire chain. Neurons were therefore dependent on both stimulus input and preceding neurons responding. However, this dependence may be more difficult to produce in different input scenarios.

Our synfire chains were relatively simple and consisted only of a few neurons responding in sequence to a pattern. We concatenated two chains together to represent a longer sequence that consisted of two stimulus patterns. There are some limitations to chain length discussed in chapter 4 however further research could look at forming more complicated chains or regular expressions.

One approach to learn more complex structures could be to use our resource-based STDP learning rule. Because resource-based STDP has advantages such as weight normalisation it may be able to learn regular expressions. Furthermore, a more complex network with either segregated inhibition or a k-winner-takes-all mechanism could be used. Such possibilities will be included in a paper extending our previous synfire chain paper (Humble et al. 2012).

Finally, experimental setups could address whether any form of resource-based STDP similar to ours is present biologically. Any such setups would need to measure synaptic efficacy on many synapses simultaneously while inducing pre- and postsynaptic activity pairings. An additional mechanism could also be included in resource-based STDP that would increase the pool on request. Such a mechanism might be used to induce learning to a new stimulus sometime after already having learnt one. This mechanism could be unsupervised or supervised. Nevertheless, the research undertaken with resource-based STDP is in a paper under preparation.

Glossary.

$W_{\max}^{\mathrm{P}}$: the upper bound of synapses. A synapse can not potentiated beyond this value.

Δ: a binning factor used to produce S. See S.

λ: a parameter which adjusts the relative contributions of potentiation and depression to the spike-timing-dependent plasticity function.

$\mathbf{P_{orig}}$: the original pattern vector used when computing Φ. See Φ.

$\mathbf{P_{perm}}$: the altered pattern vector used when computing Φ. See Φ.

$\mathbf{S}$: the spatio-temporal receptive field.

Ω: a cumulative amount of resources used when implementing resource-based spike-timing-dependent plasticity.

Φ_α: a sub-space of parameters (jitter amount and number of afferents altered) whereby the spiking neuron model still responded correctly.

Φ_β: a sub-space of parameters (jitter amount and number of afferents altered) whereby the spiking neuron model still responded correctly with additional current.

Φ_γ: a sub-space of parameters (jitter amount and number of afferents altered) whereby the spiking neuron model no longer responded correctly eve with additional current.

$\Phi_{mathrmtolerance}$: a border between Φ_α and Φ_β.

Φ: linear prediction error. The change in $C(t)$ when comparing the maximum value of $C(t)$ with the original pattern and with test input.

ψ: a parameter used in the implementation of resource-based spike-timing-dependent plasticity.

τ_a: time constant for neuronal adaptation. See neuronal adaptation.

τ_f: the fall time constant of the alpha function.

τ_m: see membrane time constant.

τ_r: the rise time constant of the alpha function.

τd: the time constant for the depression contribution the exponential spike-timing-dependent plasticity function.

τp: the time constant for the potentiation contribution the exponential spike-timing-dependent plasticity function.

θ: see Neuronal threshold.

a: amount of adaptation. See neuronal adaptation.

A_d: the negative learning rate. See learning rate.

A_p: the positive learning rate. See learning rate.

$B(t)$: the component representing the background activity.

$C(t)$: the linear predictor. See linear prediction.

D^2: squared van Rossum spike train metric. See van Rossum spike train metric.

$f(\tau)$: the spike-timing-dependent plasticity function. If $\tau \geq 0$ then a synapse is potentiated and if $\tau < 0$ then it is depressed.

$F(t)$: the component representing the fast fluctuations in the neuron's membrane potential due to spike-timing within the pattern.

$f_{LH}[f(\tau), x]$: the potentiating amount for resource-based spike-timing-dependent plasticity which depends on a function of the distance between the potentiating synapse and its neighbours and the spike-timing-dependent function.

$g(t)$: a function of the van Rossum spike train metric. See van Rossum spike train metric.

$h(t)$: a function of the van Rossum spike train metric. See van Rossum spike train metric.

I: input to a neuron. See dendrite.

I^{in}: half of the input afferents that alternate between independent Poisson spike trains and a fixed spatio-temporal pattern.

I^{noise}: half of the input afferents that continuously transmit independent Poisson spike trains.

M: the number of spikes in the original pattern.

N_{input}: the number of input afferents.

P: the pool in resource-based spike-timing-dependent plasticity.

P_{orig}: the original pattern matrix used when computing Φ. See Φ.

P_{perm}: the altered pattern matrix used when computing Φ. See Φ.

$R(t)$: the component representing both $F(t)$ and $B(t)$.

S_f: see synaptic current.

S_r: see synaptic current.

V: see membrane potential.

$W_{\max}^{\mathrm{L}}$: the maximum synaptic weight for lateral synapses between excitatory neurons.

w_i: a specific synapse indexed by i.

$x_{\max}$: the maximum distance to take resources from neighbouring synapses when implementing resource-based spike-timing-dependent plasticity.

τ_c: a parameter in the van Rossum spike train metric. See van Rossum spike train metric.

M': the number of spikes in the altered pattern.

Action potential: a pulse of chemical/electrical activity that is propagated down a neuron's axon due to its membrane potential reaching threshold.; often called a spike.

Activity-dependent plasticity: a form of plasticity that is controlled by activity.

Afferent: describes incoming synapses.

All-to-all: a form of spike-timing-dependent plasticity which includes all pre- and postsynaptic action potentials when computing synaptic efficacy changes.

Alpha function: a function describing synaptic currents. See synaptic current.

AMPA receptor: a receptor commonly found at synapses that transduces neurotransmitters to ionic current.

Axon: the output section of a neuron.

Axonal delay: the delay an action potential takes to propagate from the soma to a synapse.

Calcium: calcium is critical in synaptic plasticity as releases the extracellular NMDA block. It has also been implicated in nearly all forms of plasticity.

Computational mode: a mathematical representation of a phenomena which is usually simulated on a computer.

Dendrite: the input section of a neuron.

Depression: the decrease in a synapse's efficacy.

Efferent: describes outgoing synapses.

Excitation: the effect of excitatory synapses. See excitatory synapse.

Excitatory neuron: a neuron which has an excitatory effect on postsynaptic neurons. See excitatory synapse.

Excitatory synapse: a synapse which increases membrane potential.

Firing rate: the average rate a neuron is producing action potentials.

Hebbian: a type of synaptic plasticity learning named after Dr. Hebb. Hebbian plasticity describes an increase in synaptic efficacy for activity correlated across a synapse and a decrease in efficacy for uncorrelated activity.

Heterostasis: see heterosynaptic plasticity.

Heterosynaptic plasticity: describes cases where the induction of one form of plasticity is accompanied by the induction of another.

Hodgkin-Huxley model: the first model which models different ionic channels of neurons.

Homeostasis: see homeostatic plasticity.

Homeostatic plasticity: a form of plasticity which adjusts a neuron's synapses so some property of them (usually the average synaptic efficacy) is at a preset value.

Information theory: a theory explaining information such as mutual information. See mutual information.

Inhibition neuron: a neuron which has an inhibitory effect on postsynaptic neurons. See inhibitory synapse.

Inhibition: the effect of inhibitory synapses. See inhibitory synapse.

Inhibitory synapse: a synapse which decreases membrane potential.

Input-output relationship: the relationship between input to a neuron and any induced output action potentials or changes in membrane potential.

Integrate-and-fire model: one of the most simple models of a neuron which includes the integration of input to a threshold and the resulting action potential

Ion channel: a channel in a neuron's membrane which allows the passing of ions. These ions then adjust the potential different across the membrane.

Jitter: a adjustment in the timing of an action potential.

Latency: a delay that usually describes the delay between stimulus and response.

Leaky integrate-and-fire model: an extension of the integrate-and-fire model which includes leak currents which allow electrical current to constantly exit a neuron.

Learning rate: the rate at which synaptic efficacy is changed in a computational model. A higher rate describes a quick change in efficacy.

Linear prediction: is a method whereby future values are predicted as a linear function of previous values.

Linear predictor: a function that operates linear prediction.

Long-term depression: a long term decrease in a synapse's efficacy.

Long-term potentiation: a long term increase in a synapse's efficacy.

Membrane potential: the voltage across the membrane of a neuron.

Membrane time constant: the time constant with which the membrane potential relaxes to a resting potential.

Mutual information: the amount of information that is communicated between transmitter and receiver.

Nearest-neighbour: a form of spike-timing-dependent plasticity which only includes one pre- and one postsynaptic action potential when computing synaptic efficacy changes.

Network: more than one neuron connected via synapses.

Neuron: the specialised cell found throughout the central nervous system and brain.

Neuronal adaptation: adaptation has a negative effect on a neuron's membrane potential every time a neuron produces an action potential. This leads to the scenario where every response from a neuron makes it more difficult to produce another.

Neuronal reset value: the voltage to which a neuron is 'reset' after an action potential is produced. This value can be different to resting.

Neuronal threshold: a voltage level at which an action potential is produced. In neurons this threshold is not a fixed value however in many models such as the leaky integrate-and-fire model the value *is* fixed for simplicity

Neurotransmitter: chemicals/proteins which pass across a synapse transducing chemical/electrical activity from one neuron to another.

NMDA receptor: a receptor that is crucial to many forms of plasticity including long-term and potentiation and depression and spike-timing-dependent plasticity.

Non-potentiable synapse: a synapse which cannot undergo potentiation under an experimental protocol.

Pattern learning: a type of learning which is concerned with learning specific, often, repeated stimuli (patterns).

Plastic: see plasticity

Plasticity: a change in the efficacy of a synapse.

Poisson noise: noise which follows the Poisson distribution. That is, the probability of a number of events occurring with a given average rate independently and within a fixed interval.

Population: several neurons which often cooperate to achieve a task.

Postsynaptic: referring to the neuron after a synapse.

Potentiation: the increase in a synapse's efficacy.

Presynaptic: referring to the neuron before a synapse.

Receptive field: describes a subsection of input which a neuron is sensitive to. Receptive fields can be spatial or temporal.

Receptor: a structure which transduces incoming chemicals such as neurotransmitters into intracellular current.

Refractory period: a period after a neuron has produced an action potential within which is is difficult to produce another action potential (relative refractory period) or impossible (absolute refractory period).

Response distribution: the distribution of number of response spikes within a presented stimulus.

Resting potential: the voltage at which a neuron will rest/stay if no input is present.

Rheobase: the minimum current that will produce an action potential.

Self-organising map: often describes a network of neurons which organise without external pressure.

Silent synapse: a synapse which exhibits no detectable AMPA receptors and therefore theoretically will not transduce any bound neurotransmitter into chemical/electrical activity.

Soma: the main body section of a neuron.

Spatio-temporal receptive field: see receptive field.

Spike count: the number (count) of action potentials (spikes) within a set period.

Spike train metric: a metric which describes certain properties of a spike train.

Spike train: a series of spikes in sequence. The delays between spikes do not have to be constant and the spikes can come at various times.

Spike-timing-dependent plasticity: a type of plasticity that permits the spike time differences between pre- and postsynaptic activities to affect changes in synaptic efficacy.

Spike-timing: describing the specific times of action potentials (spikes).

Spike: see action potential.

Stimulus-response transducer: a model that characterises the transduction of stimulus into response.

Synapse: a structure that permits chemical/electrical activity to pass from one neuron to another.

Synaptic bound: a value which bounds synaptic change. For exmaple, if two synaptic bounds of 0 and 10 were enforced then a synapse could be not be set less than 0 or greater than 10.

Synaptic current: a synapse does not transduce neurotransmitters into an instantaneous increase or decrease in membrane potential but rather has a current profile that gradually increases and/or decreases.

Synaptic efficacy: how effective a synapse is at transducing incoming activity to either an increase or decrease in membrane potential.

Synaptic scaling: a form of homeostatic plasticity which adjusts synaptic efficacies so the average value is at a preset value. See homeostatic plasticity.

Synfire chain: a theoretical network where several neurons are connected in sequence allowing the propagation of activity accurately from 'layer' to layer.

van Rossum spike train metric: a certain spike train metric. See spike train metric.

Weight normalisation: a computational tool to normalise synaptic efficacies over a neuron.

Weight: see synaptic efficacy.

Winner-takes-all competition: such competition describes how, out of several neurons, one one may fire at a time due to competition. When one neuron does produce an action potential it inhibits (either directly or via an inhibitory inter-neuron) all other neurons.

List of references.

Abeles, M. (1982), *Local cortical circuits: An electrophysiological study*, Springer-Verlag New York.

Abeles, M. (1991), *Corticonics: Neural circuits of the cerebral cortex*, Cambridge Univ Pr.

Abraham, W. C., Dragunow, M. and Tate, W. (1991), 'The role of immediate early genes in the stabilization of long-term potentiation', *Molecular Neurobiology* **5**(2), 297–314.

Abraham, W. C. and Goddard, G. (1983), 'Asymmetric relationships between homosynaptic long-term potentiation and heterosynaptic long-term depression', *Nature* **305**(5936), 717–9.

Abraham, W. C., Logan, B., Greenwood, J. and Dragunow, M. (2002), 'Induction and experience-dependent consolidation of stable long-term potentiation lasting months in the hippocampus', *Journal of Neuroscience* **22**(21), 9626–34.

Abraham, W. C., Mason, S., Demmer, J., Williams, J., Richardson, C., Tate, W., Lawlor, P. and Dragunow, M. (1993), 'Correlations between immediate early gene induction and the persistence of long-term potentiation', *Neuroscience* **56**(3), 717–27.

Abraham, W. C. and Tate, W. P. (1997), 'Metaplasticity: A new vista across the field of synaptic plasticity', *Progress in Neurobiology* **52**(4), 303–23.

Aoto, J., Nam, C., Poon, M., Ting, P. and Chen, L. (2008), 'Synaptic signaling by all-trans retinoic acid in homeostatic synaptic plasticity', *Neuron* **60**(2), 308–20.

Ayzenshtat, I., Meirovithz, E., Edelman, H., Werner-Reiss, U., Bienenstock, E., Abeles, M. and Slovin, H. (2010), 'Precise spatiotemporal patterns among visual cortical areas and their relation to visual stimulus processing.', *Journal of Neuroscience* **30**(33), 11232–45.

Bacci, A., Coco, S., Pravettoni, E., Schenk, U., Armano, S., Frassoni, C., Verderio, C., De Camilli, P. and Matteoli, M. (2001), 'Chronic blockade of glutamate receptors enhances presynaptic release and downregulates the interaction between synaptophysin-synaptobrevin vesicle-associated membrane protein 2', *Journal of Neuroscience* **21**(17), 6588–96.

Barbour, B., Brunel, N., Hakim, V. and Nadal, J.-P. (2007), 'What can we learn from synaptic weight distributions?', *Trends in Neurosciences* **30**(12), 622–9.

Barria, A., Derkach, V. and Soderling, T. (1997), 'Identification of the Ca2+/Calmodulin-dependent Protein Kinase II Regulatory Phosphorylation Site in the Amino-3-hydroxyl-5-

methyl4-isoxazole-propionate-type Glutamate Receptor', *Journal of Biological Chemistry* **272**(52), 32727–30.

Bastrikova, N., Gardner, G., Reece, J., Jeromin, A. and Dudek, S. (2008), 'Synapse elimination accompanies functional plasticity in hippocampal neurons.', *Proceedings of the National Academy of Sciences of the United States of America* **105**(8), 3123–3127.

Bayer, K. U., De Koninck, P., Leonard, a. S., Hell, J. W. and Schulman, H. (2001), 'Interaction with the NMDA receptor locks CaMKII in an active conformation.', *Nature* **411**(6839), 801–5.

Beattie, E., Carroll, R., Yu, X., Morishita, W., Yasuda, H., Von Zastrow, M. and Malenka, R. (2000), 'Regulation of AMPA receptor endocytosis by a signaling mechanism shared with LTD', *Nature Neuroscience* **3**(12), 1291–300.

Bell, C., Han, V., Sugawara, Y. and Grant, K. (1997), 'Synaptic plasticity in a cerebellum-like structure depends on temporal order', *Nature* **387**, 278–81.

Benke, T., Luthi, A., Isaac, J. and Collingridge, G. (1998), 'Modulation of AMPA receptor unitary conductance by synaptic activity', *Nature* **393**(6687), 793–97.

Bernander, O., Douglas, R., Martin, K. and Koch, C. (1991), 'Synaptic background activity influences spatiotemporal integration in single pyramidal cells.', *Proceedings of the National Academy of Sciences of the United States of America* **88**(24), 11569–73.

Bi, G. and Poo, M. (1998), 'Synaptic Modifications in Cultured Hippocampal Neurons: Dependence on Spike Timing, Synaptic Strength, and Postsynaptic Cell Type', *Journal of Neuroscience* **18**(24), 10464–72.

Bi, G. and Poo, M. (1999), 'Distributed synaptic modification in neural networks induced by patterned stimulation.', *Nature* **401**(6755), 792–6.

Bi, G.-Q. (2002), 'Spatiotemporal specificity of synaptic plasticity: cellular rules and mechanisms.', *Biological cybernetics* **87**(5-6), 319–32.

Bienenstock, E. (1991), 'Notes on the growth of a composition machine', *Proceedings of First Interdisciplinary Workshop on Cognition and Neural Networks* pp. 25–43.

Bienenstock, E. (1995), 'A model of neocortex', *Network: Computation in Neural Systems* **6**(2), 179–224.

Billings, G. and Rossum, M. C. W. V. (2009), 'Memory retention and Spike Timing Dependent Plasticity', *Journal of Neurophysiology* **101**(6), 2775–88.

Bingol, B. and Schuman, E. M. (2004), 'A proteasome-sensitive connection between PSD-95 and GluR1 endocytosis.', *Neuropharmacology* **47**(5), 755–63.

Bliss, T. and Collingridge, G. (1993), 'A synaptic model of memory: long-term potentiation in the hippocampus', *Nature* **361**(6407), 31–9.

Bliss, T. and Gardner-Medwin, A. (1973), 'Long-lasting potentiation of synaptic transmission in the dentate area of the unanaesthetized rabbit following stimulation of the perforant path', *Journal of Physiology* **232**(2), 357–74.

Böhme, G., Bon, C., Stutzmann, J., Doble, A. and Blanchard, J. (1991), 'Possible involvement of nitric oxide in long-term potentiation', *European Journal of Pharmacology* **199**(3), 379–81.

Borgdorff, A. J. and Choquet, D. (2002), 'Regulation of AMPA receptor lateral movements.', *Nature* **417**(6889), 649–53.

Bradler, J. and Barrionuevo, G. (1989), 'Long-term potentiation in hippocampal CA3 neurons: Tetanized input regulates heterosynaptic efficacy', *Synapse* **4**(2), 132–42.

Branco, T., Staras, K., Darcy, K. J. and Goda, Y. (2008), 'Local dendritic activity sets release probability at hippocampal synapses.', *Neuron* **59**(3), 475–85.

Bredt, D. S. and Nicoll, R. a. (2003), 'AMPA receptor trafficking at excitatory synapses.', *Neuron* **40**(2), 361–79.

Brunel, N., Hakim, V., Isope, P., Nadal, J.-P. and Barbour, B. (2004), 'Optimal information storage and the distribution of synaptic weights: perceptron versus Purkinje cell.', *Neuron* **43**(5), 745–57.

Burkitt, A., Meffin, H. and Grayden, D. (2004), 'Spike-timing-dependent plasticity: the relationship to rate-based learning for models with weight dynamics determined by a stable fixed point', *Neural Computation* **16**(5), 885–940.

Burrone, J., Neves, G., Gomis, A., Cooke, A. and Lagnado, L. (2002), 'Endogenous calcium buffers regulate fast exocytosis in the synaptic terminal of retinal bipolar cells', *Neuron* **33**(1), 101–12.

Bush, D., Philippides, A., Husbands, P. and O'Shea, M. (2010), 'Reconciling the STDP and BCM models of synaptic plasticity in a spiking recurrent neural network.', *Neural computation* **22**(8), 2059–85.

Carroll, R., Beattie, E., Xia, H., Luscher, C., Altschuler, Y., Nicoll, R., Malenka, R. and Von Zastrow, M. (1999), 'Dynamin-dependent endocytosis of ionotropic glutamate receptors', *Proceedings of the National Academy of Sciences of the United States of America* **96**(24), 14112–7.

Casagrande, V. A. and Kaas, J. H. (1994), 'The afferent, intrinsic, and efferent connections of primary visual vortex in primates', *Cerebral Cortex* **10**, 201–59.

Câteau, H. and Fukai, T. (2003), 'A stochastic method to predict the consequence of arbitrary forms of spike-timing-dependent plasticity', *Neural Computation* **15**(3), 597–620.

Chance, F., Abbott, L. and Reyes, A. (2002), 'Gain modulation from background synaptic input', *Neuron* **35**(4), 773–82.

Chen, L., Chetkovich, D. M., Petralia, R. S., Sweeney, N. T., Kawasaki, Y., Wenthold, R. J., Bredt, D. S. and Nicoll, R. a. (2000), 'Stargazin regulates synaptic targeting of AMPA receptors by two distinct mechanisms.', *Nature* **408**(6815), 936–43.

Cheng, D., Hoogenraad, C., Rush, J., Ramm, E., Schlager, M., Duong, D., Xu, P., Wijayawardana, S., Hanfelt, J., Nakagawa, T., Sheng, M. and Peng, J. (2006), 'Relative and absolute quantification of postsynaptic density proteome isolated from rat forebrain and cerebellum', *Molecular and Cellular Proteomics* **5**(6), 1158–70.

Chistiakova, M. and Volgushev, M. (2009), 'Heterosynaptic plasticity in the neocortex.', *Experimental Brain Research* **199**(3-4), 377–90.

Choquet, D. and Triller, A. (2003), 'The role of receptor diffusion in the organization of the postsynaptic membrane.', *Nature reviews. Neuroscience* **4**(4), 251–65.

Colledge, M., Snyder, E. M., Crozier, R. a., Soderling, J. a., Jin, Y., Langeberg, L. K., Lu, H., Bear, M. F. and Scott, J. D. (2003), 'Ubiquitination regulates PSD-95 degradation and AMPA receptor surface expression.', *Neuron* **40**(3), 595–607.

Collingridge, G. L., Isaac, J. T. R. and Wang, Y. T. (2004), 'Receptor trafficking and synaptic plasticity.', *Nature reviews. Neuroscience* **5**(12), 952–62.

Coussens, C. M. and Teyler, T. J. (1996), 'Long-term potentiation induces synaptic plasticity at nontetanized adjacent synapses.', *Learning and Memory* **3**(2-3), 106–14.

Cowan, N. (1998), *Attention and memory: An integrated framework*, Oxford University Press, USA.

Davis, G. and Bezprozvanny, I. (2001), 'Maintaining the stability of neural function: a homeostatic hypothesis', *Annuual Review Physiology* **63**, 847–69.

Debanne, D., Gähwiler, B. H. and Thompson, S. M. (1999), 'Heterogeneity of synaptic plasticity at unitary CA3-CA1 and CA3-CA3 connections in rat hippocampal slice cultures.', *Journal of Neuroscience* **19**(24), 10664–71.

Derkach, V. a., Oh, M. C., Guire, E. S. and Soderling, T. R. (2007), 'Regulatory mechanisms of AMPA receptors in synaptic plasticity', *Nature Reviews Neuroscience* **8**(2), 101–13.

Desai, N. S., Cudmore, R. H., Nelson, S. B. and Turrigiano, G. G. (2002), 'Critical periods for experience-dependent synaptic scaling in visual cortex.', *Nature Neuroscience* **5**(8), 783–9.

Dunwiddie, T. and Lynch, G. (1978), 'Long-term potentiation and depression of synaptic responses in the rat hippocampus: localization and frequency dependency.', *The Journal of Physiology* **276**(1), 353–67.

Edwards, F. a., Konnerth, A. and Sakmann, B. (1990), 'Quantal analysis of inhibitory synaptic transmission in the dentate gyrus of rat hippocampal slices: a patch-clamp study.', *Journal of Physiology* **430**, 213–49.

Ehlers, M. D. (2003), 'Activity level controls postsynaptic composition and signaling via the ubiquitin-proteasome system', *Nature Neuroscience* **6**(3), 231–42.

Ehlers, M. D., Heine, M., Groc, L., Lee, M.-C. and Choquet, D. (2007), 'Diffusional trapping of GluR1 AMPA receptors by input-specific synaptic activity.', *Neuron* **54**(3), 447–60.

Ehrlich, I., Klein, M., Rumpel, S. and Malinow, R. (2007), 'PSD-95 is required for activity-driven synapse stabilization', *Proceedings of the National Academy of Sciences of the United States of America* **104**(10), 4176–81.

El-Husseini, A., Schnell, E., Dakoji, S., Sweeney, N., Zhou, Q., Prange, O., Gauthier-Campbell, C., Aguilera-Moreno, A., Nicoll, R. and Bredt, D. (2002), 'Synaptic strength regulated by palmitate cycling on PSD-95', *Cell* **108**(6), 849–63.

Feldmeyer, D., Egger, V., Lubke, J. and Sakmann, B. (1999), 'Reliable synaptic connections between pairs of excitatory layer 4 neurones within a single 'barrel' of developing rat somatosensory cortex.', *Journal of Physiology* **521 Pt 1**, 169–90.

Feldmeyer, D., Lübke, J. and Sakmann, B. (2006), 'Efficacy and connectivity of intracolumnar pairs of layer 2/3 pyramidal cells in the barrel cortex of juvenile rats.', *Journal of Physiology* **575**(Pt 2), 583–602.

Fellous, J., Rudolph, M., Destexhe, A. and Sejnowski, T. (2003), 'Synaptic background noise controls the input/output characteristics of single cells in an in vitro model of in vivo activity', *Neuroscience* **122**(3), 811–29.

Fox, K. (2008), *Barrel Cortex*, Cambridge University Press.

Frerking, M., Borges, S. and Wilson, M. (1995), 'Variation in GABA mini amplitude is the consequence of variation in transmitter concentration', *Neuron* **15**(4), 885–95.

Gally, J. a., Montague, P. R., Reeke, G. N. and Edelman, G. M. (1990), 'The NO hypothesis: possible effects of a short-lived, rapidly diffusible signal in the development and function of the nervous system.', *Proceedings of the National Academy of Sciences of the United States of America* **87**(9), 3547–51.

Gerstner, W. and Kistler, W. (2002), *Spiking Neuron Models*, Cambridge University Press.

Goel, A. and Lee, H.-K. (2007), 'Persistence of experience-induced homeostatic synaptic plasticity through adulthood in superficial layers of mouse visual cortex.', *Journal of Neuroscience* **27**(25), 6692–700.

Goel, M., Sinkins, W. and Schilling, W. (2002), 'Selective association of TRPC channel subunits in rat brain synaptosomes', *Journal of Biological Chemistry* **277**(50), 48303–10.

Groc, L., Heine, M., Cognet, L., Brickley, K., Stephenson, F., Lounis, B. and Choquet, D. (2004), 'Differential activity-dependent regulation of the lateral mobilities of AMPA and NMDA receptors', *Nature Neuroscience* **7**(7), 695–6.

Grunwald, M. E., Mellem, J. E., Strutz, N., Maricq, A. V. and Kaplan, J. M. (2004), 'Clathrin-mediated endocytosis is required for compensatory regulation of GLR-1 glutamate receptors after activity blockade.', *Proceedings of the National Academy of Sciences of the United States of America* **101**(9), 3190–5.

Gütig, R., Aharonov, R., Rotter, S. and Sompolinsky, H. (2003), 'Learning input correlations through nonlinear temporally asymmetric Hebbian plasticity.', *Journal of Neuroscience* **23**(9), 3697–714.

Guyonneau, R., van Rullen, R. and Thorpe, S. (2005), 'Neurons tune to the earliest spikes through STDP.', *Neural Computation* **17**(4), 859–79.

Hahnloser, R. H. R., Kozhevnikov, A. a. and Fee, M. S. (2002), 'An ultra-sparse code underlies the generation of neural sequences in a songbird.', *Nature* **419**(6902), 65–70.

Hanson, P. and Schulman, H. (1992), 'Neuronal Ca2+/calmodulin-dependent protein kinases', *Annual Review of Biochemistry* **61**, 559–601.

Harris, K. M. and Stevens, J. K. (1989), 'Dendritic spines of CA 1 pyramidal cells in the rat hippocampus: serial electron microscopy with reference to their biophysical characteristics.', *Journal of Neuroscience* **9**(8), 2982–97.

Harvey, C. D. and Svoboda, K. (2007), 'Locally dynamic synaptic learning rules in pyramidal neuron dendrites.', *Nature* **450**(7173), 1195–200.

Hayashi, Y., Shi, S., Esteban, J., Piccini, A., Poncer, J. and Malinow, R. (2000), 'Driving AMPA Receptors into Synapses by LTP and CaMKII: Requirement for GluR1 and PDZ Domain Interaction', *Science* **287**(5461), 2262–7.

Hertz, J. and Prügel-Bennett, A. (1996), 'Learning synfire chains: Turning noise into signal', *International Journal of Neural Systems* **7**(4), 445–450.

Hirokawa, N. and Takemura, R. (2005), 'Molecular motors and mechanisms of directional transport in neurons.', *Nature Reviews Neuroscience* **6**(3), 201–14.

Hirsch, J., Alonso, J., Reid, R. and Martinez, L. (1998), 'Synaptic integration in striate cortical simple cells', *Journal of Neuroscience* **18**(22), 9517–28.

Hirsch, J., Barrionuevo, G. and Crepel, F. (1992), 'Homo- and heterosynaptic changes in efficacy are expressed in prefrontal neurons: An in vitro study in the rat', *Synapse* **12**(1), 82–5.

Hô, N. and Destexhe, A. (2000), 'Synaptic background activity enhances the responsiveness of neocortical pyramidal neurons.', *Journal of Neurophysiology* **84**(3), 1488–96.

Hodgkin, A. L. and Huxley, A. F. (1952), 'A quantitative description of membrane current and its application to conduction and excitation in nerve', *The Journal of Physiology* **117**(4), 500–544.

Holmgren, C., Harkany, T., Svennenfors, B. and Zilberter, Y. (2003), 'Pyramidal cell communication within local networks in layer 2/3 of rat neocortex.', *Journal of Physiology* **551**(Pt 1), 139–53.

Horton, A. C. and Ehlers, M. D. (2003), 'Dual modes of endoplasmic reticulum-to-Golgi transport in dendrites revealed by live-cell imaging.', *Journal of Neuroscience* **23**(15), 6188–99.

Horton, A. and Ehlers, M. (2004), 'Secretory trafficking in neuronal dendrites', *Nature Cell Biology* **6**(7), 585–91.

Horton, J. C. and Hocking, D. R. (1996), 'Anatomical demonstration of ocular dominance columns in striate cortex of the squirrel monkey.', *The Journal of Neuroscience* **16**(17), 5510–22.

Hosaka, R., Araki, O. and Ikeguchi, T. (2008), 'STDP provides the substrate for igniting synfire chains by spatiotemporal input patterns.', *Neural computation* **20**(2), 415–35.

Hou, Q., Zhang, D., Jarzylo, L., Huganir, R. L. and Man, H.-Y. (2008), 'Homeostatic regulation of AMPA receptor expression at single hippocampal synapses.', *Proceedings of the National Academy of Sciences of the United States of America* **105**(2), 775–80.

Humble, J., Denham, S. and Wennekers, T. (in preparation), What can a neuron learn with STDP?

Humble, J., Denham, S. and Wennekers, T. (in preparation), Synaptic homeostasis arising from spike-timing-dependent plasticity with heterostasis.

Humble, J., Denham, S. and Wennekers, T. (2012), 'Spatio-temporal pattern recognizers using spiking neurons and spike-timing-dependent plasticity', *Frontiers in Computational Neuroscience* **6**(October), 1–12.

Humble, J., Furber, S., Denham, S. and Wennekers, T. (2010), STDP pattern onset learning depends on background activity, *in* 'Proceedings of BICS 2010 - Brain Inspired Cognitive Systems'.

Ibata, K., Sun, Q. and Turrigiano, G. G. (2008), 'Rapid synaptic scaling induced by changes in postsynaptic firing.', *Neuron* **57**(6), 819–26.

Ikegaya, Y., Aaron, G., Cossart, R., Aronov, D., Lampl, I., Ferster, D. and Yuste, R. (2004), 'Synfire chains and cortical songs: temporal modules of cortical activity.', *Science* **304**(5670), 559–64.

Isope, P. and Barbour, B. (2002), 'Properties of unitary granule cell–>Purkinje cell synapses in adult rat cerebellar slices.', *Journal of Neuroscience* **22**(22), 9668–78.

Izhikevich, E. and Hoppensteadt, F. (2009), 'Polychronous Wavefront Computations', *International Journal of Bifurcation and Chaos* **19**, 1733–9.

Izhikevich, E. M. (2006), 'Polychronization: computation with spikes.', *Neural Computation* **18**(2), 245–82.

Izhikevich, E. M. and Desai, N. S. (2003), 'Relating STDP to BCM.', *Neural computation* **15**(7), 1511–23.

Jaffe, D., Johnston, D., Lasser-Ross, N., Lisman, J., Miyakawa, H. and Ross, W. (1992), 'The spread of Na+ spikes determines the pattern of dendritic Ca2+ entry into hippocampal neurons', *Nature* **357**(6375), 244–6.

Ju, W., Morishita, W., Tsui, J., Gaietta, G., Deerinck, T. J., Adams, S. R., Garner, C. C., Tsien, R. Y., Ellisman, M. H. and Malenka, R. C. (2004), 'Activity-dependent regulation of dendritic synthesis and trafficking of AMPA receptors.', *Nature Neuroscience* **7**(3), 244–53.

Kennedy, M., Bennett, M., Bulleit, R., Erondu, N., Jennings, V., Miller, S., Molloy, S., Patton, B. and Schenker, L. (1990), Structure and regulation of type II calcium/calmodulin-dependent protein kinase in central nervous system neurons, *in* 'Cold Spring Harbor Symposia on Quantitative Biology', Vol. 55, Cold Spring Harbor Laboratory Press, pp. 101–10.

Kepecs, A., Wang, X.-J. and Lisman, J. (2002), 'Bursting neurons signal input slope.', *The Journal of Neuroscience* **22**(20), 9053–62.

Koester, H. J. and Johnston, D. (2005), 'Target cell-dependent normalization of transmitter release at neocortical synapses.', *Science* **308**(5723), 863–6.

Kohonen, T. (1995), *Self-Organizing Maps*, Vol. 30 of *Springer Series in Information Sciences*, Springer.

Kossel, A., Bonhoeffer, T. and Bolz, J. (1990), 'Non-Hebbian synapses in rat visual cortex.', *Neuroreport* **1**(2), 115–8.

Lapicque, L. (1907), 'Recherches quantitatives Sur l'excitation electrique des nerfs traitee comme une polarisation', *Journal de physiologie* **9**, 620–635.

Lee, H. K., Barbarosie, M., Kameyama, K., Bear, M. F. and Huganir, R. L. (2000), 'Regulation of distinct AMPA receptor phosphorylation sites during bidirectional synaptic plasticity.', *Nature* **405**(6789), 955–9.

Lee, S., Valtschanoff, J., Kharazia, V., Weinberg, R. and Sheng, M. (2001), 'Biochemical and morphological characterization of an intracellular membrane compartment containing AMPA receptors', *Neuropharmacology* **41**(6), 680–92.

Legenstein, R., Naeger, C. and Maass, W. (2005), 'What can a neuron learn with spike-timing-dependent plasticity?', *Neural Computation* **17**(11), 2337–82.

Leonard, A., Lim, I., Hemsworth, D., Horne, M. and Hell, J. (1999), 'Calcium/calmodulin-dependent protein kinase II is associated with the N-methyl-D-aspartate receptor', *Proceedings of the National Academy of Sciences of the United States of America* **96**(6), 3239–44.

Levy, W. and Steward, O. (1979), 'Synapses as associative memory elements in the hippocampal formation', *Brain Research* **175**(2), 233–45.

Levy, W. and Steward, O. (1983), 'Temporal contiguity requirements for long-term associative potentiation/depression in the hippocampus.', *Neuroscience* **8**(4), 791–7.

Linden, D. and Connor, J. (1995), 'Long-term synaptic depression', *Annual Review of Neuroscience* **18**, 319–57.

Linsker, R. (1988), Self-organization in a perceptual network, Technical report.

Lisé, M., Wong, T., Trinh, A., Hines, R., Liu, L., Kang, R., Hines, D., Lu, J., Goldenring, J., Wang, Y. and A., E.-H. (2006), 'Involvement of myosin Vb in glutamate receptor trafficking', *Journal of Biological Chemistry* **281**(6), 3669–78.

Lisman, J. (1994), 'The CaM kinase II hypothesis for the storage of synaptic memory', *Trends in Neurosciences* **17**(10), 406–12.

Lisman, J., Schulman, H. and Cline, H. (2002), 'The molecular basis of CaMKII function in synaptic and behavioural memory.', *Nature Reviews Neuroscience* **3**(3), 175–90.

Lissin, D., Carroll, R., Nicoll, R., Malenka, R. and von Zastrow, M. (1999), 'Rapid, activation-induced redistribution of ionotropic glutamate receptors in cultured hippocampal neurons', *Journal of Neuroscience* **19**(4), 1263–72.

Lissin, D. V., Gomperts, S. N., Carroll, R. C., Christine, C. W., Kalman, D., Kitamura, M., Hardy, S., Nicoll, R. a., Malenka, R. C. and von Zastrow, M. (1998), 'Activity differentially regulates the surface expression of synaptic AMPA and NMDA glutamate receptors.', *Proceedings of the National Academy of Sciences of the United States of America* **95**(12), 7097–102.

Luthi, A., Chittajallu, R., Duprat, F., Palmer, M., Benke, T., Kidd, F., Henley, J., Isaac, J. and Collingridge, G. (1999), 'Hippocampal LTD expression involves a pool of AMPARs regulated by the NSF-GluR2 interaction', *Neuron* **24**(2), 389–99.

MacKay, D. and Miller, K. (1990), 'Analysis of Linsker's application of Hebbian rules to linear networks', *Network: Computation in Neural Systems* **1**(3), 257–97.

Maffei, A., Nelson, S. and Turrigiano, G. (2004), 'Selective reconfiguration of layer 4 visual cortical circuitry by visual deprivation', *Nature Neuroscience* **7**(12), 1353–9.

Maghsoodi, B., Poon, M., Nam, C., Aoto, J., Ting, P. and Chen, L. (2008), 'Retinoic acid regulates RARα-mediated control of translation in dendritic RNA granules during homeostatic synaptic plasticity', *Proceedings of the National Academy of Sciences of the United States of America* **105**(41), 16015–20.

Mammen, a. L., Huganir, R. L. and O'Brien, R. J. (1997), 'Redistribution and stabilization of cell surface glutamate receptors during synapse formation.', *Journal of Neuroscience* **17**(19), 7351–8.

Man, H. Y., Lin, J. W., Ju, W. H., Ahmadian, G., Liu, L., Becker, L. E., Sheng, M. and Wang, Y. T. (2000), 'Regulation of AMPA receptor-mediated synaptic transmission by clathrin-dependent receptor internalization.', *Neuron* **25**(3), 649–62.

Markram, H., Lubke, J., Frotscher, M. and Sakmann, B. (1997), 'Regulation of synaptic efficacy by coincidence of postsynaptic APs and EPSPs', *Science* **275**(5297), 213–5.

Mason, A., Nicoll, A. and Stratford, K. (1991), 'Synaptic transmission between individual pyramidal neurons of the rat visual cortex in vitro', *Journal of Neuroscience* **11**(1), 72–84.

Masquelier, T., Guyonneau, R. and Thorpe, S. (2008), 'Spike timing dependent plasticity finds the start of repeating patterns in continuous spike trains', *PLoS ONE* **3**(1), e1377.

Masquelier, T., Guyonneau, R. and Thorpe, S. (2009), 'Competitive STDP-based spike pattern learning', *Neural Computation* **21**(5), 1259–76.

Masquelier, T. and Thorpe, S. (2007), 'Unsupervised Learning of Visual Features through spike Timing Dependent Plasticity', *PloS Computational Biology* **3**(2), e31.

Miles, R. (1990), 'Variation in strength of inhibitory synapses in the CA3 region of guinea-pig hippocampus in vitro.', *Journal of Physiology* **431**(1), 659–76.

Miller, K. D. (1996), 'Synaptic economics: competition and cooperation in synaptic plasticity.', *Neuron* **17**(3), 371–4.

Misgeld, U., Sarvey, J. and Klee, M. (1979), 'Heterosynaptic postactivation potentiation in hippocampal CA 3 neurons: long-term changes of the postsynaptic potentials', *Experimental Brain Research* **37**(2), 217–29.

Mokeichev, A., Okun, M., Barak, O., Katz, Y., Ben-Shahar, O. and Lampl, I. (2007), 'Stochastic emergence of repeating cortical motifs in spontaneous membrane potential fluctuations in vivo.', *Neuron* **53**(3), 413–25.

Montgomery, J. M., Pavlidis, P. and Madison, D. V. (2001), 'Pair recordings reveal all-silent synaptic connections and the postsynaptic expression of long-term potentiation.', *Neuron* **29**(3), 691–701.

Montgomery, J. and Madison, D. (2004), 'Discrete synaptic states define a major mechanism of synapse plasticity', *Trends in Neurosciences* **27**(12), 744–50.

Morrison, A., Diesmann, M. and Gerstner, W. (2008), 'Phenomenological models of synaptic plasticity based on spike timing.', *Biological Cybernetics* **98**(6), 459–78.

Moulder, K., Jiang, X., Taylor, A., Olney, J. and Mennerick, S. (2006), 'Physiological activity depresses synaptic function through an effect on vesicle priming', *Journal of Neuroscience* **26**(24), 6618–26.

Moulder, K., Meeks, J., Shute, A., Hamilton, C., de Erausquin, G. and Mennerick, S. (2004), 'Plastic elimination of functional glutamate release sites by depolarization', *Neuron* **42**(3), 423–35.

Mu, Y., Otsuka, T., Horton, A., Scott, D. and Ehlers, M. (2003), 'Activity-dependent mRNA splicing controls ER export and synaptic delivery of NMDA receptors', *Neuron* **40**(3), 581–94.

Muller, D., Hefft, S. and Figurov, A. (1995), 'Heterosynaptic interactions between UP and LTD in CA1 hippocampal slices', *Neuron* **14**(3), 599–605.

Nádasdy, Z., Hirase, H., Czurkó, a., Csicsvari, J. and Buzsáki, G. (1999), 'Replay and time compression of recurring spike sequences in the hippocampus.', *Journal of Neuroscience* **19**(21), 9497–507.

Nicoll, R. and Malenka, R. (1995), 'Contrasting properties of two forms of long-term potentiation in the hippocampus', *Nature* **377**(6545), 115–8.

Nicoll, R., Tomita, S. and Bredt, D. (2006), 'Auxiliary subunits assist AMPA-type glutamate receptors', *Science* **311**(5765), 1253–6.

Niell, C. M., Meyer, M. P. and Smith, S. J. (2004), 'In vivo imaging of synapse formation on a growing dendritic arbor.', *Nature Neuroscience* **7**(3), 254–60.

Niethammer, M., Kim, E. and Sheng, M. (1996), 'Interaction between the C terminus of NMDA receptor subunits and multiple members of the PSD-95 family of membrane-associated guanylate kinases', *Journal of Neuroscience* **16**(7), 2157–63.

Nusser, Z., Lujan, R., Laube, G., Roberts, J. D., Molnar, E. and Somogyi, P. (1998), 'Cell type and pathway dependence of synaptic AMPA receptor number and variability in the hippocampus.', *Neuron* **21**(3), 545–59.

O'Brien, R. J., Kamboj, S., Ehlers, M. D., Rosen, K. R., Fischbach, G. D. and Huganir, R. L. (1998), 'Activity-dependent modulation of synaptic AMPA receptor accumulation.', *Neuron* **21**(5), 1067–78.

O'Dell, T. J., Hawkins, R. D., Kandel, E. R. and Arancio, O. (1991), 'Tests of the roles of two diffusible substances in long-term potentiation: evidence for nitric oxide as a possible early retrograde messenger.', *Proceedings of the National Academy of Sciences of the United States of America* **88**(24), 11285–9.

Oh, M. C., Derkach, V. a., Guire, E. S. and Soderling, T. R. (2006), 'Extrasynaptic membrane trafficking regulated by GluR1 serine 845 phosphorylation primes AMPA receptors for long-term potentiation.', *Journal of Biological Chemistry* **281**(2), 752–8.

Okabe, S., Kim, H., Miwa, A., Kuriu, T. and Okado, H. (1999), 'Continual remodeling of postsynaptic density and its regulation by synaptic activity', *Nature Neuroscience* **2**(9), 804–11.

Osterweil, E., Wells, D. and Mooseker, M. (2005), 'A role for myosin VI in postsynaptic structure and glutamate receptor endocytosis', *Journal of Cell Biology* **168**(2), 329–38.

Ouyang, Y., Kantor, D., Harris, K., Schuman, E. and Kennedy, M. (1997), 'Visualization of the distribution of autophosphorylated calcium/calmodulin-dependent protein kinase II after tetanic stimulation in the CA1 area of the hippocampus', *Journal of Neuroscience* **17**(14), 5416–27.

Palm, G. (1991), 'Memory capacities of local rules for synaptic modification', *Concepts in Neuroscience* **2**(1), 97–128.

Park, M., Penick, E., Edwards, J., Kauer, J. and Ehlers, M. (2004), 'Recycling endosomes supply AMPA receptors for LTP.', *Science (New York, N.Y.)* **305**(5692), 1972–5.

Park, M., Salgado, J. M., Ostroff, L., Helton, T. D., Robinson, C. G., Harris, K. M. and Ehlers, M. D. (2006), 'Plasticity-induced growth of dendritic spines by exocytic trafficking from recycling endosomes.', *Neuron* **52**(5), 817–30.

Passafaro, M., Piech, V. and Sheng, M. (2001), 'Subunit-specific temporal and spatial patterns of AMPA receptor exocytosis in hippocampal neurons', *Nature Neuroscience* **4**(9), 917–26.

Pérez-Otaño, I. and Ehlers, M. D. (2005), 'Homeostatic plasticity and NMDA receptor trafficking.', *Trends in Neurosciences* **28**(5), 229–38.

Petersen, C., Malenka, R., Nicoll, R. and Hopfield, J. (1998), 'All-or-none potentiation at CA3-CA1 synapses', *Proceedings of the National Academy of Sciences of the United States of America* **95**(8), 4732–7.

Petersen, S. a., Fetter, R. D., Noordermeer, J. N., Goodman, C. S. and DiAntonio, a. (1997), 'Genetic analysis of glutamate receptors in Drosophila reveals a retrograde signal regulating presynaptic transmitter release.', *Neuron* **19**(6), 1237–48.

Petrozzino, J. and Connor, J. (1994), 'Dendritic Ca2+ accumulations and metabotropic glutamate receptor activation associated with an n-methyl-d-aspartate receptor-independent long-term potentiation in hippocampal CA1 neurons', *Hippocampus* **4**(5), 546–58.

Poncer, J., Esteban, J. and Malinow, R. (2002), 'Multiple Mechanisms for the Potentiation of AMPA Receptor-Mediated Transmission by α-Ca2+/Calmodulin-Dependent Protein Kinase II', *Journal of Neuroscience* **22**(11), 4406–11.

Popivanova, B., Kitamura, K., Wu, Y., Kondo, T., Kagaya, T., Kaneko, S., Oshima, M., Fujii, C. and Mukaida, N. (2008), 'Blocking TNF-α in mice reduces colorectal carcinogenesis associated with chronic colitis', *Journal of Clinical Investigation* **118**(2), 560–70.

Pratt, K., Dong, W. and Aizenmann, C. (2008), 'Development and spike timing-dependent plasticity of recurrent excitation in the Xenopus optic tectum', *Nature Neuroscience* **11**(4), 467–75.

Pratt, K. G., Watt, A. J., Griffith, L. C., Nelson, S. B. and Turrigiano, G. G. (2003), 'Activity-dependent remodeling of presynaptic inputs by postsynaptic expression of activated CaMKII.', *Neuron* **39**(2), 269–81.

Prekeris, R., Klumperman, J., Chen, Y. and Scheller, R. (1998), 'Syntaxin 13 mediates cycling of plasma membrane proteins via tubulovesicular recycling endosomes', *Journal of Cell Biology* **143**(4), 957–71.

Prekeris, R., Yang, B., Oorschot, V., Klumperman, J. and Scheller, R. (1999), 'Differential roles of syntaxin 7 and syntaxin 8 in endosomal trafficking', *Molecular Biology of the Cell* **10**(11), 3891–908.

Prut, Y., Vaadia, E., Bergman, H., Haalman, I., Slovin, H. and Abeles, M. (1998), 'Spatiotemporal structure of cortical activity: properties and behavioral relevance', *Journal of Neurophysiology* **79**(6), 2657–74.

Rabinowitch, I. and Segev, I. (2008), 'Two opposing plasticity mechanisms pulling a single synapse', *Trends in Neurosciences* **31**(8), 377–83.

Racine, R., Milgram, N. and Hafner, S. (1983), 'Long-term potentiation phenomena in the rat limbic forebrain', *Brain Research* **260**(2), 217–31.

Rácz, B., Blanpied, T., Ehlers, M. and Weinberg, R. (2004), 'Lateral organization of endocytic machinery in dendritic spines', *Nature Neuroscience* **7**(9), 917–8.

Rao, R. P. and Ballard, D. H. (1997), 'Dynamic model of visual recognition predicts neural response properties in the visual cortex.', *Neural Computation* **9**(4), 721–63.

Raymond, C., Thompson, V., Tate, W. and Abraham, W. C. (2000), 'Metabotropic glutamate receptors trigger homosynaptic protein synthesis to prolong long-term potentiation', *Journal of Neuroscience* **20**(3), 969–76.

Rial Verde, E. M., Lee-Osbourne, J., Worley, P. F., Malinow, R. and Cline, H. T. (2006), 'Increased expression of the immediate-early gene arc/arg3.1 reduces AMPA receptor-mediated synaptic transmission.', *Neuron* **52**(3), 461–74.

Roche, K., O'Brien, R., Mammen, A., Bernhardt, J. and Huganir, R. (1996), 'Characterization of multiple phosphorylation sites on the AMPA receptor GluR1 subunit', *Neuron* **16**(6), 1179–88.

Rosa, M. G. P. (2002), 'Visual maps in the adult primate cerebral cortex: some implications for brain development and evolution.', *Brazilian Journal of Medical and Biological Research* **35**(12), 1485–98.

Royer, S. and Paré, D. (2003), 'Conservation of total synaptic weight through balanced synaptic depression and potentiation', *Nature* **422**(6931), 518–22.

Rubin, J., Lee, D. and Sompolinsky, H. (2001), 'Equilibrium properties of temporally asymmetric Hebbian plasticity', *Physical Review Letters* **86**(2), 364–67.

Rutherford, L. C., Nelson, S. B. and Turrigiano, G. G. (1998), 'BDNF has opposite effects on the quantal amplitude of pyramidal neuron and interneuron excitatory synapses.', *Neuron* **21**(3), 521–30.

Sayer, R., Friedlander, M. and Redman, S. (1990), 'The time course and amplitude of EPSPs evoked at synapses between pairs of CA3/CA1 neurons in the hippocampal slice', *Journal of Neuroscience* **10**(3), 826–36.

Schiller, J., Helmchen, F. and Sakmann, B. (1995), 'Spatial profile of dendritic calcium transients evoked by action potentials in rat neocortical pyramidal neurones.', *Journal of Physiology* **487 (Pt 3)**, 583–600.

Schuman, E. and Madison, D. (1994), 'Nitric oxide and synaptic function', *Annual Review of Neuroscience* **17**, 153–83.

Seidenman, K., Steinberg, J., Huganir, R. and Malinow, R. (2003), 'Glutamate receptor subunit 2 Serine 880 phosphorylation modulates synaptic transmission and mediates plasticity in CA1 pyramidal cells', *Journal of Neuroscience* **23**(27), 9220–8.

Senn, W. and Fusi, S. (2005), 'Learning only when necessary: better memories of correlated patterns in networks with bounded synapses', *Neural Computation* **17**(10), 2106–38.

Serulle, Y., Zhang, S., Ninan, I., Puzzo, D., McCarthy, M., Khatri, L., Arancio, O. and Ziff, E. B. (2007), 'A GluR1-cGKII interaction regulates AMPA receptor trafficking.', *Neuron* **56**(4), 670–88.

Sharma, K., Fong, D. K. and Craig, A. M. (2006), 'Postsynaptic protein mobility in dendritic spines: long-term regulation by synaptic NMDA receptor activation.', *Molecular and Cellular Neurosciences* **31**(4), 702–12.

Shepherd, J. D., Rumbaugh, G., Wu, J., Chowdhury, S., Plath, N., Kuhl, D., Huganir, R. L. and Worley, P. F. (2006), 'Arc/Arg3.1 mediates homeostatic synaptic scaling of AMPA receptors.', *Neuron* **52**(3), 475–84.

Shi, S., Hayashi, Y., Esteban, J. a. and Malinow, R. (2001), 'Subunit-specific rules governing AMPA receptor trafficking to synapses in hippocampal pyramidal neurons.', *Cell* **105**(3), 331–43.

Shi, S., Hayashi, Y., Petralia, R., Zaman, S., Wenthold, R., Svoboda, K. and Malinow, R. (1999), 'Rapid Spine Delivery and Redistribution of AMPA Receptors After Synaptic NMDA Receptor Activation', *Science* **284**(5421), 1811–6.

Shmiel, T. and Drori, R. (2006), 'Neurons of the cerebral cortex exhibit precise interspike timing in correspondence to behavior', *Proceedings of the National Academy of Sciences of the United States of America* **102**(51), 18655–7.

Shu, Y., Hasenstaub, A., Badoual, M., Bal, T. and McCormick, D. (2003), 'Barrages of synaptic activity control the gain and sensitivity of cortical neurons', *Journal of Neuroscience* **23**(32), 10388–401.

Siegelbaum, S. and Kandel, E. (1991), 'Learning-related synaptic plasticity: LTP and LTD', *Current Opinion in Neurobiology* **1**(1), 113–20.

Silver, R. (2010), 'Neuronal arithmetic.', *Nature Reviews Neuroscience* **11**(7), 474–89.

Silver, R. A., Lubke, J., Sakmann, B. and Feldmeyer, D. (2003), 'High-probability uniquantal transmission at excitatory synapses in barrel cortex.', *Science* **302**(5652), 1981–4.

Sjöström, P., Turrigiano, G. and Nelson, S. (2001), 'Rate, timing, and cooperativity jointly determine cortical synaptic plasticity', *Neuron* **32**(6), 1149–64.

Song, S. and Abbott, L. (2001), 'Cortical Remapping through Spike Timing-Dependent Plasticity', *Neuron* **32**(2), 339–50.

Song, S., Miller, K. and Abbott, L. (2000), 'Competitive Hebbian learning through spike-timing-dependent synaptic plasticity', *Nature Neuroscience* **3**(9), 919–26.

Song, S., Sjöström, P., Reigl, M., Nelson, S. and Chklovskii, D. B. (2005), 'Highly nonrandom features of synaptic connectivity in local cortical circuits.', *PLoS Biology* **3**(3), e68.

Stacey, W. and Durand, D. (2001), 'Synaptic noise improves detection of subthreshold signals in hippocampal CA1 neurons', *Journal of Neurophysiology* **86**(3), 1104–12.

Standage, D., Jalil, S. and Trappenberg, T. (2007), 'Computational consequences of experimentally derived spike-time and weight dependent plasticity rules.', *Biological Cybernetics* **96**(6), 615–23.

Standage, D. and Trappenberg, T. (2007), 'The trouble with weight-dependent STDP', *Neural Networks* pp. 1348–53.

Staubli, U. and Ji, Z. (1996), 'The induction of homo -vs. heterosynaptic LTD in area CA1 of hippocampal slices from adult rats', *Brain research* **714**(1-2), 169–76.

Staubli, U. and Lynch, G. (1990), 'Stable depression of potentiated synaptic responses in the hippocampus with 1-5 Hz stimulation', *Brain Research* **513**(1), 113–8.

Stein, R. B. (1967), 'Some Models of Neuronal Variability', *Biophysical Journal* **7**(1), 37–68.

Stellwagen, D. and Malenka, R. (2006), 'Synaptic scaling mediated by glial TNF-α', *Nature* **440**(7087), 1054–9.

Sugiyama, Y., Kawabata, I., Sobue, K. and Okabe, S. (2005), 'Determination of absolute protein numbers in single synapses by a GFP-based calibration technique', *Nature Methods* **2**(9), 677–84.

Sutton, M. a., Ito, H. T., Cressy, P., Kempf, C., Woo, J. C. and Schuman, E. M. (2006), 'Miniature neurotransmission stabilizes synaptic function via tonic suppression of local dendritic protein synthesis.', *Cell* **125**(4), 785–99.

Swindale, N. (1982), 'A model for the formation of orientation columns.', *Proceedings of the Royal Society* **215**, 211–30.

Takahashi, M., Itakura, M. and Kataoka, M. (2003), 'New aspects of neurotransmitter release and exocytosis: Regulation of neurotransmitter release by phosphorylation', *Journal of Pharmacological Sciences* **93**(1), 41–5.

Takumi, Y., Ramirez-León, V., Laake, P., Rinvik, E. and Ottersen, O. (1999), 'Different modes of expression of AMPA and NMDA receptors in hippocampal synapses', *Nature Neuroscience* **2**(7), 618–24.

Thiagarajan, T. C., Lindskog, M. and Tsien, R. W. (2005), 'Adaptation to synaptic inactivity in hippocampal neurons.', *Neuron* **47**(5), 725–37.

Thiagarajan, T., Lindskog, M., Malgaroli, A. and Tsien, R. (2007), 'LTP and adaptation to inactivity : Overlapping mechanisms and implications for metaplasticity', *Neuropharmacology* **52**(1), 156–75.

Tomita, S., Stein, V., Stocker, T., Nicoll, R. and Bredt, D. (2005), 'Bidirectional synaptic plasticity regulated by phosphorylation of stargazin-like TARPs.', *Neuron* **45**(2), 269–77.

Toyoizumi, T., Pfister, J.-P., Aihara, K. and Gerstner, W. (2007), 'Optimality model of unsupervised spike-timing-dependent plasticity: synaptic memory and weight distribution.', *Neural Computation* **19**(3), 639–71.

Triller, a. and Choquet, D. (2005), 'Surface trafficking of receptors between synaptic and extrasynaptic membranes: and yet they do move!', *Trends in Neurosciences* **28**(3), 133–9.

Tsumoto, T., Creutzfeldt, O. and Legendy, C. (1978), 'Functional organization of the corticofugal system from visual cortex to lateral geniculate nucleus in the cat (with an appendix on geniculo-cortical mono-synaptic connections)', *Experimental Brain Research* **32**(3), 345–64.

Tsuriel, S., Geva, R., Zamorano, P., Dresbach, T., Boeckers, T., Gundelfinger, E. D., Garner, C. C. and Ziv, N. E. (2006), 'Local sharing as a predominant determinant of synaptic matrix molecular dynamics.', *PLoS biology* **4**(9), e271.

Turrigiano, G. (1999), 'Homeostatic plasticity in neuronal networks : the more things change , the more they stay the same', *Trends in Neurosciences* **22**, 221–7.

Turrigiano, G. (2008), 'The Self-Tuning Neuron : Synaptic Scaling of Excitatory Synapses', *Cell* **135**(3), 422–35.

Turrigiano, G., Leslie, K., Desai, N., Rutherford, L. and Nelson, S. (1998), 'Activity-dependent scaling of quantal amplitude in neocortical neurons', *Nature* **391**(6670), 892–6.

Tzingounis, A. and Nicoll, R. (2006), 'Arc/Arg3. 1: linking gene expression to synaptic plasticity and memory', *Neuron* **52**(3), 403–7.

van Rossum, M. (2001), 'A novel spike distance.', *Neural Computation* **13**(4), 751–63.

van Rossum, M., Bi, G. and Turrigiano, G. (2000), 'Stable Hebbian learning from spike timing-dependent plasticity', *Journal of Neuroscience* **20**(23), 8812–21.

Wandell, B. A. and Winawer, J. (2011), 'Imaging retinotopic maps in the human brain.', *Vision Research* **51**(7), 718–37.

Wang, H., Gerkin, R., Nauen, D. and Bi, G. (2005), 'Coactivation and timing-dependent integration of synaptic potentiation and depression.', *Nature Neuroscience* **8**(2), 187–93.

Washbourne, P., Bennett, J. E. and McAllister, a. K. (2002), 'Rapid recruitment of NMDA receptor transport packets to nascent synapses.', *Nature Neuroscience* **5**(8), 751–9.

Watt, a. J., van Rossum, M., MacLeod, K. M., Nelson, S. B. and Turrigiano, G. G. (2000), 'Activity coregulates quantal AMPA and NMDA currents at neocortical synapses.', *Neuron* **26**(3), 659–70.

Wennekers, T. (2000), 'Dynamics of spatio-temporal patterns in associative networks of spiking neurons', *Neurocomputing* **32-33**(1-4), 597–602.

Wennekers, T. (2003), 'Editorial: Cell Assemblies', *Theory in Biosciences* **122**(1), 1–4.

Wennekers, T. and Ay, N. (2005), 'Finite state automata resulting from temporal information maximization and a temporal learning rule.', *Neural Computation* **17**(10), 2258–90.

Wennekers, T. and Ay, N. (2006), 'A temporal learning rule in recurrent systems supports high spatio-temporal stochastic interactions', *Neurocomputing* **69**(10-12), 1199–202.

Wennekers, T. and Palm, G. (1996), 'Controlling the speed of synfire chains', *Lecture Notes in Computer Science* **1112**, 451–6.

Wennekers, T. and Palm, G. (2007), 'Modelling generic cognitive functions with operational Hebbian cell assemblies', *Neuronal Network Research Horizons* **49**(0), 225–94.

White, E. (1989), *Cortical Circuits: Synaptic Organization of the Cerebral Cortex. Structure, Function and Theory*, Birkhäuser Verlag AG.

White, G., Levy, W. and Steward, O. (1990), 'Spatial overlap between populations of synapses determines the extent of their associative interaction during the induction of long-term potentiation and depression', *Journal of Neurophysiology* **64**(4), 1186–98.

Wierenga, C., Ibata, K. and Turrigiano, G. (2005), 'Postsynaptic expression of homeostatic plasticity at neocortical synapses', *Journal of Neuroscience* **25**(11), 2895–905.

Winder, D. G., Mansuy, I. M., Osman, M., Moallem, T. M. and Kandel, E. R. (1998), 'Genetic and pharmacological evidence for a novel, intermediate phase of long-term potentiation suppressed by calcineurin.', *Cell* **92**(1), 25–37.

Wittenberg, G. and Wang, S. (2006), 'Malleability of spike-timing-dependent plasticity at the CA3-CA1 synapse', *Journal of Neuroscience* **26**(24), 6610–7.

Wöhrl, R., Von Haebler, D. and Heinemann, U. (2007), 'Low-frequency stimulation of the direct cortical input to area CA1 induces homosynaptic LTD and heterosynaptic LTP in the rat hippocampal entorhinal cortex slice preparation', *European Journal of Neuroscience* **25**(1), 251–8.

Wolfart, J., Debay, D., Masson, G. L., Destexhe, A. and Bal, T. (2005), 'Synaptic background activity controls spike transfer from thalamus to cortex.', *Nature Neuroscience* **8**(12), 1760–7.

Wolfe, J., Houweling, A. R. and Brecht, M. (2010), 'Sparse and powerful cortical spikes.', *Current Opinion in Neurobiology* **20**(3), 306–12.

Yang, S., Tang, Y. and Zucker, R. (1999), 'Selective induction of LTP and LTD by postsynaptic [Ca2+]i elevation', *Journal of Neurophysiology* **81**(2), 781–7.

Yang, Y., Wang, X.-B., Frerking, M. and Zhou, Q. (2008), 'Delivery of AMPA receptors to perisynaptic sites precedes the full expression of long-term potentiation.', *Proceedings of the National Academy of Sciences of the United States of America* **105**(32), 11388–93.

Yu, Y.-C., Bultje, R. S., Wang, X. and Shi, S.-H. (2009), 'Specific synapses develop preferentially among sister excitatory neurons in the neocortex.', *Nature* **458**(7237), 501–4.

Yuste, R., Gutnick, M., Saar, D., Delaney, K. and Tank, D. (1994), 'Ca2+ accumulations in dendrites of neocortical pyramidal neurons: an apical band and evidence for two functional compartments', *Neuron* **13**(1), 23–43.